Collaboration:
A. Castaneda[4], S. Dildick[2], T. Elkafrawy[1], T. Kamon[3], H. Kim[3], P. Padley[2], A. Safonov[3] and W. Shi[2]
[1] Florida Institute of Technology
[2] Rice University
[3] Texas A&M
[4] University of Sonora

CMS Compact Muon Solenoid

Vector-Portal to The Dark Sector

A Dark Matter Search at the LHC

General Muon Meeting

Mehdi Rahmani & Marcus Hohlmann
Florida Institute of Technology

Contact: mrahmani2015@my.fit.edu

Feb 28, 2022

FLORIDA TECH

Introduction

The Dark Matter Problem

- The Standard Model of particle physics (SM) is a mathematically tight theory that describes fundamental physics and provides high-precision predictions consistent with decades of experimental studies.

Introduction

The Dark Matter Problem

- The Standard Model of particle physics (SM) is a mathematically tight theory that describes fundamental physics and provides high-precision predictions consistent with decades of experimental studies.

- There are several important shortcomings that are of primary interest for current research in the field. Related to the research reported here is the fact that the SM offers no explanation for the existence of dark matter (DM), for which there is abundant astronomical evidence.

Introduction

The Dark Matter Problem

- The Standard Model of particle physics (SM) is a mathematically tight theory that describes fundamental physics and provides high-precision predictions consistent with decades of experimental studies.

- There are several important shortcomings that are of primary interest for current research in the field. Related to the research reported here is the fact that the SM offers no explanation for the existence of dark matter (DM), for which there is abundant astronomical evidence.

- Experimentally, DM has not yet been observed, and there is not yet any evidence for non-gravitational interactions between DM and Standard Model particles.

Introduction

The Dark Matter Problem

- The Standard Model of particle physics (SM) is a mathematically tight theory that describes fundamental physics and provides high-precision predictions consistent with decades of experimental studies.

- There are several important shortcomings that are of primary interest for current research in the field. Related to the research reported here is the fact that the SM offers no explanation for the existence of dark matter (DM), for which there is abundant astronomical evidence.

- Experimentally, DM has not yet been observed, and there is not yet any evidence for non-gravitational interactions between DM and Standard Model particles.

- The DM searches are perused in three major fronts:
    - Direct detection experiments
    - Indirect searches
    - **Collider searches**

Introduction

The Dark Matter Problem

- The Standard Model of particle physics (SM) is a mathematically tight theory that describes fundamental physics and provides high-precision predictions consistent with decades of experimental studies.

- There are several important shortcomings that are of primary interest for current research in the field. Related to the research reported here is the fact that the SM offers no explanation for the existence of dark matter (DM), for which there is abundant astronomical evidence.

- Experimentally, DM has not yet been observed, and there is not yet any evidence for non-gravitational interactions between DM and Standard Model particles.

- The DM searches are perused in three major fronts:
  - Direct detection experiments
  - Indirect searches
  - **Collider searches** →
    - Model-dependent searches
    - EFT model-independent searches
    - **Simplified model-independent searches** [1,2,3]

Introduction

The Dark Sector - Continued

- ***Dark Sector Models:*** if the DM does not seemingly interact with the SM sector, the implication is that it is charged under a *dark* symmetry group [4,5]

Introduction

The Dark Sector - Continued

- ***Dark Sector Models:*** if the DM does not seemingly interact with the SM sector, the implication is that it is charged under a *dark* symmetry group [4,5]

- If this new sector communicates with SM sector through a weak portal, then detection is possible at the LHC

Introduction

The Dark Sector - Continued

- ***Dark Sector Models:*** if the DM does not seemingly interact with the SM sector, the implication is that it is charged under a *dark* symmetry group [4,5]

- If this new sector communicates with SM sector through a weak portal, then detection is possible at the LHC.

- The portal may assume different forms based on the spin of the portal operator: **Spin 1-Vector**, Spin-1/2 Neutrinos, Spin0-Higgs (scalar), or Axions (pseudo-scalar).

Introduction

The Dark Sector - Continued

- ***Dark Sector Models:*** if the DM does not seemingly interact with the SM sector, the implication is that it is charged under a *dark* symmetry group [4,5]

- If this new sector communicates with SM sector through a weak portal, then detection is possible at the LHC.

- The portal may assume different forms based on the spin of the portal operator: **Spin 1-Vector**, Spin-1/2 Neutrinos, Spin0-Higgs (scalar), or Axions (pseudo-scalar).

- The focus of my research is the **Spin 1-Vector portal** where a dark gauge boson interacts with an SM gauge boson through ***kinetic mixing*** between one dark and one visible Abelian gauge boson. This gauge boson is called the the dark Z (Z_D) [6].

Introduction

The Dark Sector - Continued

- ***Dark Sector Models:*** if the DM does not seemingly interact with the SM sector, the implication is that it is charged under a *dark* symmetry group [4,5]

- If this new sector communicates with SM sector through a weak portal, then detection is possible at the LHC.

- The portal may assume different forms based on the spin of the portal operator: **Spin 1-Vector**, Spin-1/2 Neutrinos, Spin0-Higgs (scalar), or Axions (pseudo-scalar).

- The focus of my research is the **Spin 1-Vector portal** where a dark gauge boson interacts with an SM gauge boson through ***kinetic mixing*** between one dark and one visible Abelian gauge boson. This gauge boson is called the the dark Z (Z_D) [6].

$$\mathscr{L} = -\frac{1}{4}B^{\mu\nu}B_{\mu\nu} - \frac{1}{4}B'^{\mu\nu}B'_{\mu\nu} - \epsilon B^{\mu\nu}B'_{\mu\nu}$$

- $B^{\mu\nu}$ is the SM electromagnetic field tensor
- $B'^{\mu\nu}$ The field tensor in the dark sector
- ϵ is the kinetic mixing parameter

Model-Independent Search

The 2018 Analysis

- We explored the **pair production of new bosons** at the LHC in collaboration with research groups from Texas A&M, Rice University, and University of Sonora.

Model-Independent Search

The 2018 Analysis

- We explored the **pair production of new bosons** at the LHC in collaboration with research groups from Texas A&M, Rice University, and University of Sonora.

- Our analysis presents a search for new light bosons decaying into muon pairs, corresponding to an integrated luminosity of $59.7\ fb^{-1}$ at the center-of-mass energy $\sqrt{s} = 13\ TeV$, recorded during 2018 at the CMS.

Model-Independent Search

The 2018 Analysis

•We explored the **pair production of new bosons** at the LHC in collaboration with research groups from Texas A&M, Rice University, and University of Sonora.

•Our analysis presents a search for new light bosons decaying into muon pairs, corresponding to an integrated luminosity of $59.7\ fb^{-1}$ at the center-of-mass energy $\sqrt{s} = 13\ TeV$, recorded during 2018 at the CMS.

•The parameter space probed is $0.25 < m < 60\ GeV$ for the mass of the mediator [7].

Model-Independent Search

The 2018 Analysis

•We explored the **pair production of new bosons** at the LHC in collaboration with research groups from Texas A&M, Rice University, and University of Sonora.

•Our analysis presents a search for new light bosons decaying into muon pairs, corresponding to an integrated luminosity of $59.7\ fb^{-1}$ at the center-of-mass energy $\sqrt{s} = 13\ TeV$, recorded during 2018 at the CMS.

•The parameter space probed is $0.25 < m < 60\ GeV$ for the mass of the mediator [7].

✳Displaced analysis (Long Lived signature): $c\tau =$ 0-100 mm (MSSMD bench-mark model)

Model-Independent Search

The 2018 Analysis

•We explored the **pair production of new bosons** at the LHC in collaboration with research groups from Texas A&M, Rice University, and University of Sonora.

•Our analysis presents a search for new light bosons decaying into muon pairs, corresponding to an integrated luminosity of $59.7\ fb^{-1}$ at the center-of-mass energy $\sqrt{s} = 13\ TeV$, recorded during 2018 at the CMS.

•The parameter space probed is $0.25 < m < 60\ GeV$ for the mass of the mediator [7].

✴Displaced analysis (Long Lived signature): $c\tau =$ 0-100 mm (MSSMD bench-mark model)

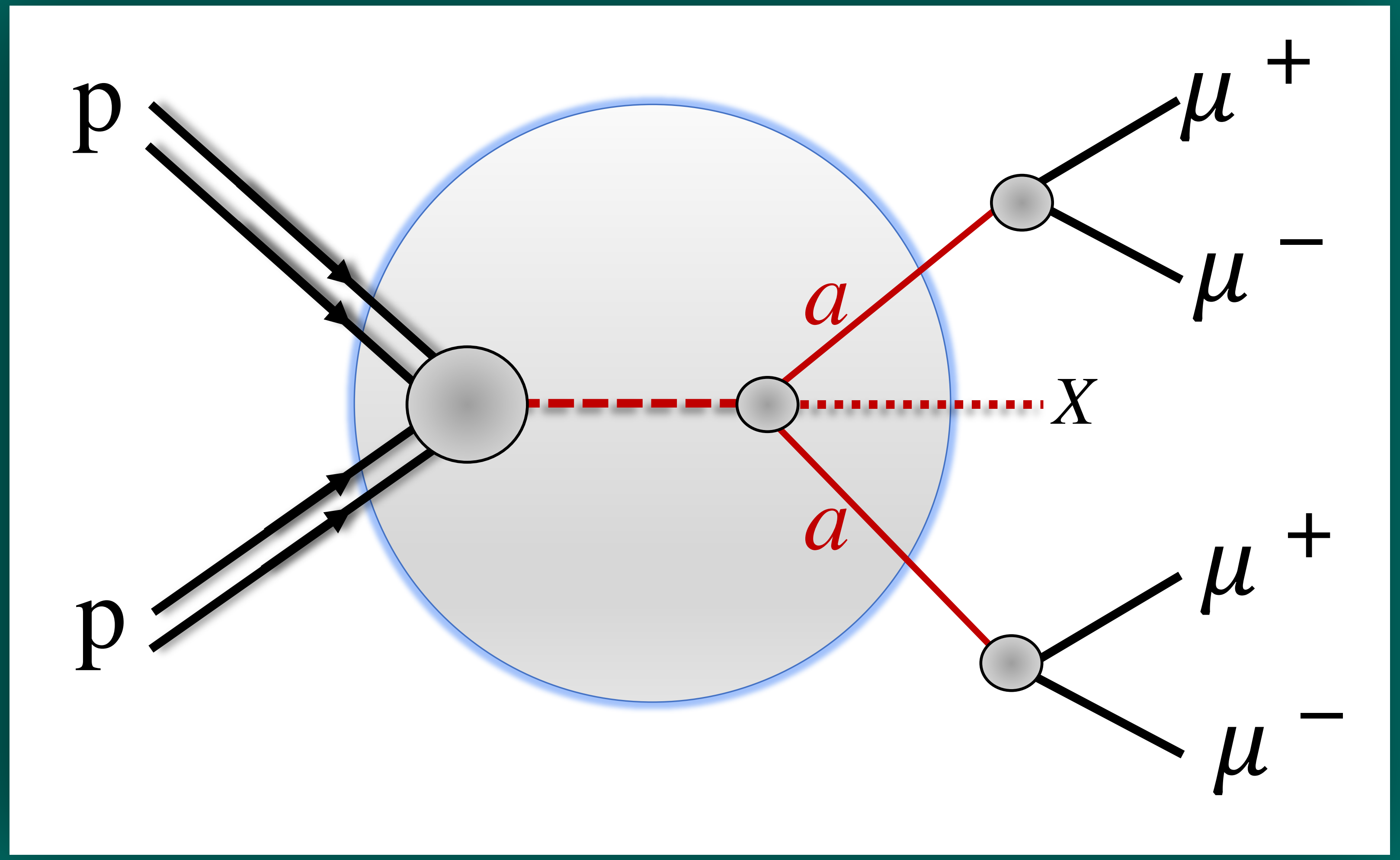

Figure1: Schematic example of the pp interaction that produces a pair of new bosons of which each decays into a muon pair. The grey circle indicate the dark sector interactions. The X particle is to signify any excess processes other than the four lepton final state.

Model-Independent Search

The 2018 Analysis

We have a CADI line with AN and draft paper based on Run II 2018 data:

- CADI: HIG-21-004
- Pre-approval talk: Feb 16 , 2021
- Unblinded results: Apr 28 , 2021
- Twiki: HIG21004Run2

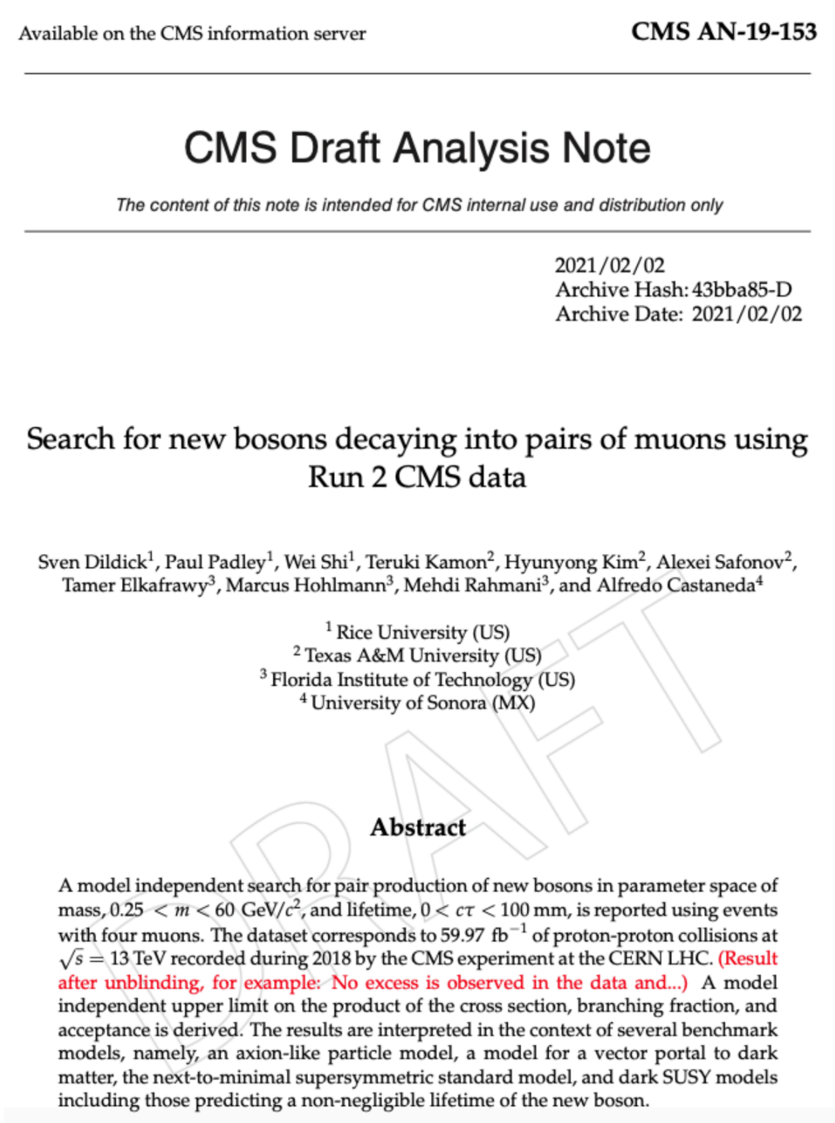

Available on the CMS information server — CMS AN-19-153

CMS Draft Analysis Note

The content of this note is intended for CMS internal use and distribution only

2021/02/02
Archive Hash: 43bba85-D
Archive Date: 2021/02/02

Search for new bosons decaying into pairs of muons using Run 2 CMS data

Sven Dildick[1], Paul Padley[1], Wei Shi[1], Teruki Kamon[2], Hyunyong Kim[2], Alexei Safonov[2], Tamer Elkafrawy[3], Marcus Hohlmann[3], Mehdi Rahmani[3], and Alfredo Castaneda[4]

[1] Rice University (US)
[2] Texas A&M University (US)
[3] Florida Institute of Technology (US)
[4] University of Sonora (MX)

Abstract

A model independent search for pair production of new bosons in parameter space of mass, $0.25 < m < 60$ GeV/c^2, and lifetime, $0 < c\tau < 100$ mm, is reported using events with four muons. The dataset corresponds to 59.97 fb^{-1} of proton-proton collisions at $\sqrt{s} = 13$ TeV recorded during 2018 by the CMS experiment at the CERN LHC. (Result after unblinding, for example: No excess is observed in the data and...) A model independent upper limit on the product of the cross section, branching fraction, and acceptance is derived. The results are interpreted in the context of several benchmark models, namely, an axion-like particle model, a model for a vector portal to dark matter, the next-to-minimal supersymmetric standard model, and dark SUSY models including those predicting a non-negligible lifetime of the new boson.

Thank conveners:

Keti Kaadze
Stephane Cooperstein

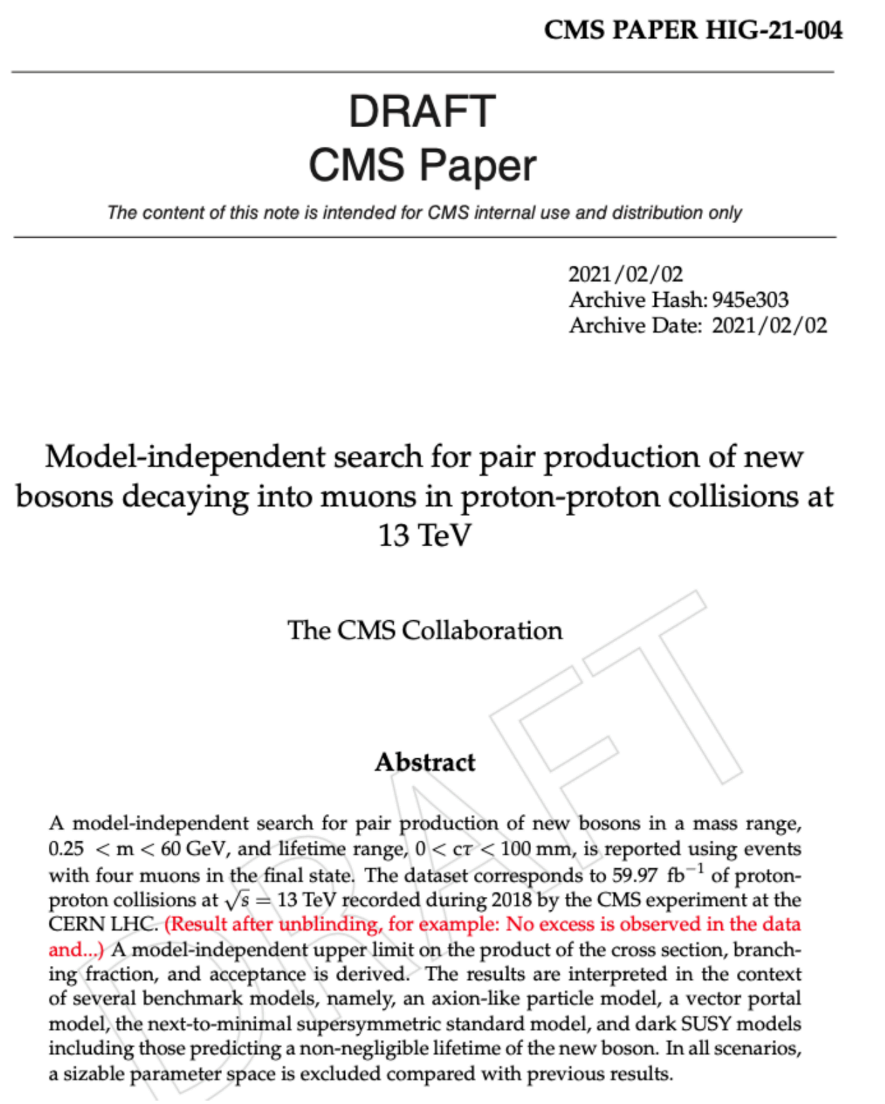

CMS PAPER HIG-21-004

DRAFT
CMS Paper

The content of this note is intended for CMS internal use and distribution only

2021/02/02
Archive Hash: 945e303
Archive Date: 2021/02/02

Model-independent search for pair production of new bosons decaying into muons in proton-proton collisions at 13 TeV

The CMS Collaboration

Abstract

A model-independent search for pair production of new bosons in a mass range, $0.25 < m < 60$ GeV, and lifetime range, $0 < c\tau < 100$ mm, is reported using events with four muons in the final state. The dataset corresponds to 59.97 fb^{-1} of proton-proton collisions at $\sqrt{s} = 13$ TeV recorded during 2018 by the CMS experiment at the CERN LHC. (Result after unblinding, for example: No excess is observed in the data and...) A model-independent upper limit on the product of the cross section, branching fraction, and acceptance is derived. The results are interpreted in the context of several benchmark models, namely, an axion-like particle model, a vector portal model, the next-to-minimal supersymmetric standard model, and dark SUSY models including those predicting a non-negligible lifetime of the new boson. In all scenarios, a sizable parameter space is excluded compared with previous results.

Bench-Mark Models

The Dark Scalar Model

- In this model, the Z_D particle is produced via kinetic mixing mechanism between the SM Z and the dark boson Z_D (gauge boson of a new $U(1)_D$ symmetry group.)
- The mixing parameter: ϵ

$$pp \to Z_D \to s_D\overline{s_D} \to \mu^+\mu^-\mu^+\mu^-$$

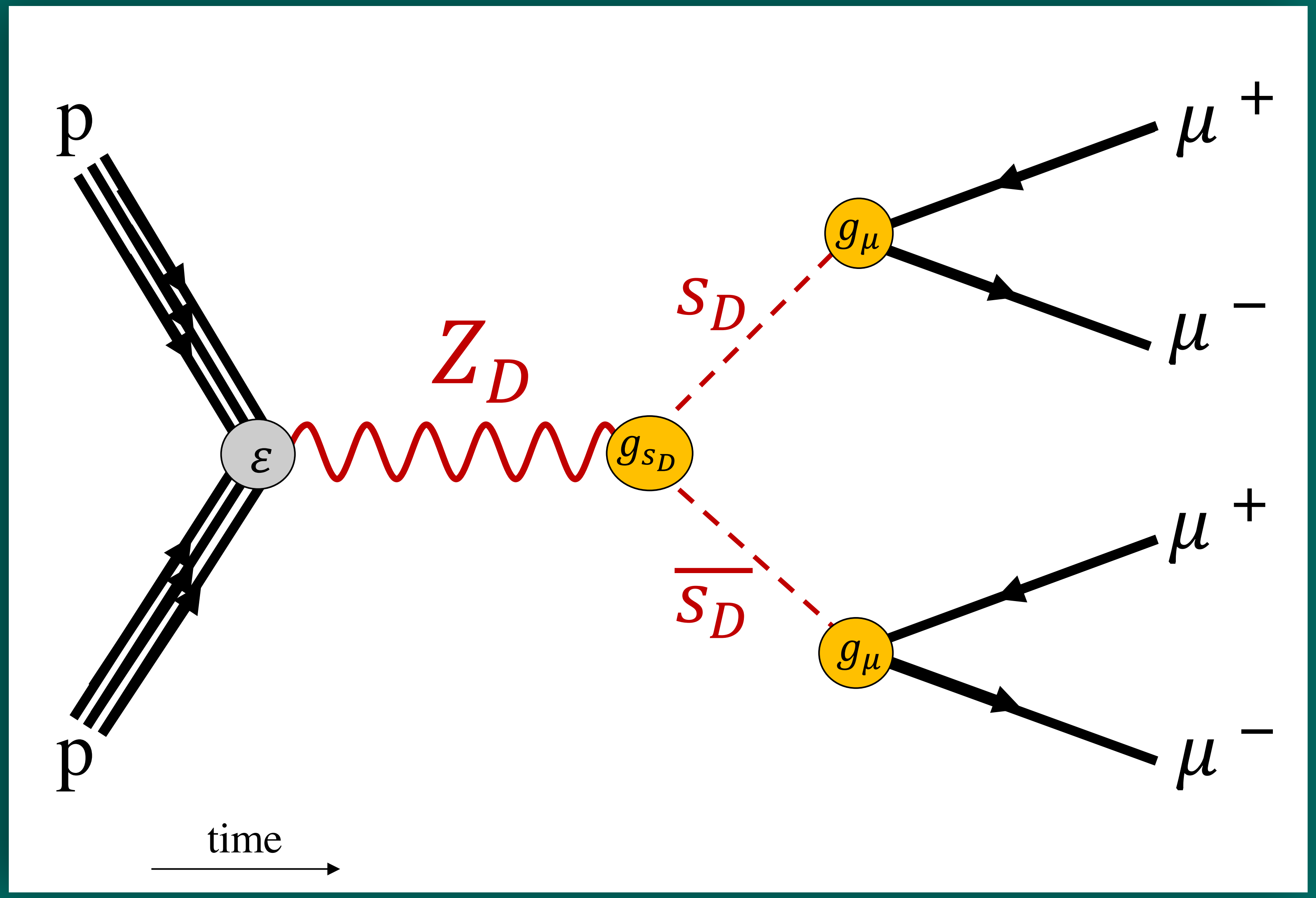

Figure2: Z_D *decays into a pair of scalar dark matter particles which then each subsequently decay into two oppositely charged muons.*

Bench-Mark Models

The Dark Scalar Model

Other bench-mark models in this search: App. A

Kinematics of hard process simulation: App. H

$$pp \to Z_D \to s_D\overline{s_D} \to \mu^+\mu^-\mu^+\mu^-$$

- In this model, the Z_D particle is produced via kinetic mixing mechanism between the SM Z and the dark boson Z_D (gauge boson of a new $U(1)_D$ symmetry group.)
- The mixing parameter: ϵ
- The dark scalar s_D, a complex scalar field, is assumed to be *not* self-conjugate
- For the purposes of simplicity the branching fraction $\mathscr{B}$ of s_D to muons is considered to be 100% [8, 9].
- Prompt signatures only

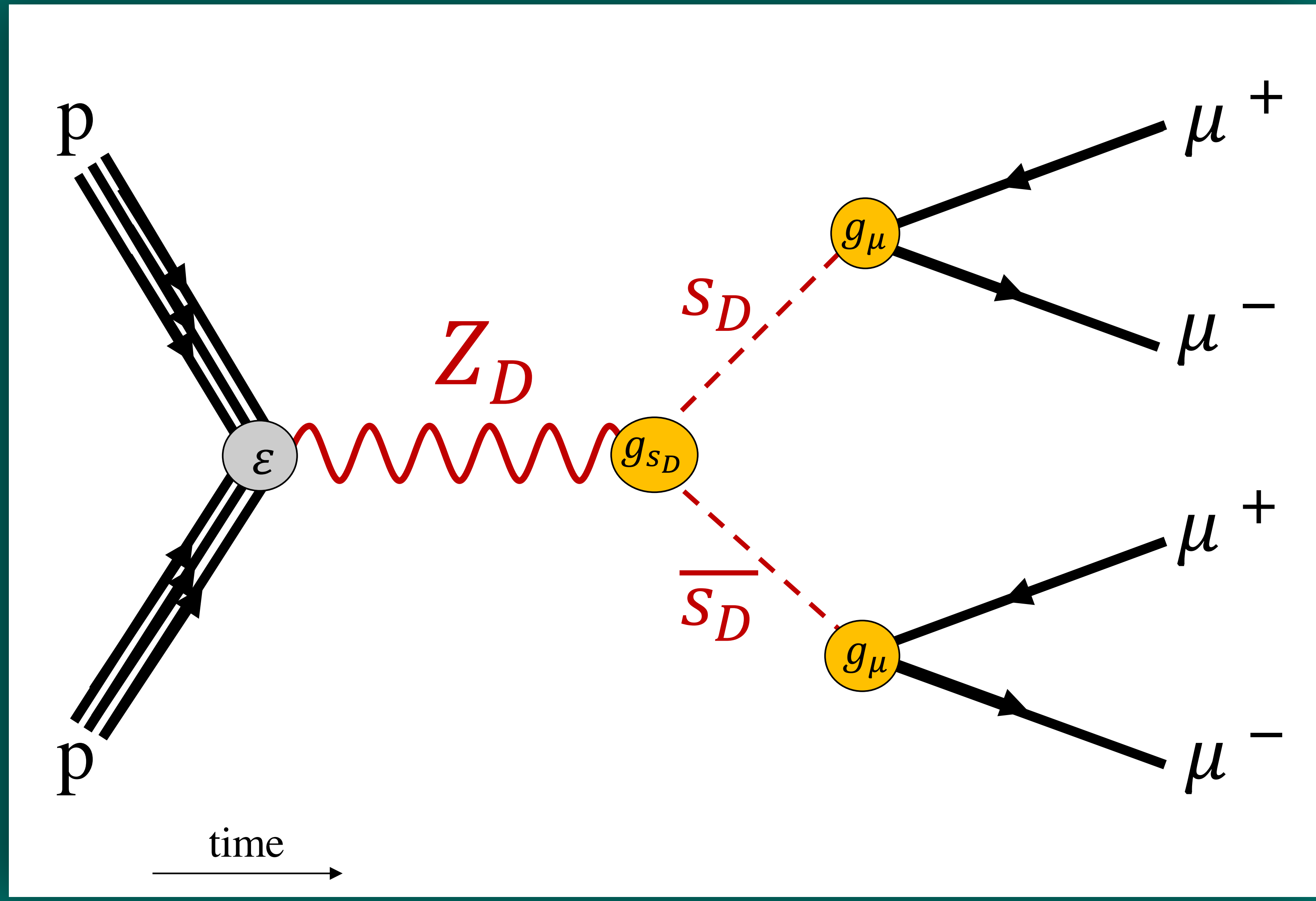

Figure2: Z_D *decays into a pair of scalar dark matter particles which then each subsequently decay into two oppositely charged muons.*

Samples

Monte-Carlo Simulation & Data

MC Simulation

Simulation Process	Description
Model Implementation	Feynrules
Hard Scattering Simulation	amc@nlo v2.6.5
Parton showering	PYTHIA 8
Hadronization, detector response, & reconstruction	CMSSW 10 2 X

Samples

Monte-Carlo Simulation & Data

MC Simulation

Simulation Process	Description
Model Implementation	Feynrules
Hard Scattering Simulation	amc@nlo v2.6.5
Parton showering	PYTHIA 8
Hadronization, detector response, & reconstruction	CMSSW 10 2 X

2018 Data

Dataset Labels	Number of Events
/DoubleMuon/Run2018A-17Sep2018-v2/MINIAOD	75 499 908
/DoubleMuon/Run2018B-17Sep2018-v1/MINIAOD	35 057 758
/DoubleMuon/Run2018C-17Sep2018-v1/MINIAOD	34 565 869
/DoubleMuon/Run2018D-PromptReco-v2/MINIAOD	169 225 355
Total	314 348 890

Analysis

Trigger and Muon Selection

Trigger Paths
HLT_DoubleL2Mu23NoVtx_2Cha
HLT_Mu18_Mu9_SameSign
HLT_TrkMu12_DoubleTrkMu5NoFiltersNoVtx,
HLT_TripleMu_12_10_5

For more on triggers see App. D

Analysis

Trigger and Muon Selection

Trigger Paths
HLT_DoubleL2Mu23NoVtx_2Cha
HLT_Mu18_Mu9_SameSign
HLT_TrkMu12_DoubleTrkMu5NoFiltersNoVtx,
HLT_TripleMu_12_10_5

For more on triggers: **App. D**

Muon selection
slimmedMuons in MiniAOD
PF Loose muon (>=3) + standalone-only (SA) muon (>=1)
Two muons: p_T >24 GeV, |eta| < 2
Four muons: p_T >8 GeV, |eta| < 2.4

Analysis

High-Level Selection

Selection	Description
Pixel Hit	Valid pixel hit for at least one muon in the muon pair: $L_{xy} < 16$ cm, $L_Z < 51.6$ cm (See **App. E**)
Dimuon Vertex	Fit dimuon vertex of each muon pair using KalmanVertexFitter, $P_{\mu\mu} > P(L_{xy}, f(\Delta R), N_{SA-\mu})$ (See **App. E**)
Mass Window	Two signal dimuon required to have consistent invariant mass (**See App. E)**

Muon pairing algorithm : **App. I**

Model-Indepence Performance

Generator v.s. Reco Efficiency

- Model independent ratio: $\epsilon_{Full}/\alpha_{Gen}$
  - α_{Gen} : generator level acceptance
    - 4 gen-muons p_T and η selection + fiducial cuts
  - ϵ_{Full}: full analysis efficiency
    - 4 reco-muons p_T and η selection + fiducial cuts+ full selection

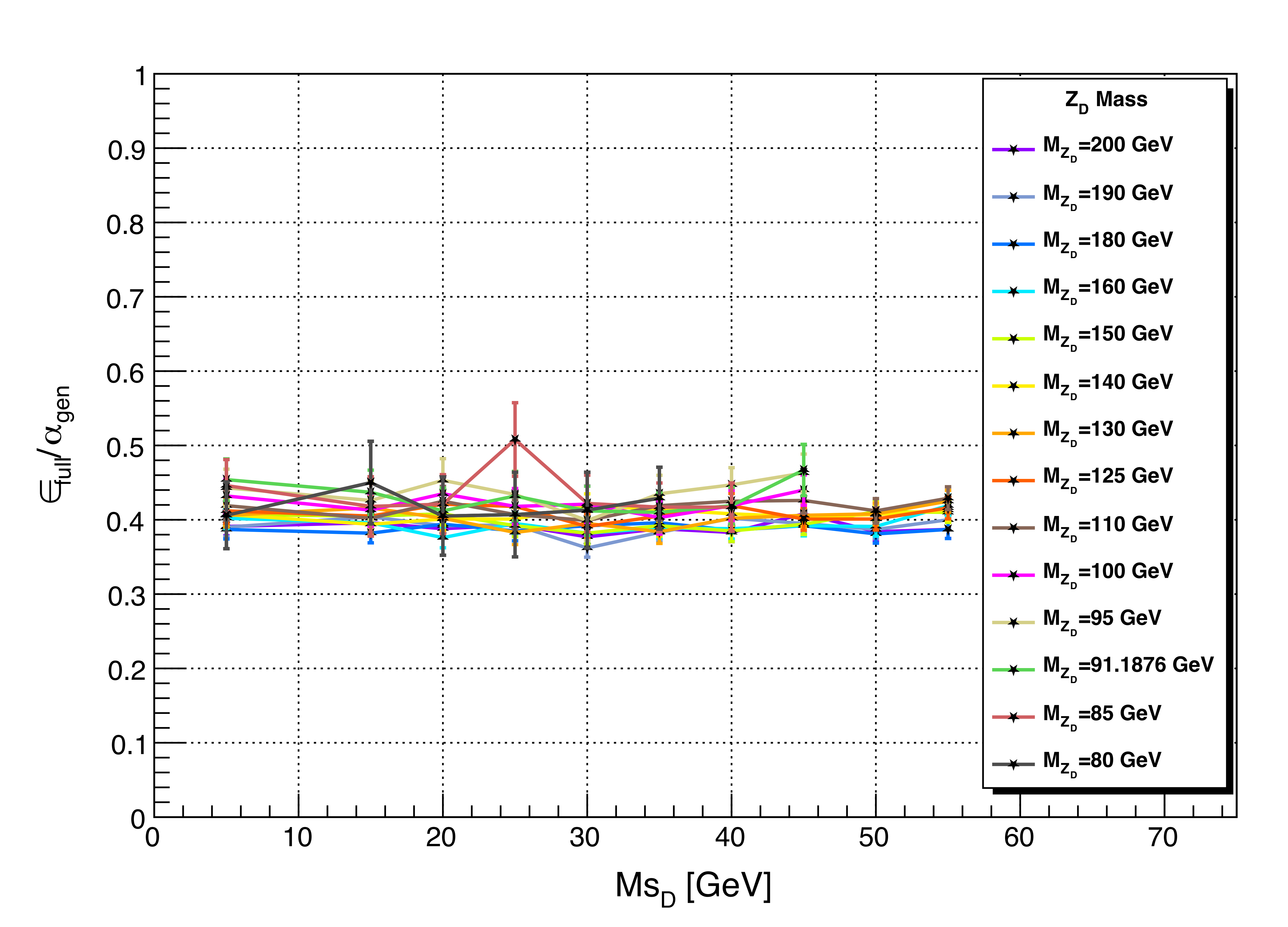

Figure3: Total selection efficiency over generator level selection acceptance, $\epsilon_{Full}/\alpha_{gen}$ as a function of the s_D mass for various Z_D masses in the vector portal model. The KM parameter, ϵ, is 10^{-2}.

Model-Indepence Performance

Generator v.s. Reco Efficiency

- Model independent ratio: $\epsilon_{Full}/\alpha_{Gen}$
  - α_{Gen} : generator level acceptance
    - 4 gen-muons p_T and η selection + fiducial cuts
  - ϵ_{Full}: full analysis efficiency
    - 4 reco-muons p_T and η selection + fiducial cuts+ full selection
- Constant $\epsilon_{Full}/\alpha_{Gen}$ indicates that the model performance is independent of its parameters

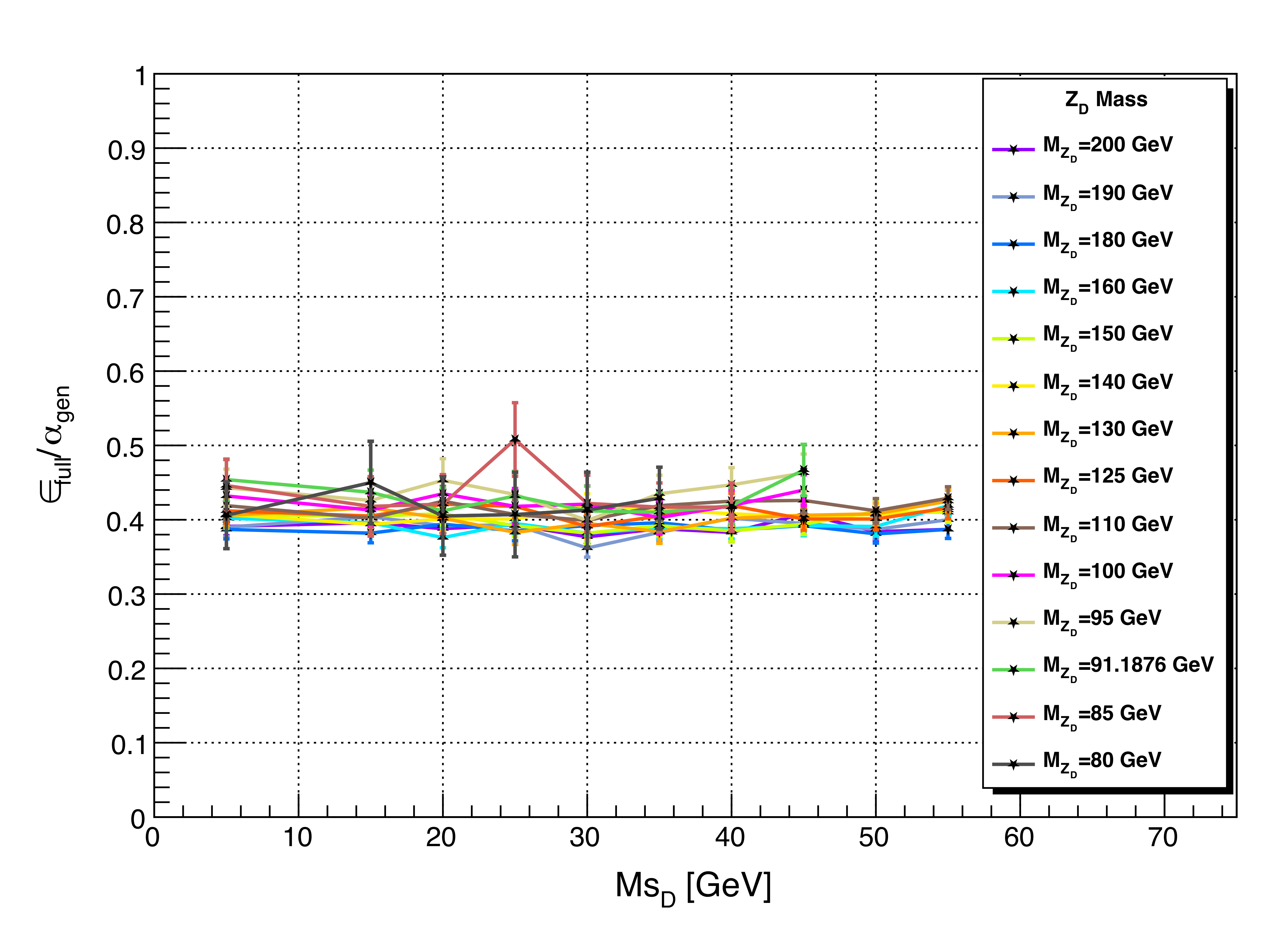

Figure3: Total selection efficiency over generator level selection acceptance, $\epsilon_{Full}/\alpha_{gen}$ as a function of the s_D mass for various Z_D masses in the vector portal model. The KM parameter, ϵ, is 10^{-2}.

Model-Indepence Performance

Generator v.s. Reco Efficiency

- Model independent ratio: $\epsilon_{Full}/\alpha_{Gen}$
  - α_{Gen} : generator level acceptance
    - 4 gen-muons p_T and η selection + fiducial cuts
  - ϵ_{Full}: full analysis efficiency
    - 4 reco-muons p_T and η selection + fiducial cuts+ full selection
- Constant $\epsilon_{Full}/\alpha_{Gen}$ indicates that the model performance is independent of its parameters
- Average $\epsilon_{Full}/\alpha_{Gen}$ = 0.418, is consistent with other benchmark models in the analysis

Other bench-mark models in this search: App. A

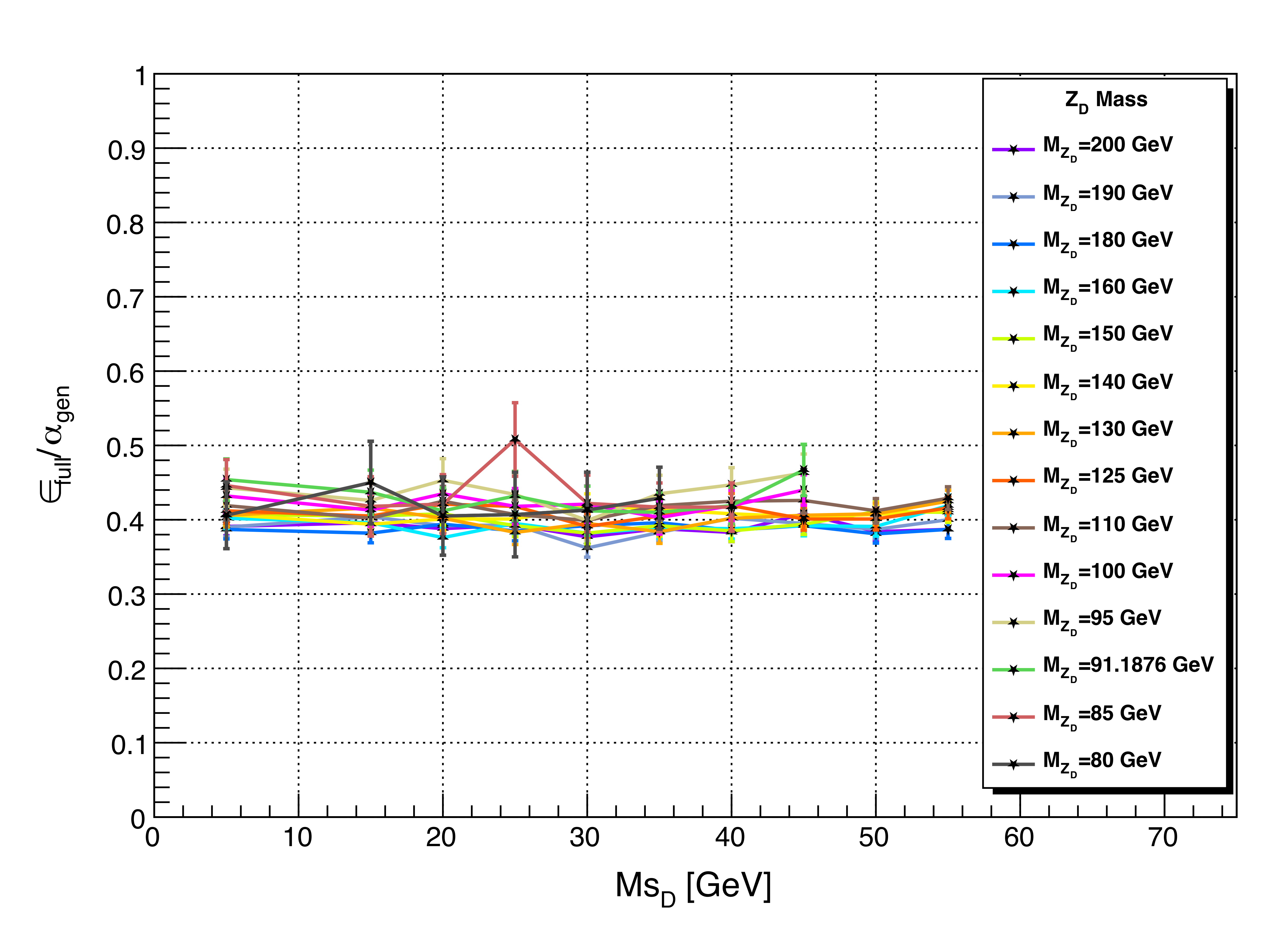

Figure3: Total selection efficiency over generator level selection acceptance, $\epsilon_{Full}/\alpha_{gen}$ as a function of the s_D mass for various Z_D masses in the vector portal model. The KM parameter, ϵ, is 10^{-2}.

Background Estimation

Below Upsilon (ϒ) Resonances (0.25-9 GeV)

•Dominated by QCD multi-jet processes, especially contributions from $b\bar{b}$

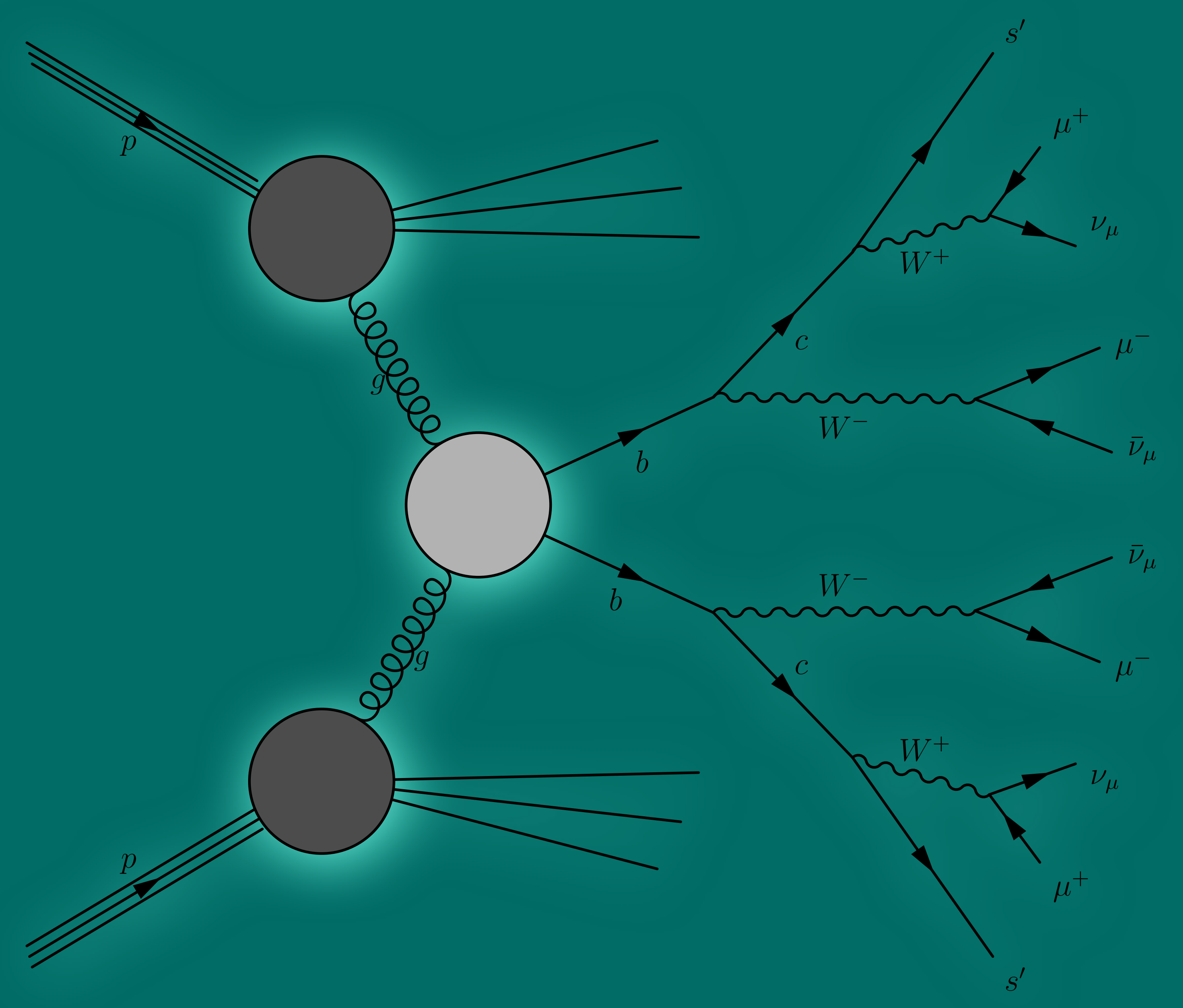

Figure4: Double semi-leptonic $b\bar{b}$ decays

Background Estimation

Below Upsilon (Υ) Resonances (0.25-9 GeV)

- Dominated by QCD multi-jet processes, especially contributions from $b\bar{b}$

- Double semi-leptonic decay or decay via resonances ($\eta, \omega, \phi, J/\psi(1S), \psi(2S)$)

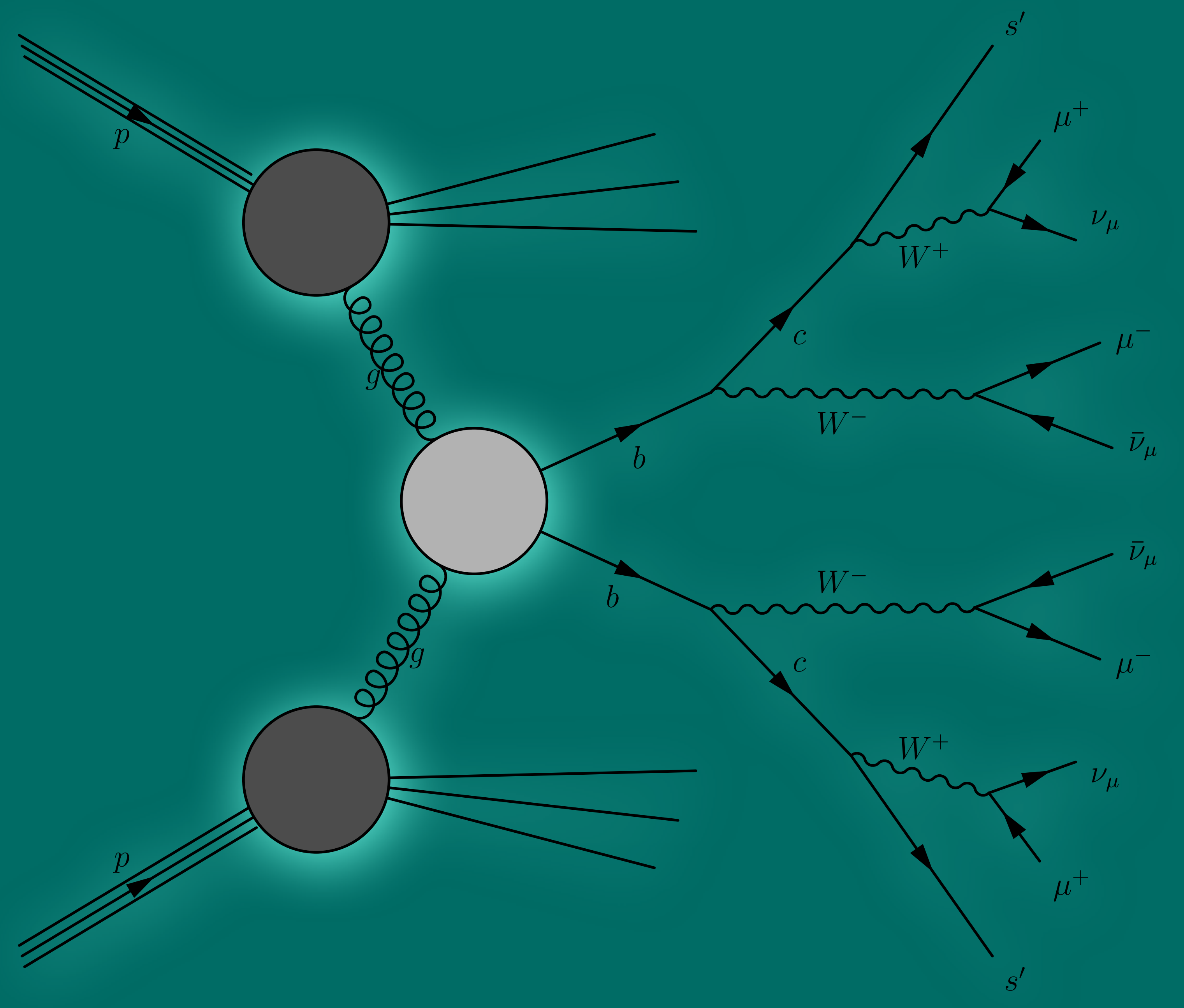

Figure4: Double semi-leptonic $b\bar{b}$ decays

Background Estimation

Below Upsilon (Υ) Resonances (0.25-9 GeV)

- Dominated by QCD multi-jet processes, especially contributions from $b\bar{b}$

- Double semi-leptonic decay or decay via resonances $(\eta, \omega, \phi, J/\psi(1S), \psi(2S))$

- Data driven (2018 DoubleMuon): because, MC for QCD processes are limited

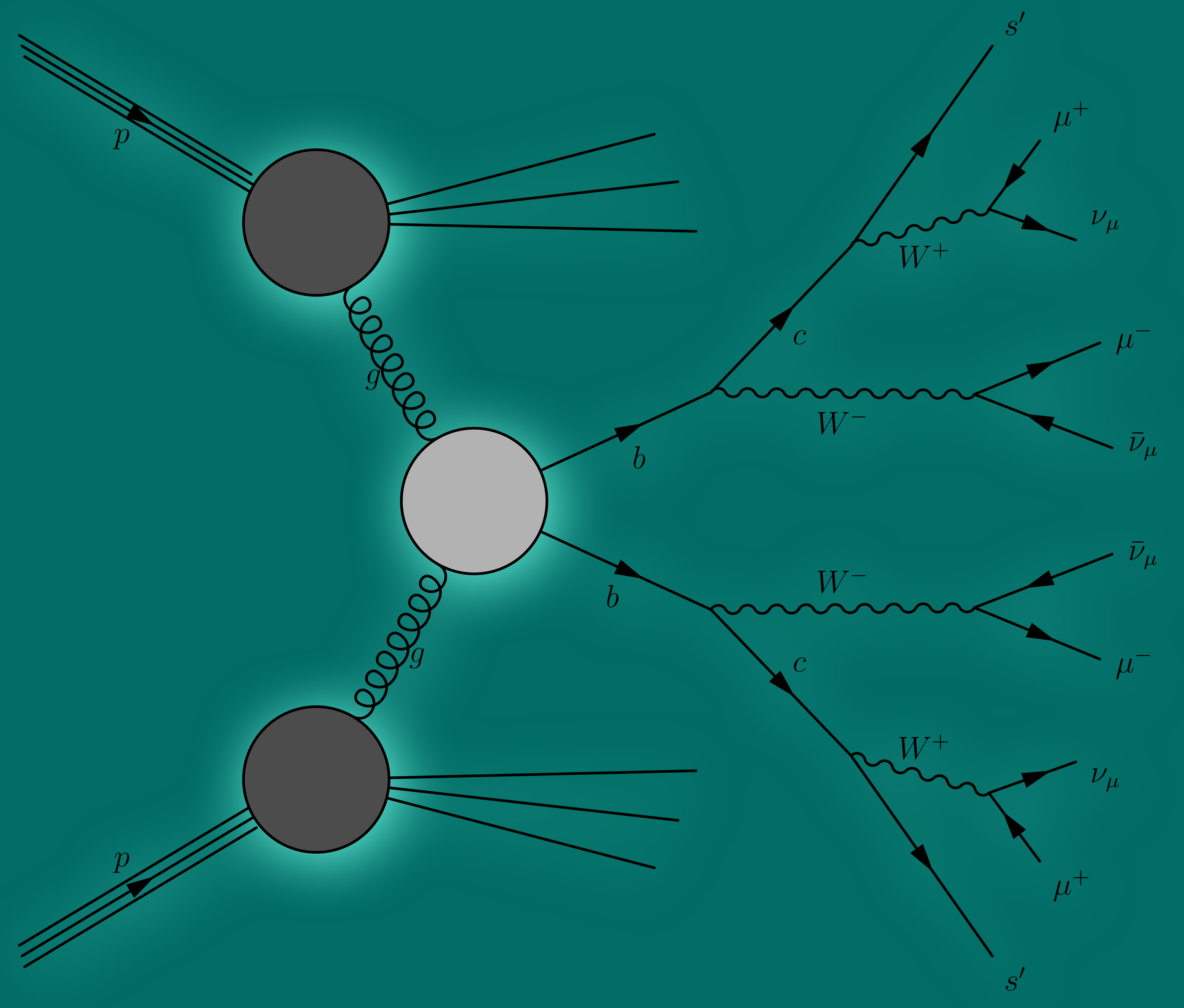

Figure4: Double semi-leptonic $b\bar{b}$ decays

Background Estimation

Below Upsilon (Υ) Resonances (0.25-9 GeV)

- Dominated by QCD multi-jet processes, especially contributions from $b\bar{b}$

- Double semi-leptonic decay or decay via resonances ($\eta, \omega, \phi, J/\psi(1S), \psi(2S)$)

- Data driven (2018 DoubleMuon): because, MC for QCD processes are limited

- Construct 2D background templates, based on 1D MC distributions and fitting them -> $f(m_{\mu\mu_1}) \otimes f(m_{\mu\mu_2})$. (See **App. B**)

- Estimate the number of background events in the signal region

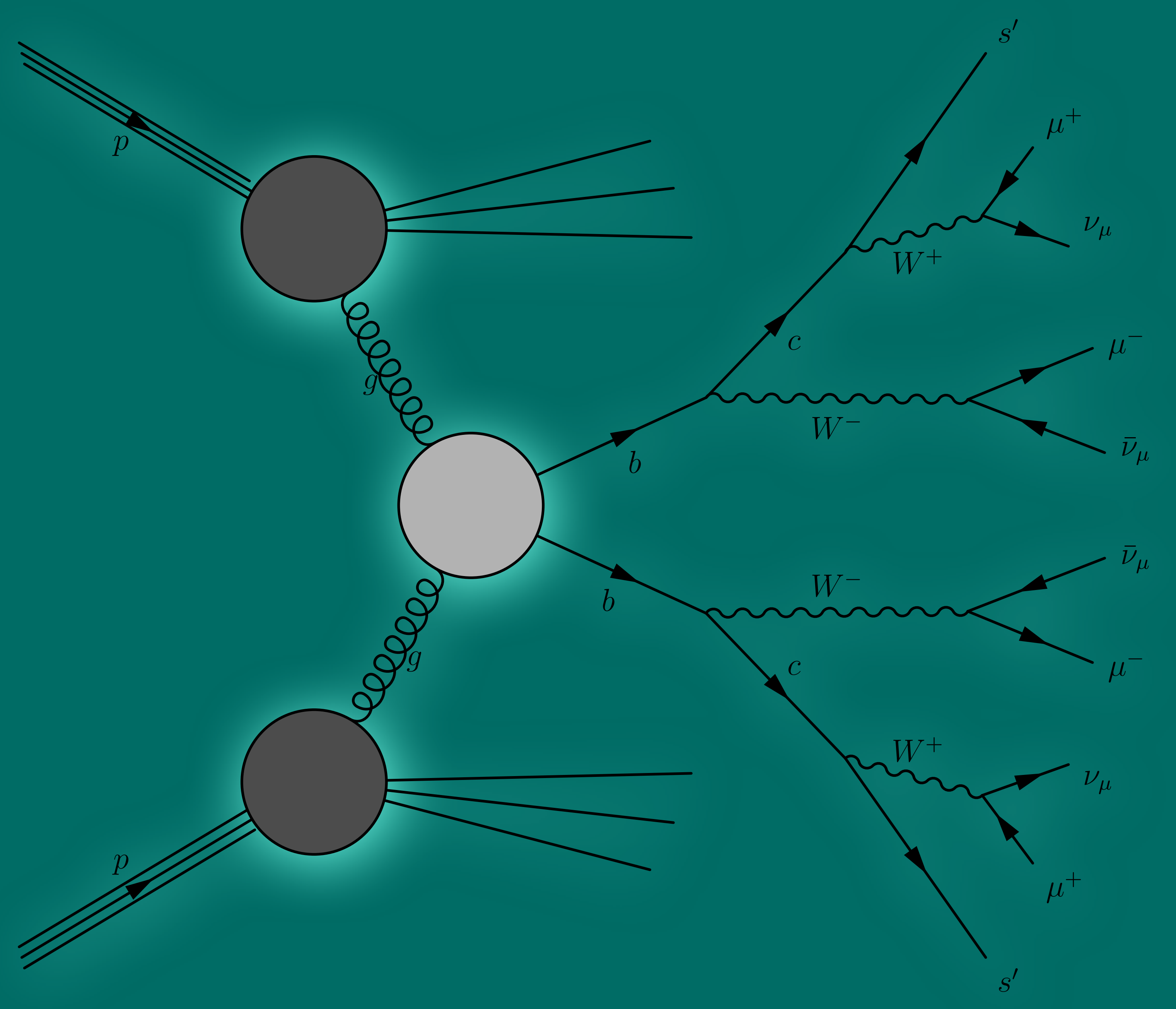

Figure4: Double semi-leptonic $b\bar{b}$ decays

Background Estimation

Below Upsilon (ϒ) Resonances (0.25-9 GeV)

Definition SR and CR: **App. E**

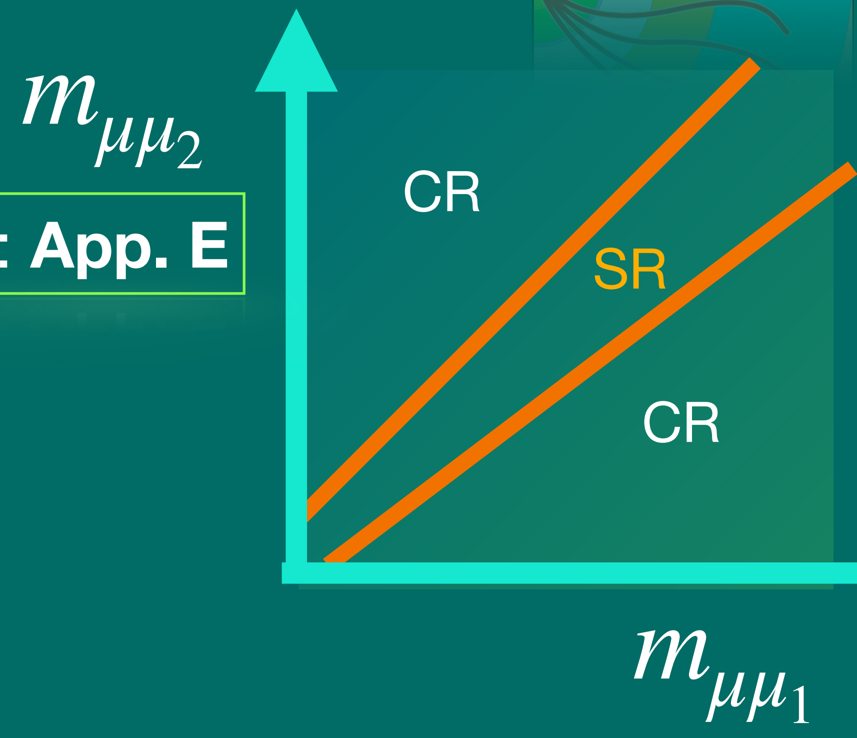

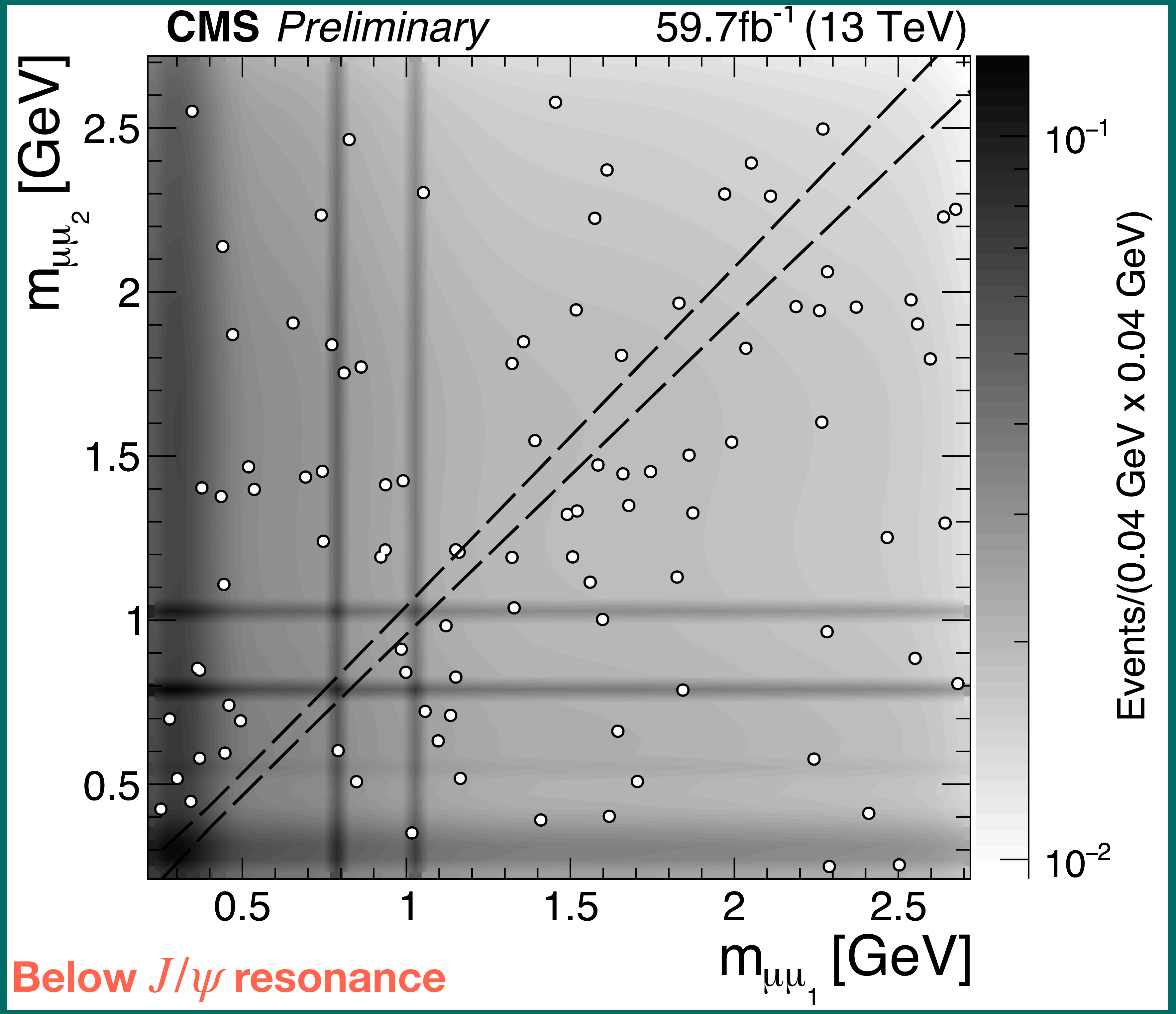

Figure5: 2D QCD background template + data at the CR

- 2D template integral SR/CR = 0.043/0.969
- 2-dimu events at CR: 98 (**SR remain blinded**)
- Estimated BKG events at SR: **4.34 +/- 0.44** (stat.)

Background Estimation

Below Upsilon (ϒ) Resonances (0.25-9 GeV)

Definition SR and CR: **App. E**

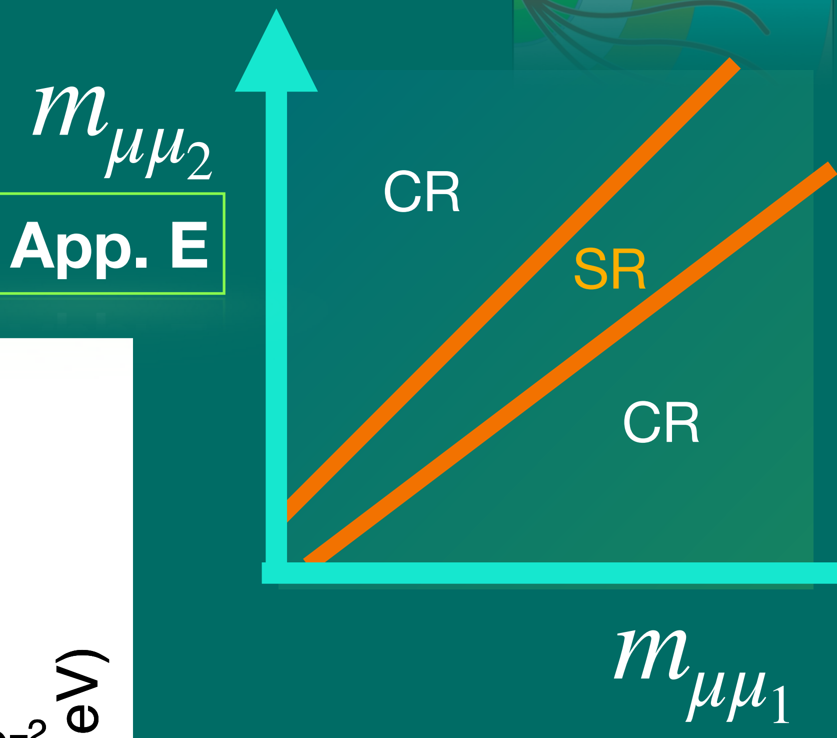

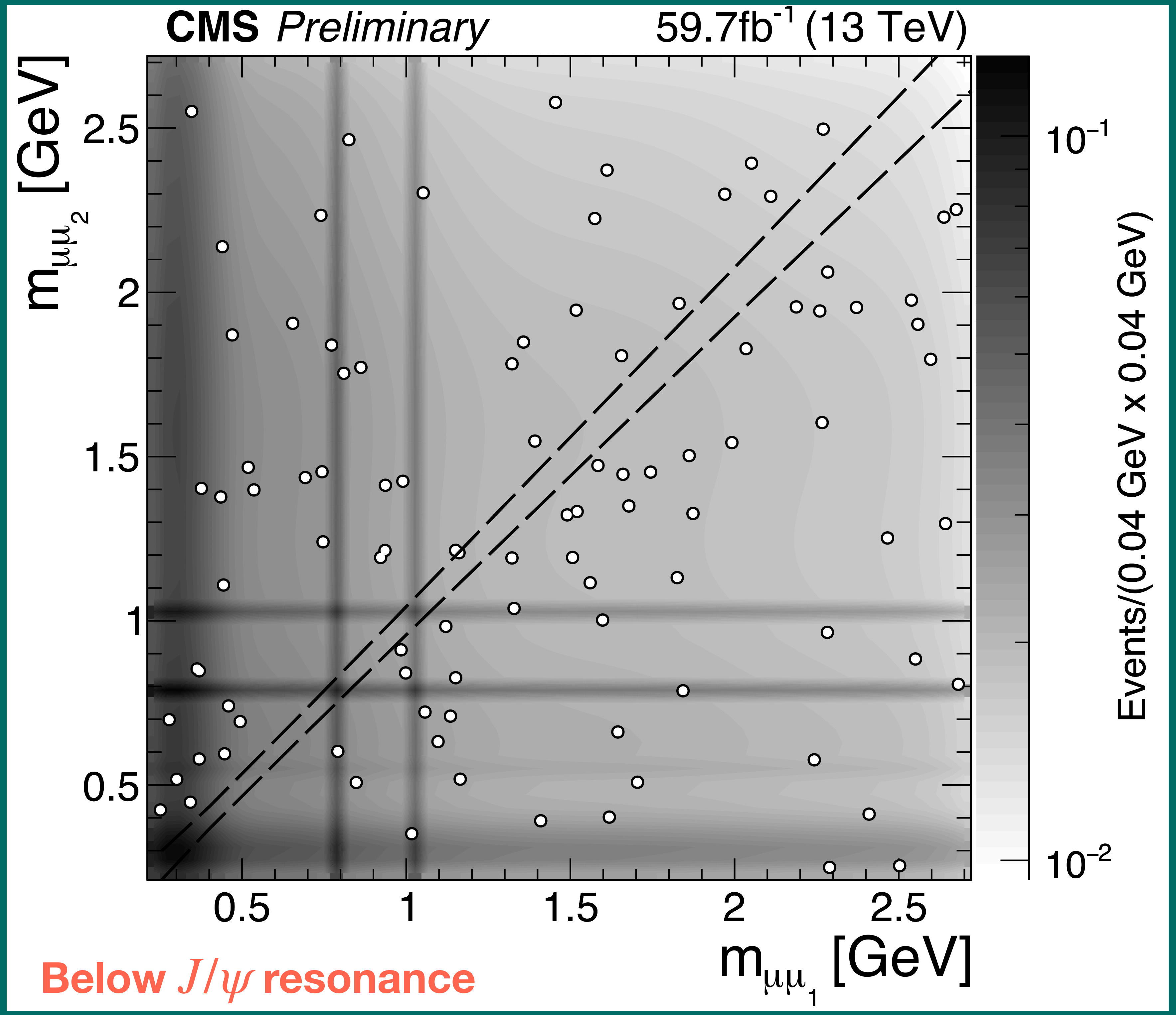

Figure5: 2D QCD background template + data at the CR

- 2D template integral SR/CR = 0.043/0.969
- 2-dimu events at CR: 98 (**SR remain blinded**)
- Estimated BKG events at SR: **4.34 +/- 0.44** (stat.)

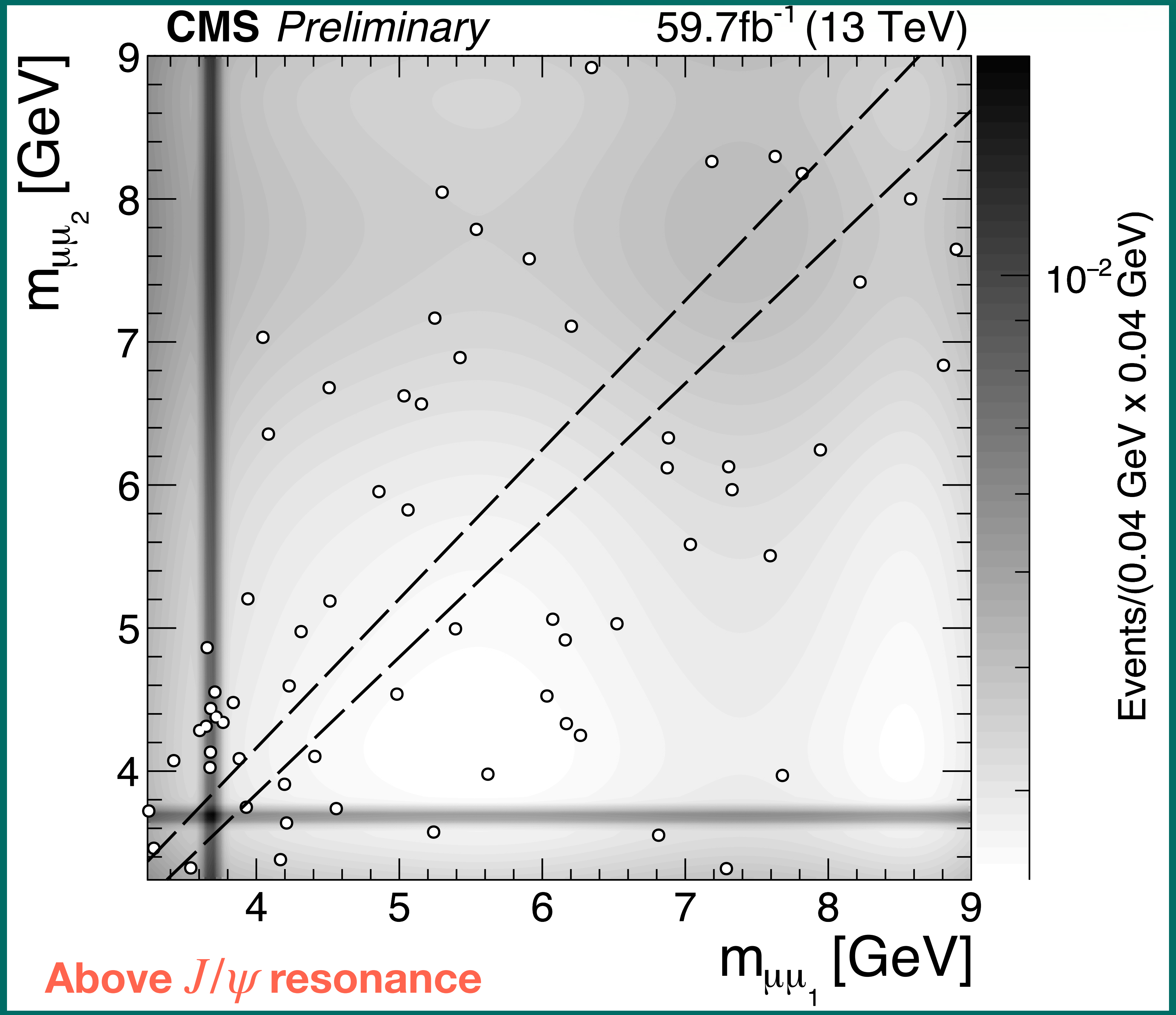

Figure6: 2D QCD background template + data at the CR

- 2D template integral SR/CR = 0.035/0.965
- 2-dimu events at CR: 66 (**SR remain blinded**)
- Estimated BKG events at SR: **6.16 +/- 0.76** (stat.)

Background Estimation

Above Upsilon (ϒ) Resonances (11-60 GeV)

•QED radiated high-energy photons produces muon pairs, each muon is then paired with Drell-Yan (DY) single muons which mimics our di-muon signal

•Reject the events with QED background

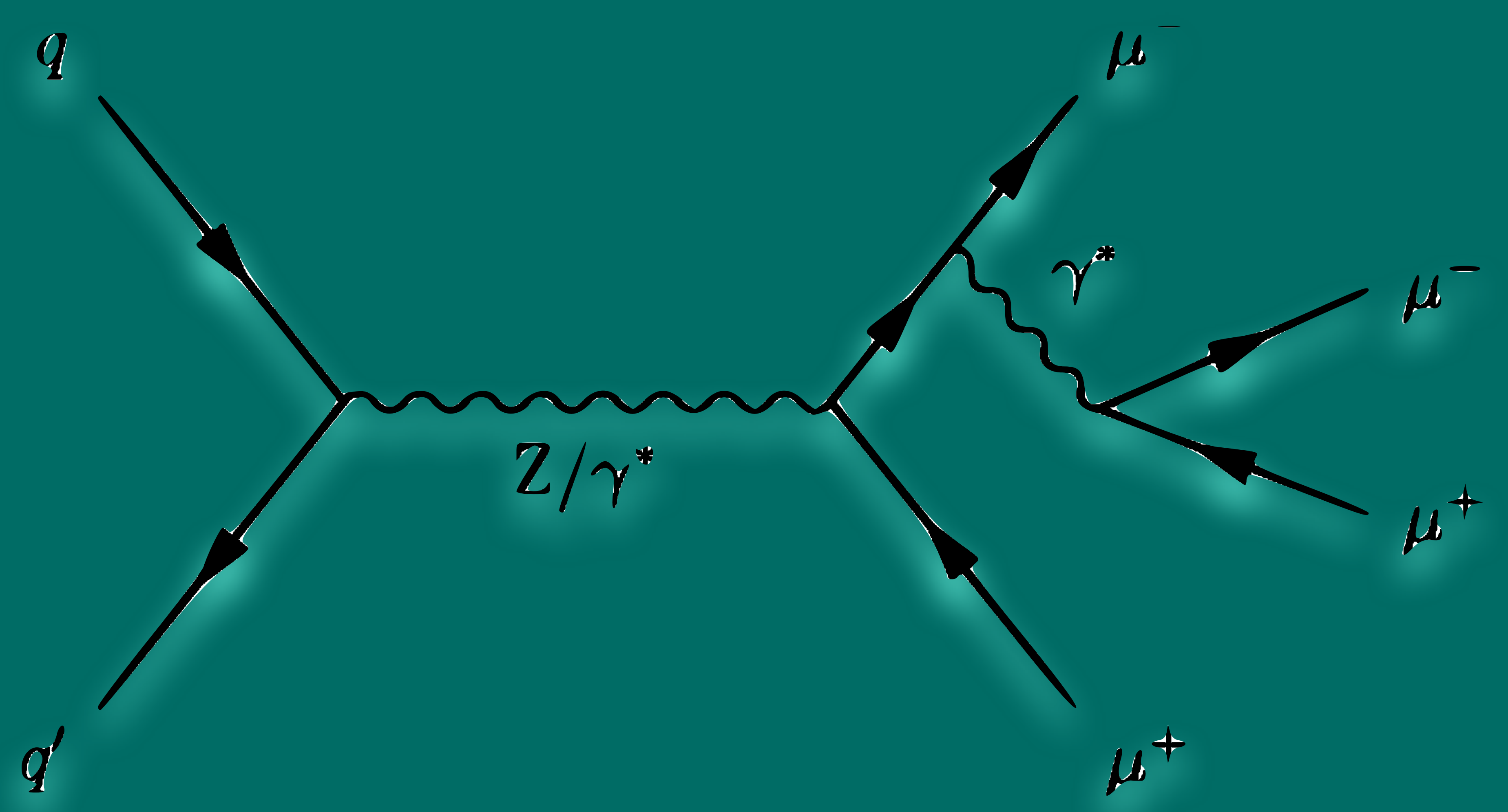

Figure7: The Feynman diagram for QED radiation in DY process. The pairing of the muon decaying in the DY with muon decaying from the QED radiation mimics our signal

Background Estimation

Above Upsilon (ϒ) Resonances (11-60 GeV)

•QED radiated high-energy photons produces muon pairs, each muon is then paired with Drell-Yan (DY) single muons which mimics our di-muon signal

•Reject the events with QED background

•Alternative pairing: pair the QED radiated muon with the DY muon

•Reject the event if:

  - •Alternative pairing trailing mass < 3 GeV
  - •Alternative pairing trailing $\Delta R < 0.2$

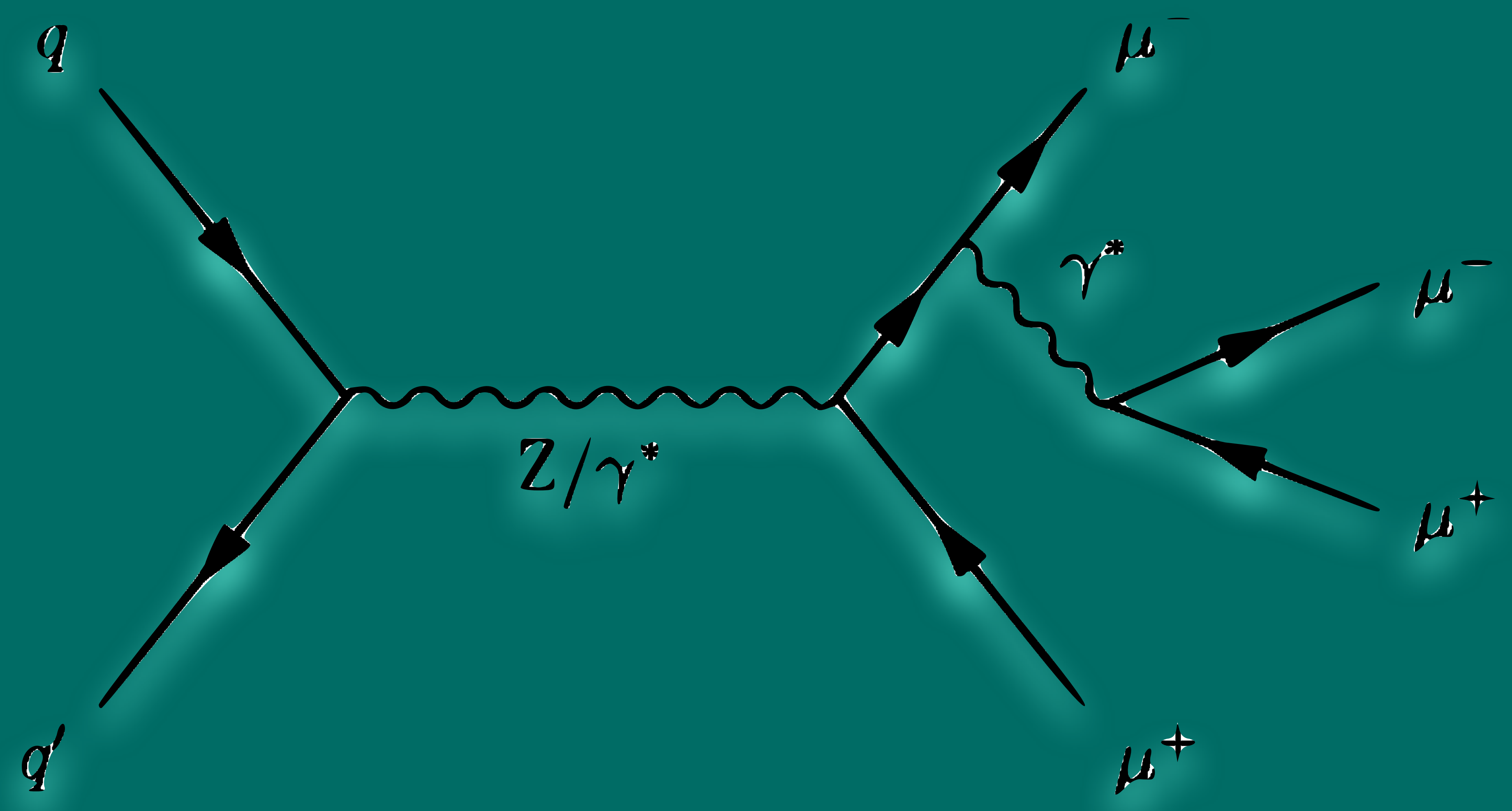

Figure7: The Feynman diagram for QED radiation in DY process. The pairing of the muon decaying in the DY with muon decaying from the QED radiation mimics our signal

Background Estimation

Above Upsilon (ϒ) Resonances (11-60 GeV) - Control Region

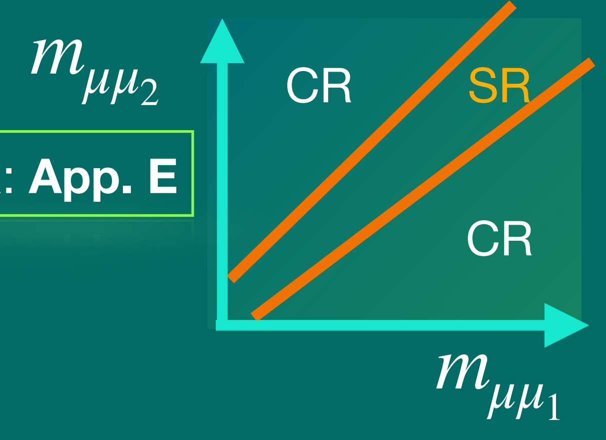

Definition SR and CR: **App. E**

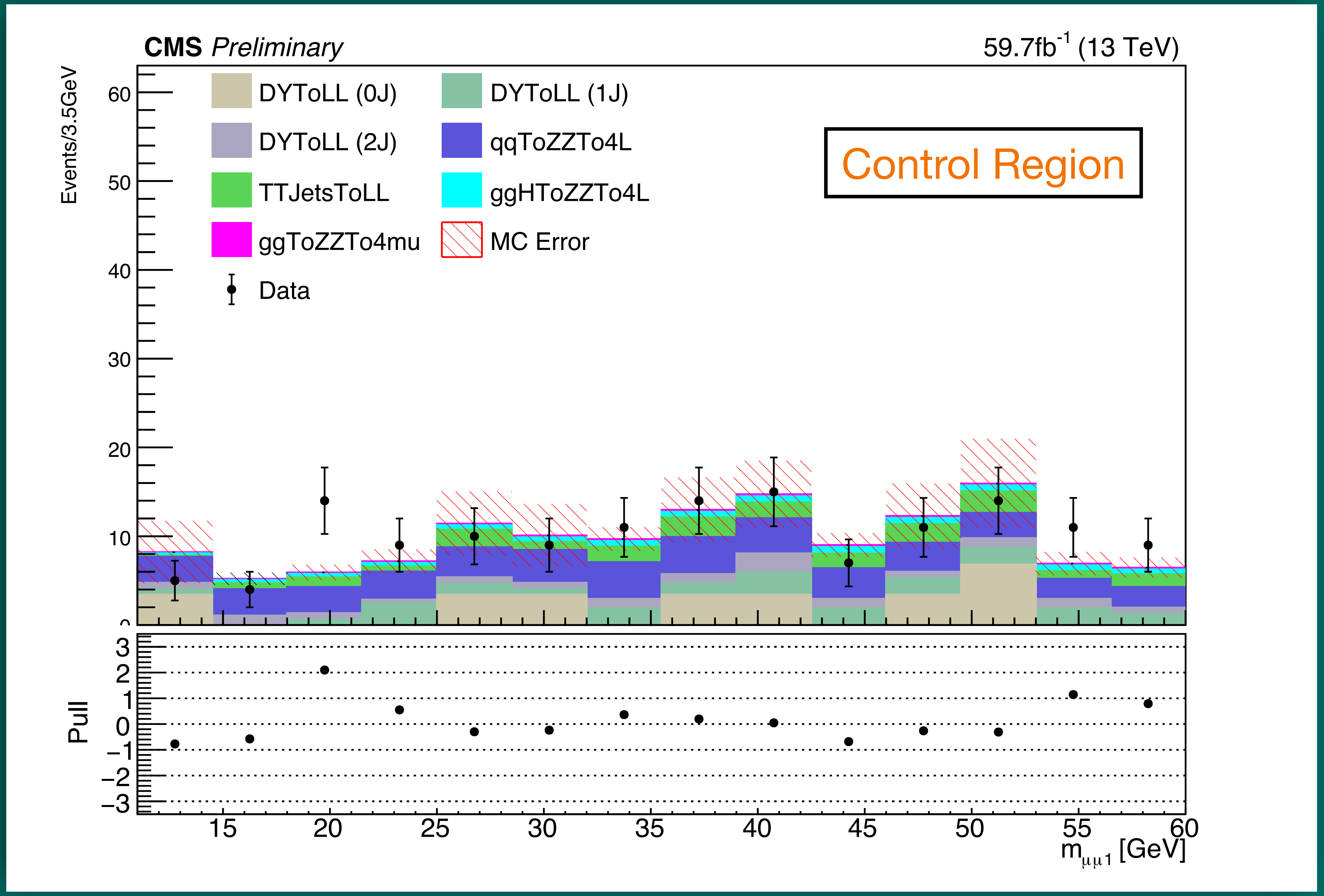

Figure8: MC simulation compared with the data in control region for muon pair 1.

Background Estimation

Above Upsilon (Υ) Resonances (11-60 GeV) - Control Region

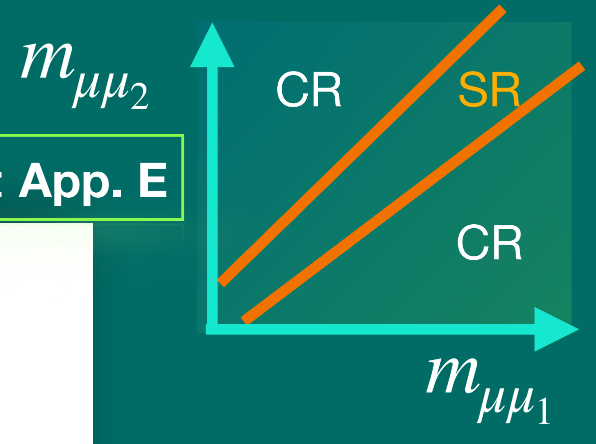

Definition SR and CR: **App. E**

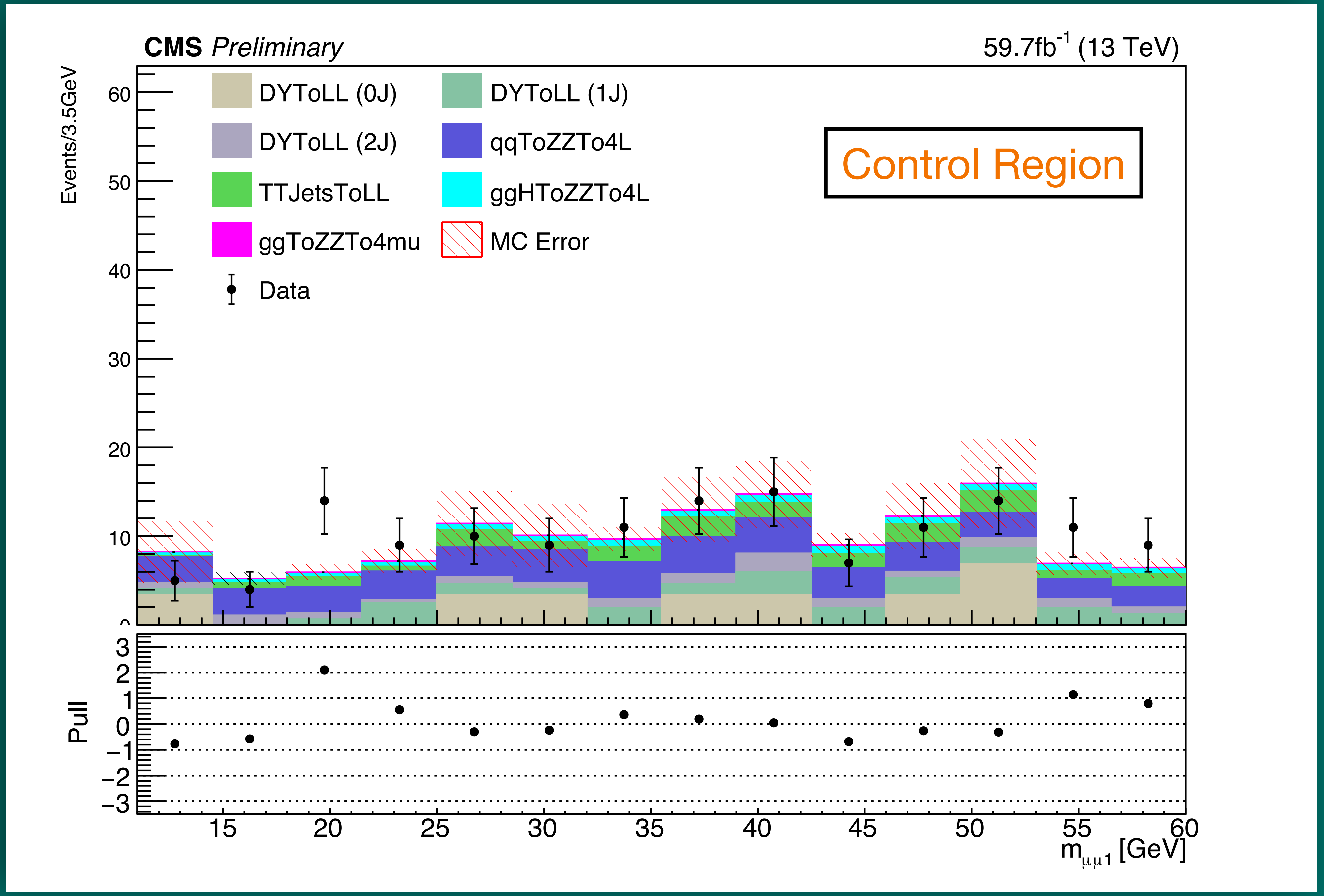

Figure8: MC simulation compared with the data in control region for muon pair 1.

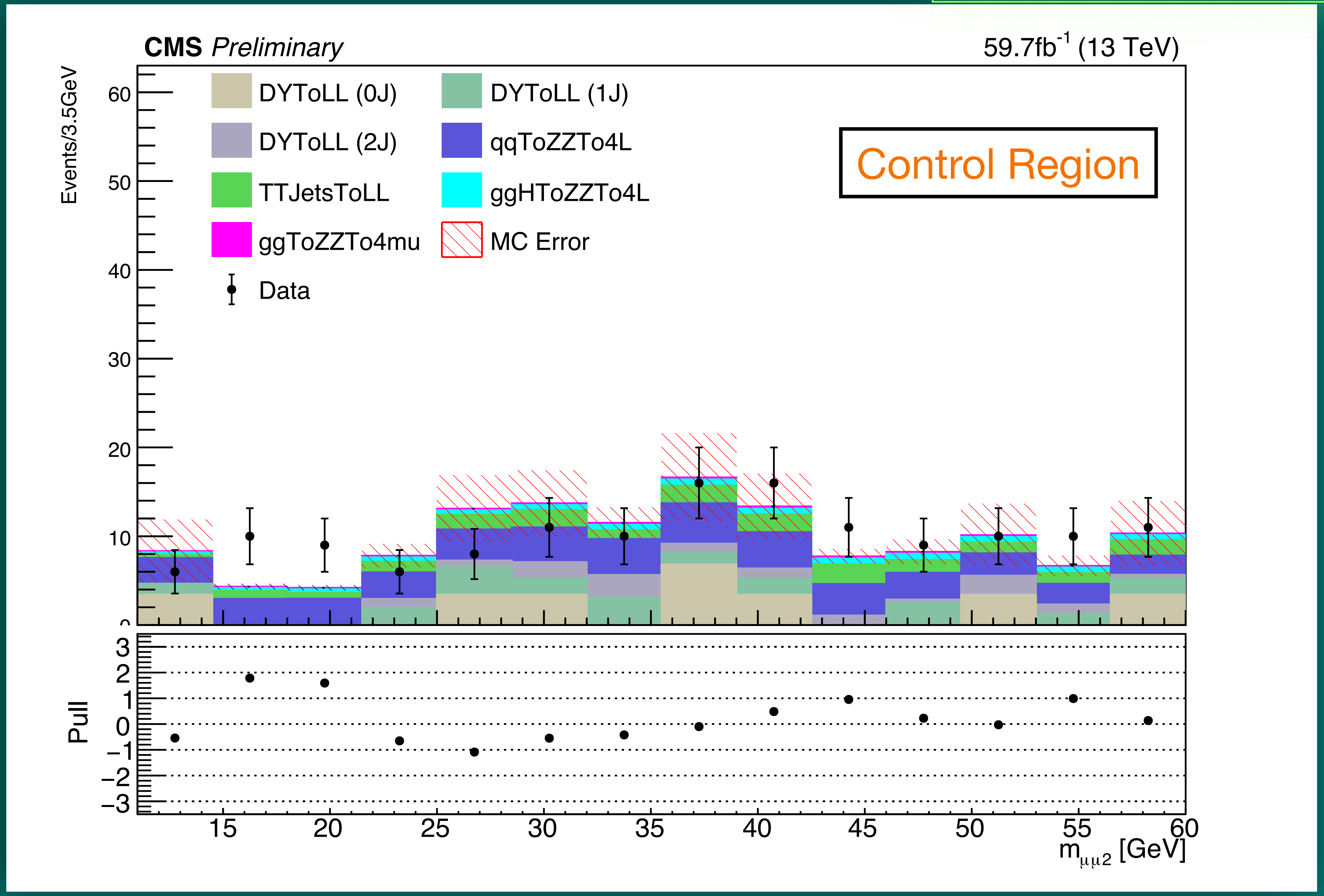

Figure9: MC simulation compared with the data in control region for muon pair 2.

Background Estimation

Above Upsilon (ϒ) Resonances (11-60 GeV) - Control Region

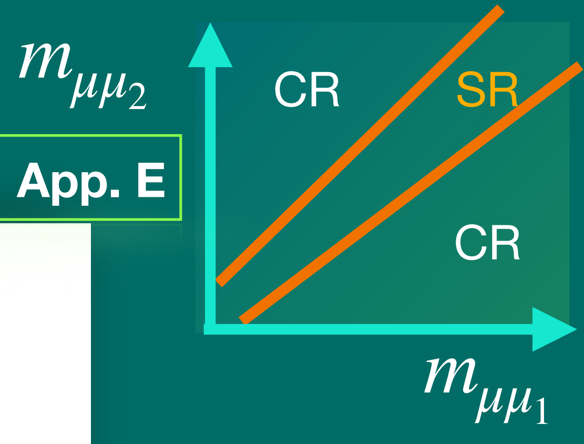

Definition SR and CR: **App. E**

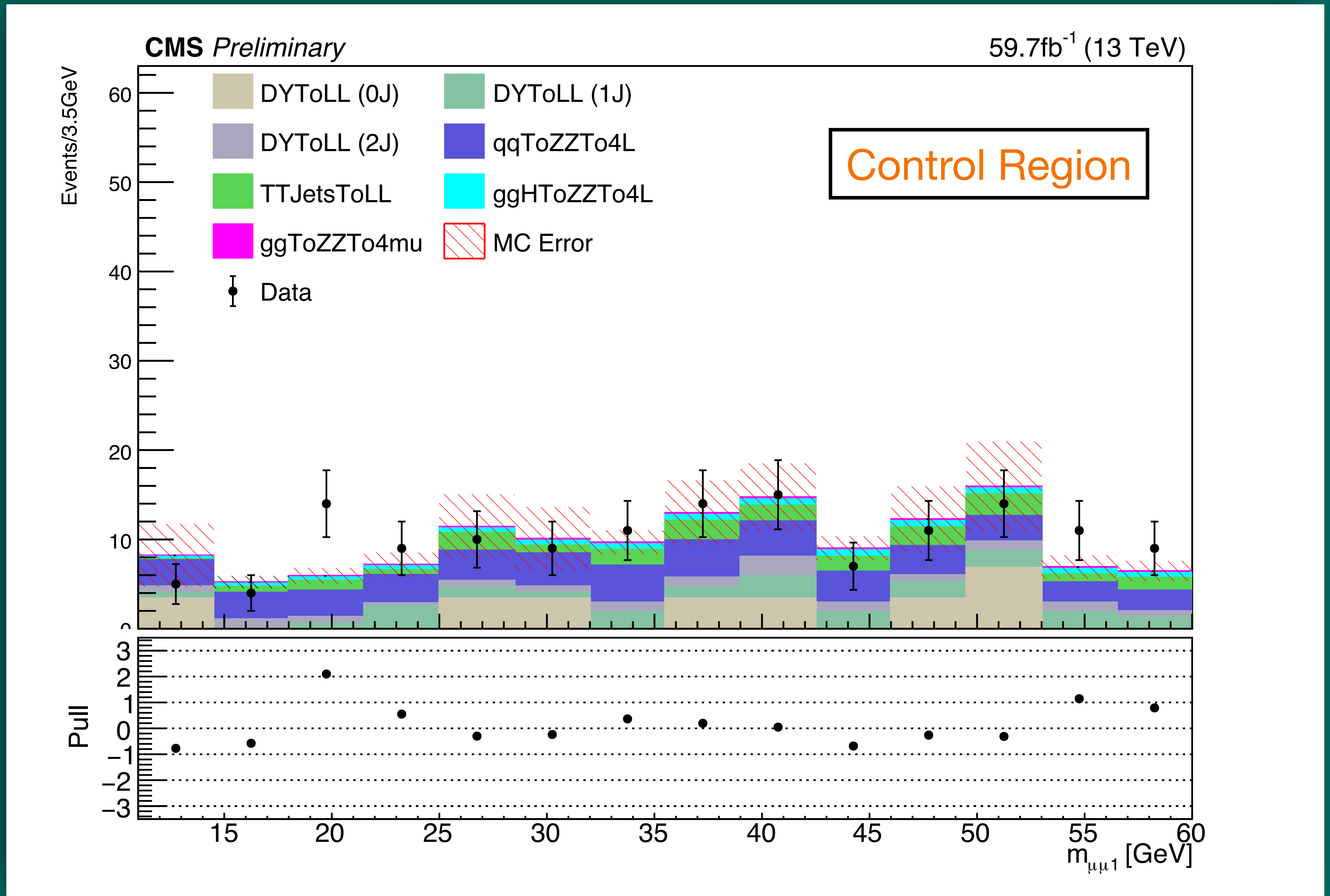

Figure8: MC simulation compared with the data in control region for muon pair 1.

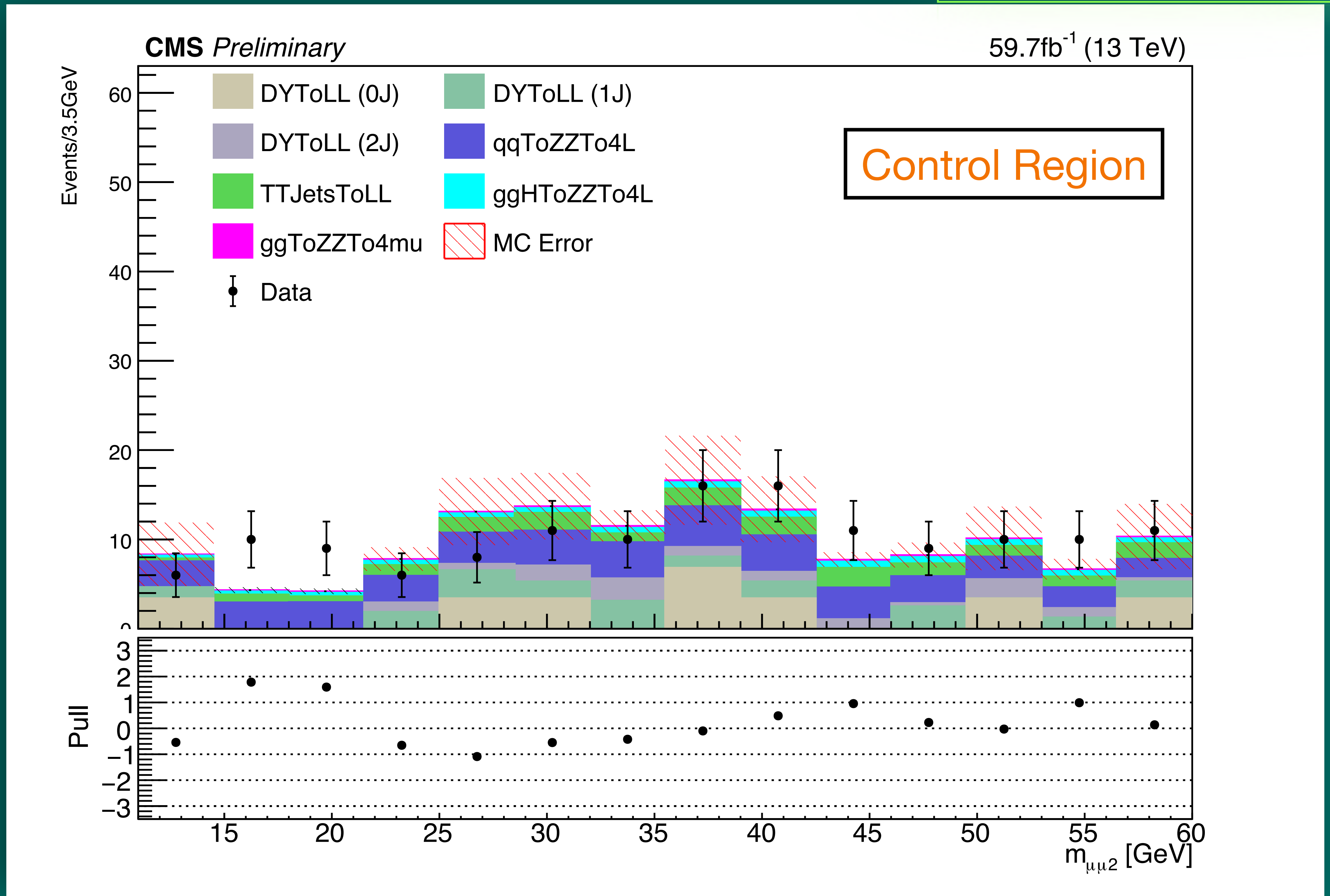

Figure9: MC simulation compared with the data in control region for muon pair 2.

Good agreement between data and MC in control region

$$\frac{data}{MC} = 1.05 \pm 0.12$$

Background Estimation

Above Upsilon (Υ) Resonances (11-60 GeV) - Signal Region

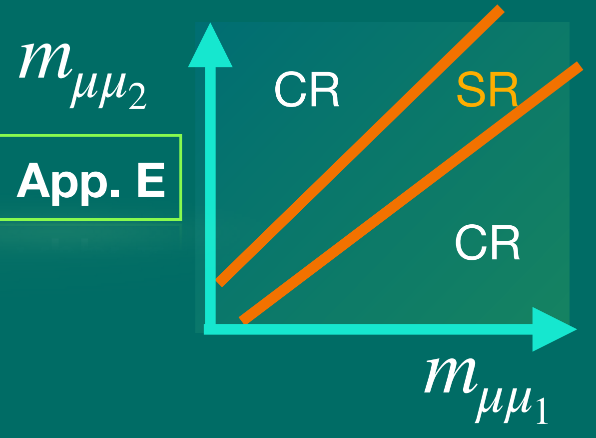

Definition SR and CR: **App. E**

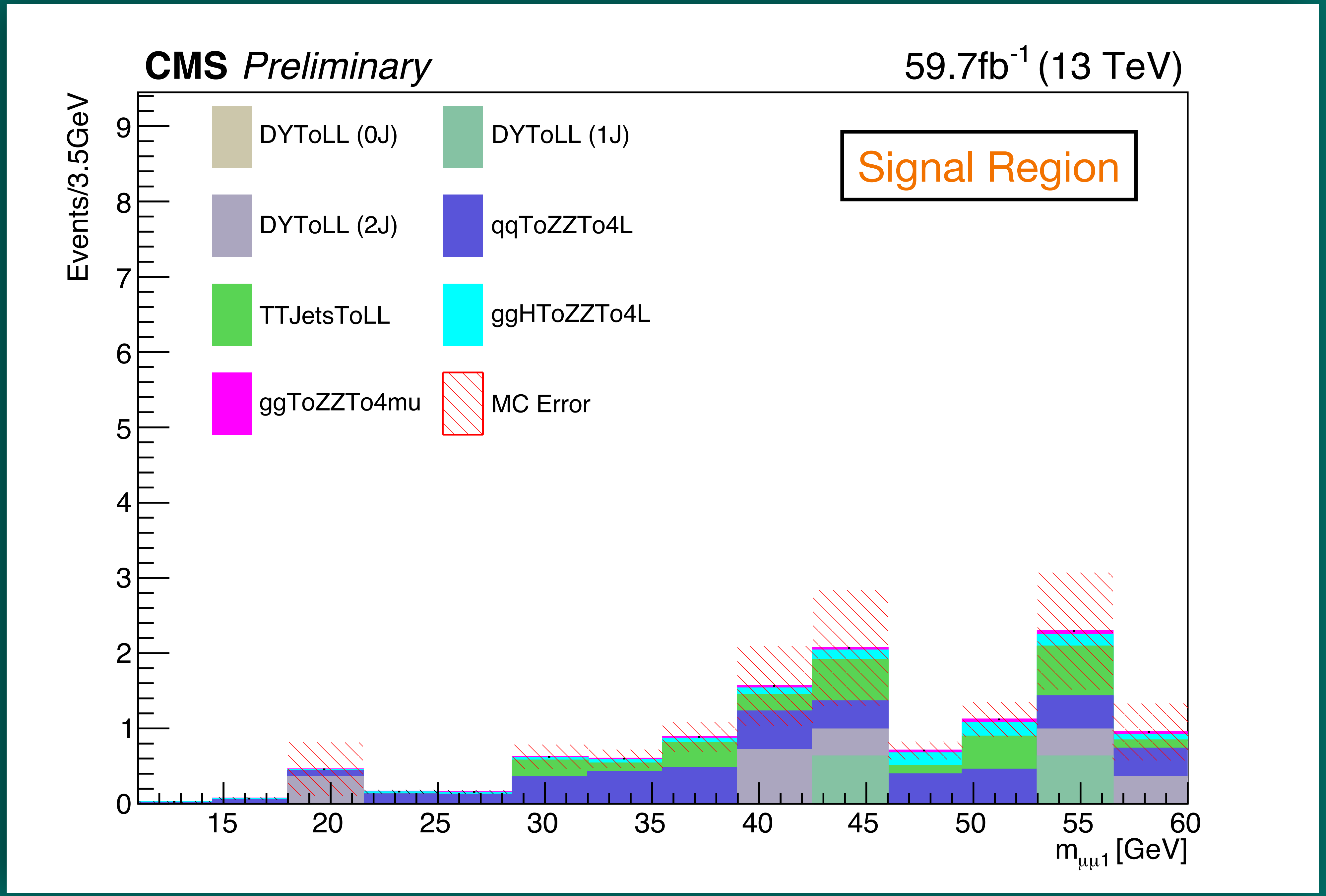

Fig10: MC simulation in signal region for muon pair 1.

Background Estimation

Above Upsilon (ϒ) Resonances (11-60 GeV) - Signal Region

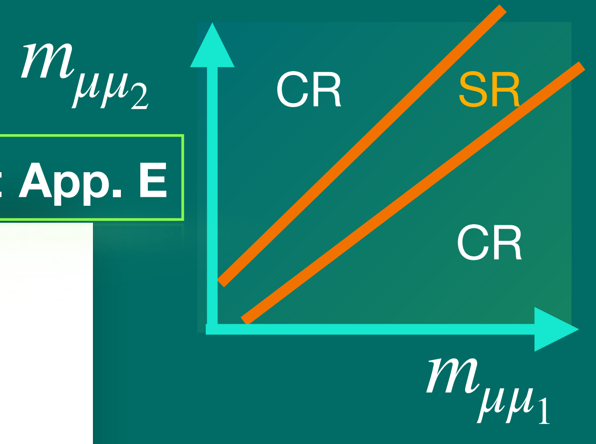

Definition SR and CR: **App. E**

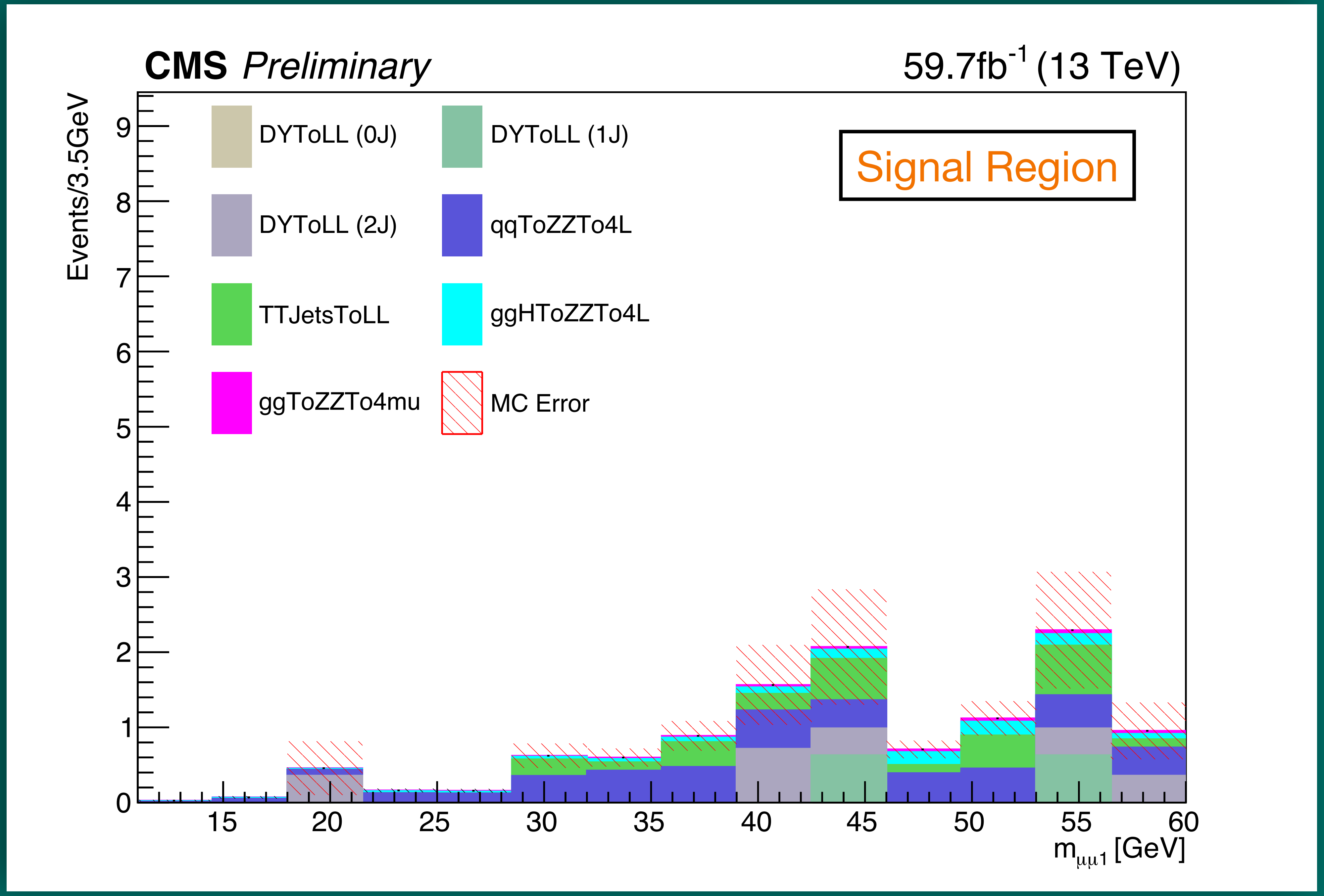

Fig10: MC simulation in signal region for muon pair 1.

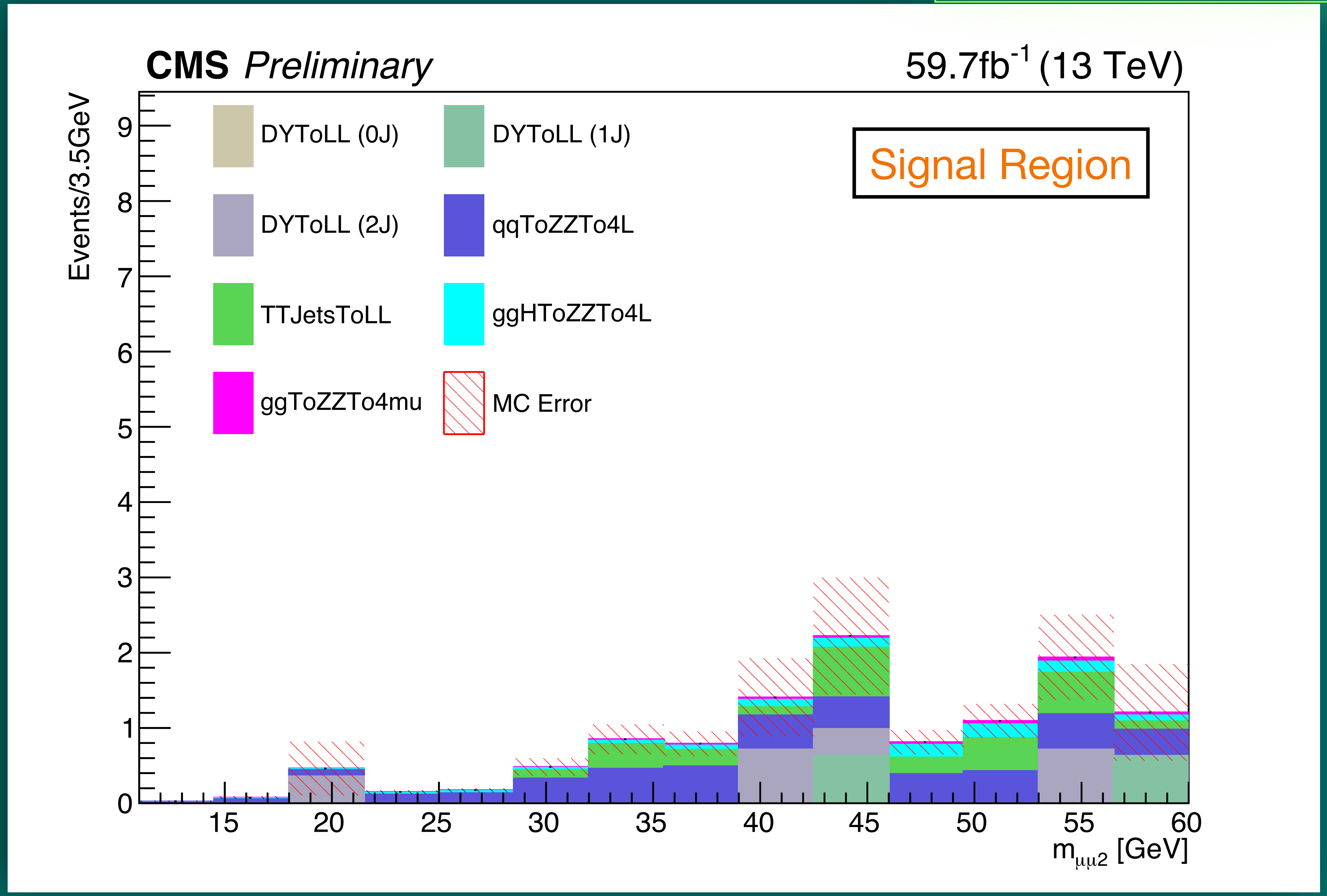

Fig11: MC simulation in signal region for muon pair 2.

Background Estimation

Above Upsilon (ϒ) Resonances (11-60 GeV) - Signal Region

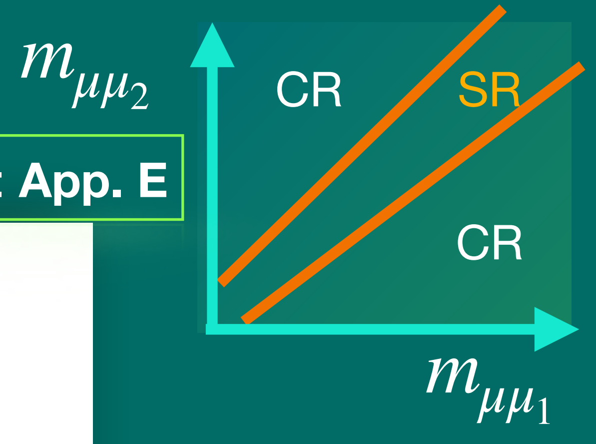

Definition SR and CR: **App. E**

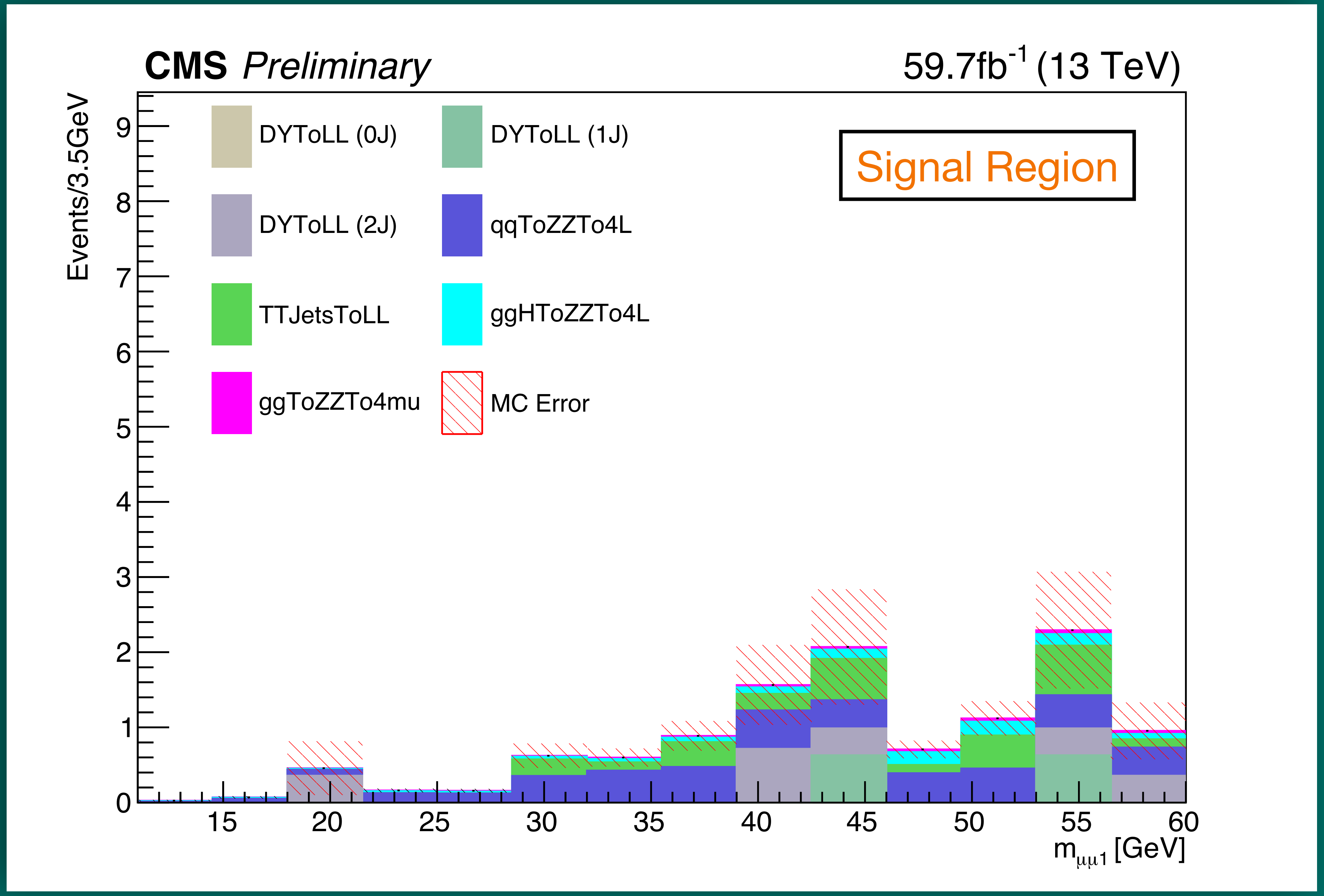

Fig10: MC simulation in signal region for muon pair 1.

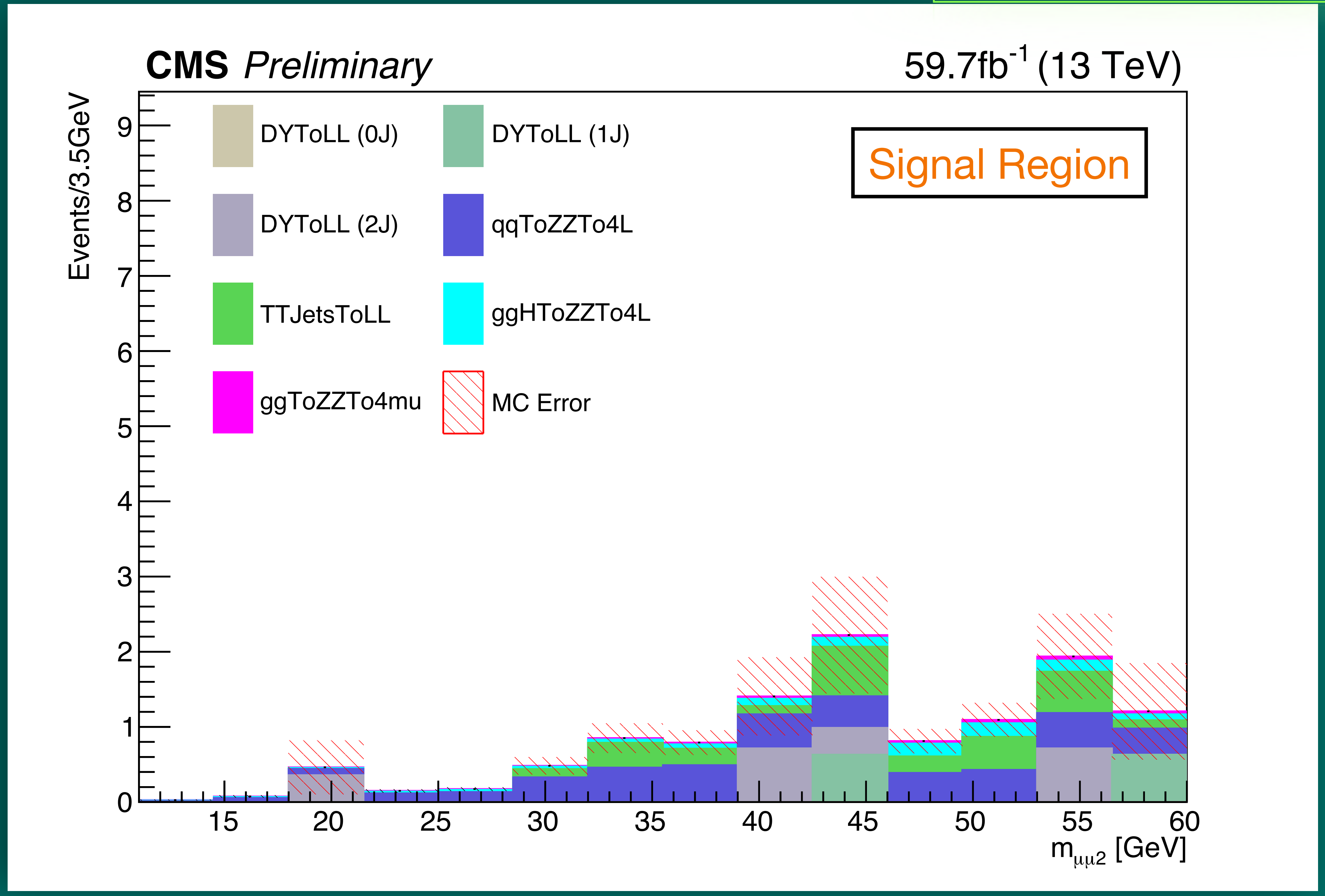

Fig11: MC simulation in signal region for muon pair 2.

Smooth background shape in the SR is obtained via adaptive Kernel Density Estimation (KDE). See **App. C**

Estimated number of background events in the SR

$$SR : 12.28 \pm 2.01$$

Expected Limits

Expected Limit on Kinetic Mixing parameter

- Close to zero background analysis: expected 95% CL upper limit is ~3 events at each mass point

  - $\sigma(pp \to Z_D)\mathscr{B}(Z_D \to s_D\overline{s_D})\mathscr{B}^2(s_D \to \mu^+\mu^-) \times \alpha_{gen} \leq \frac{N_{\mu\mu}}{L \times r}$
  - $N_{\mu\mu}$: 95% CL upper limit on the number of events
  - $\mathscr{L} = 59.7\ fb^{-1},\ r = SF_{\epsilon_{Full}} \times \epsilon^{MC}_{Full}/\alpha_{Gen}$ HLT SF calculation: **App.F**

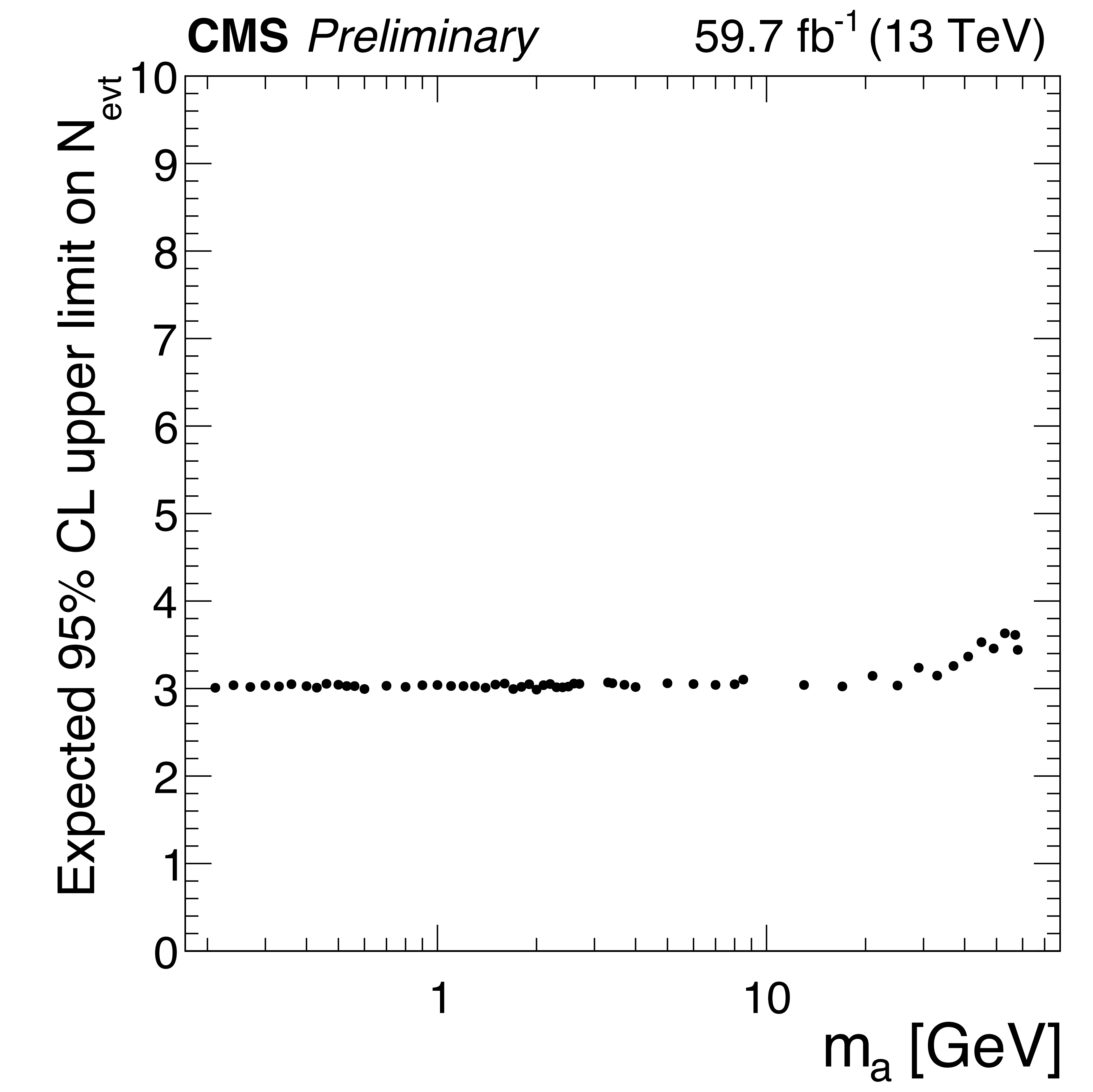

Figure12A: 95% upper limit on expected number of events

Expected Limits

Expected Limit on Kinetic Mixing parameter

- Close to zero background analysis: expected 95% CL upper limit is ~3 events at each mass point

  - $\sigma(pp \rightarrow Z_D)\mathscr{B}(Z_D \rightarrow s_D\overline{s_D})\mathscr{B}^2(s_D \rightarrow \mu^+\mu^-) \times \alpha_{gen} \leq \frac{N_{\mu\mu}}{L \times r}$
  - $N_{\mu\mu}$: 95% CL upper limit on the number of events
  - $\mathscr{L} = 59.7\ fb^{-1},\ r = SF_{\epsilon_{Full}} \times \epsilon^{MC}_{Full}/\alpha_{Gen}$ HLT SF calculation: **App.F**

- By translating the production cross-section to ϵ^2, we set 95% CL limit on

$$\epsilon^2\mathscr{B}(Z_D \rightarrow s_D\overline{s_D})\mathscr{B}^2(s_D \rightarrow \mu^+\mu^-)$$

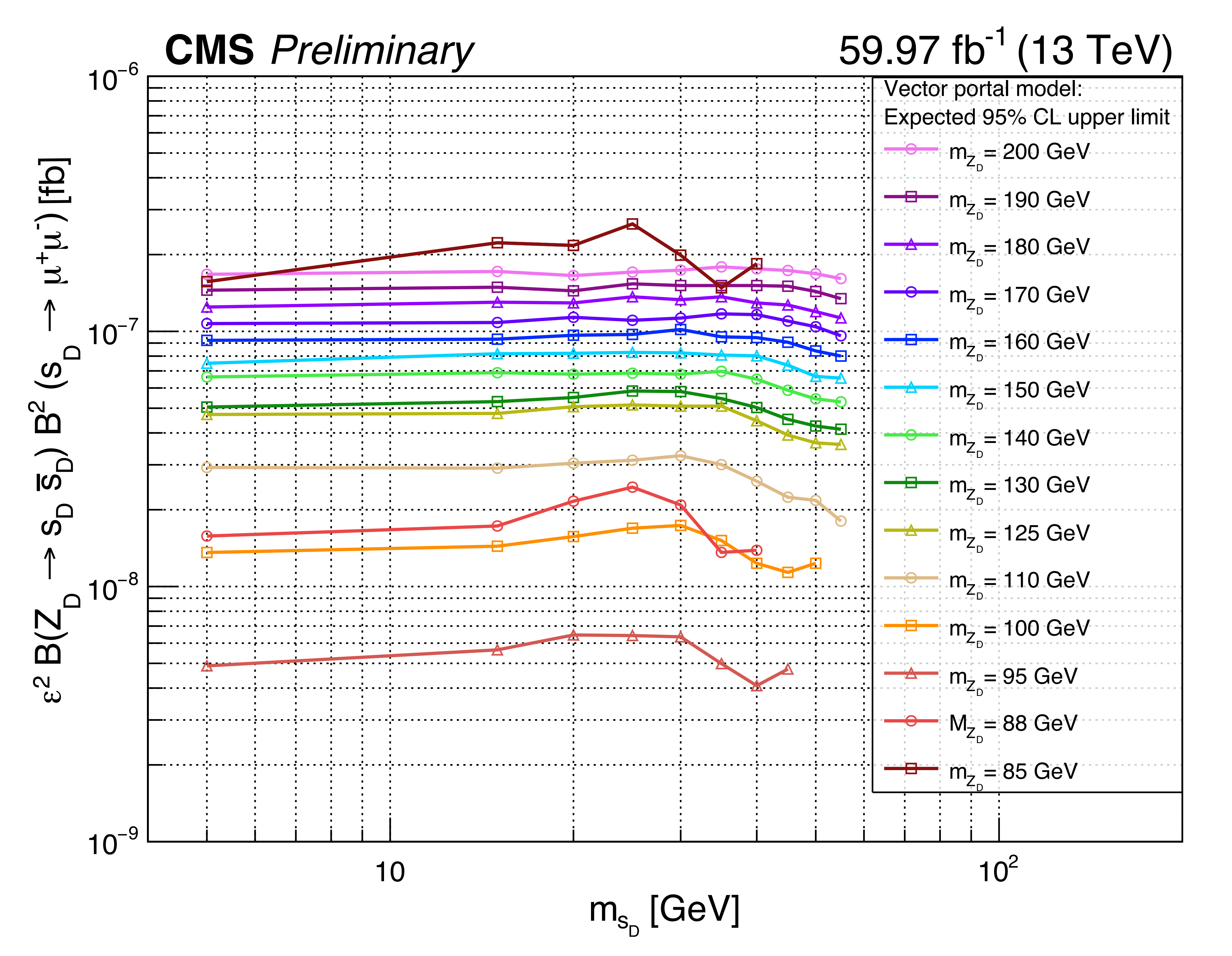

Figure12B: The expected 95% CL upper limits function of the dark scalar mass m_{s_D} and the dark vector boson mass m_{Z_D}

Expected Limits

Expected Limit on Kinetic Mixing parameter

- Close to zero background analysis: expected 95% CL upper limit is ~3 events at each mass point

  - $\sigma(pp \to Z_D)\mathscr{B}(Z_D \to s_D\overline{s_D})\mathscr{B}^2(s_D \to \mu^+\mu^-) \times \alpha_{gen} \leq \frac{N_{\mu\mu}}{L \times r}$
  - $N_{\mu\mu}$: 95% CL upper limit on the number of events
  - $\mathscr{L} = 59.7\ fb^{-1},\ r = SF_{\epsilon_{Full}} \times \epsilon_{Full}^{MC}/\alpha_{Gen}$ HLT SF calculation: **App.F**

- By translating the production cross-section to ϵ^2, we set 95% CL limit on

$$\epsilon^2\mathscr{B}(Z_D \to s_D\overline{s_D})\mathscr{B}^2(s_D \to \mu^+\mu^-)$$

- The limit curves exhibit a structure with an increase and a dip as the s_D mass approaches the kinematic limit of $m_{Z_D}/2$.

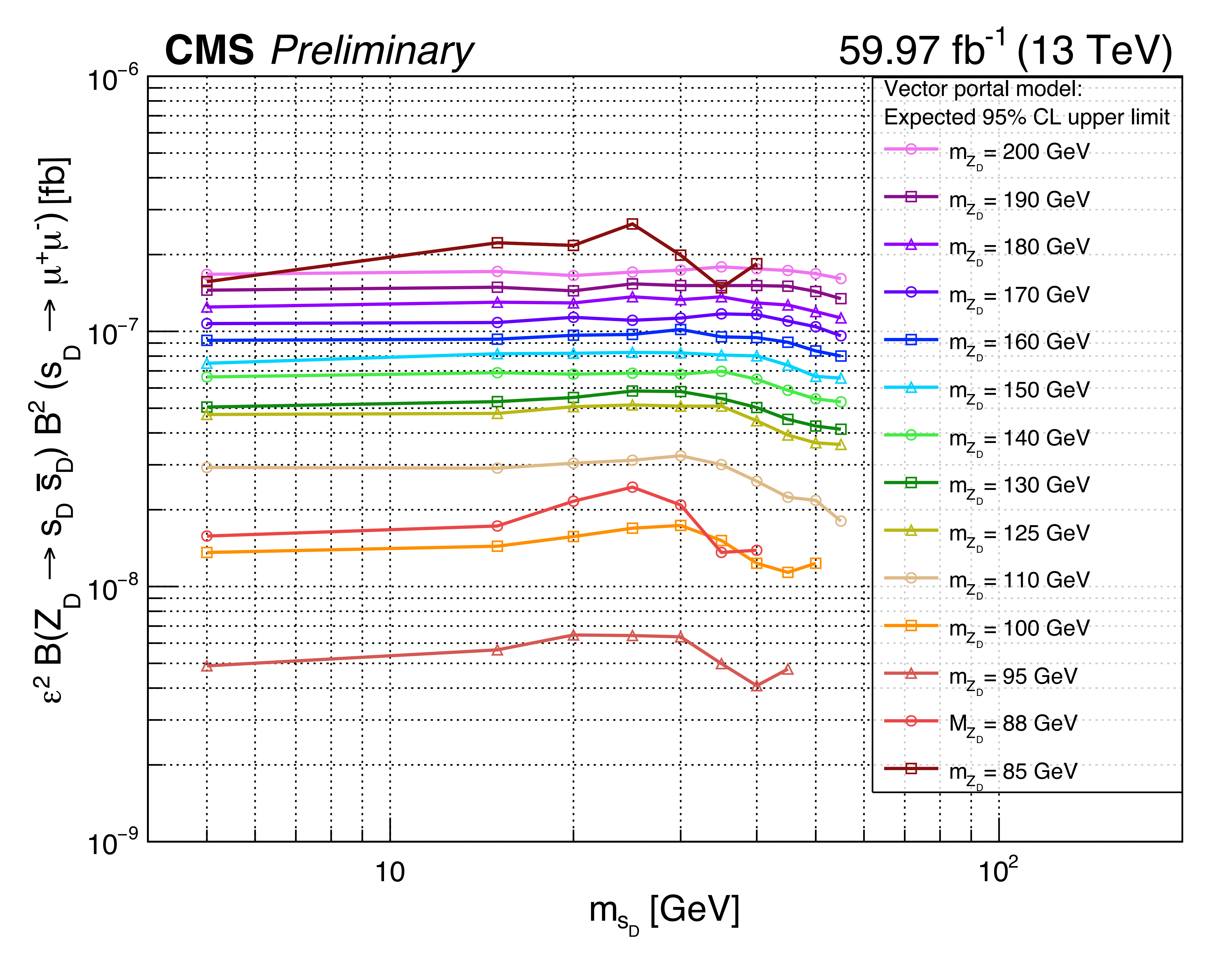

Figure12B: The expected 95% CL upper limits function of the dark scalar mass m_{s_D} and the dark vector boson mass m_{Z_D}

Unblinding The Signal Region

Below Below Upsilon (Υ) Background

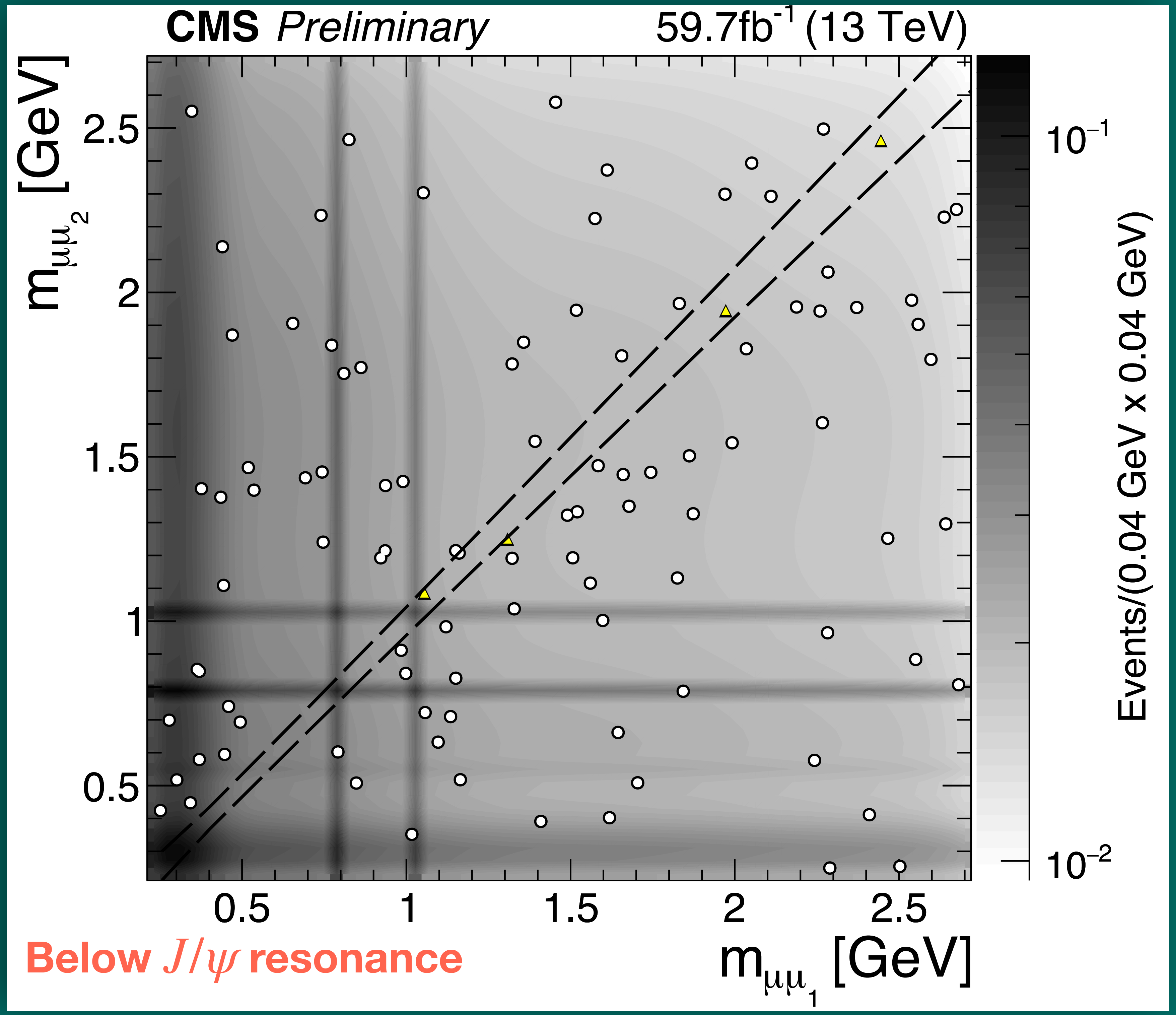

Figure13: 2D QCD background at SR

- Estimated Background events at SR:
  $4.34 \pm 0.44(stat.) \pm 0.18(sys.)$
- Observed: 4 events

Unblinding The Signal Region

Below Below Upsilon (Υ) Background

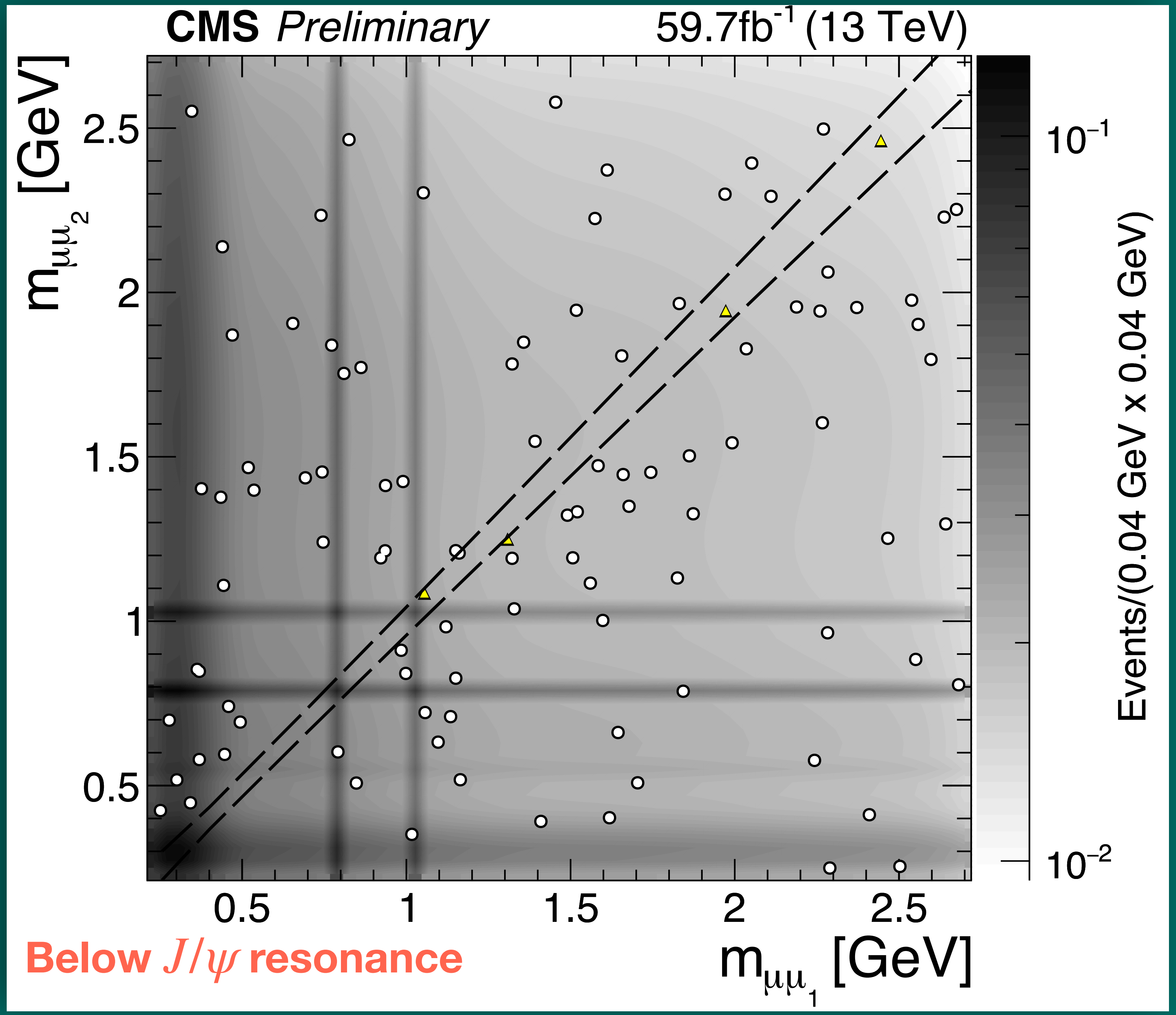

Figure13: 2D QCD background at SR

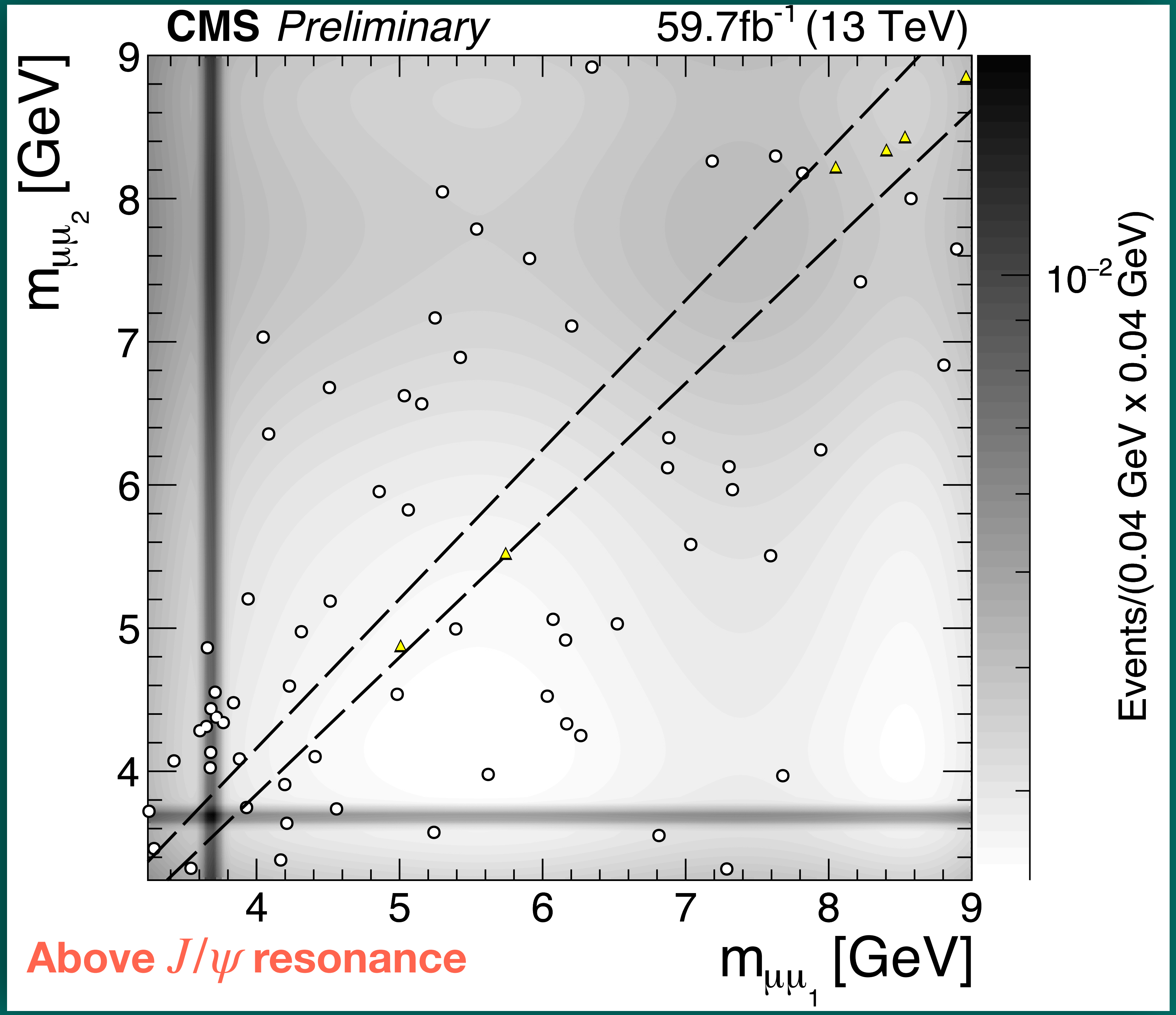

Figure14: 2D QCD background at SR

- Estimated Background events at SR: $4.34 \pm 0.44(stat.) \pm 0.18(sys.)$
- Observed: 4 events

- Estimated Background events at SR: $6.16 \pm 0.76(stat.) \pm 0.09(sys.)$
- Observed: 6 events

Unblinding The Signal Region

Above Upsilon (ϒ) Background

Definition SR and CR: **App. E**

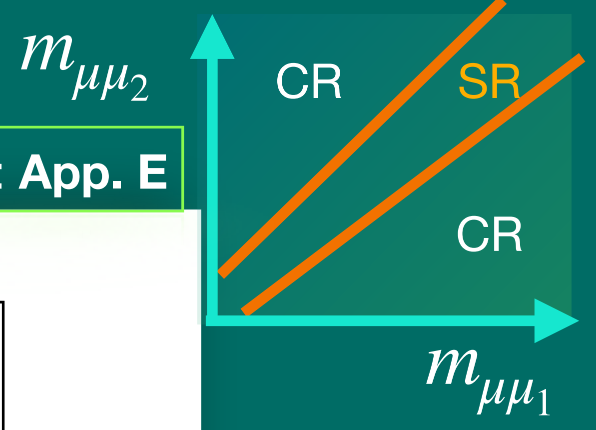

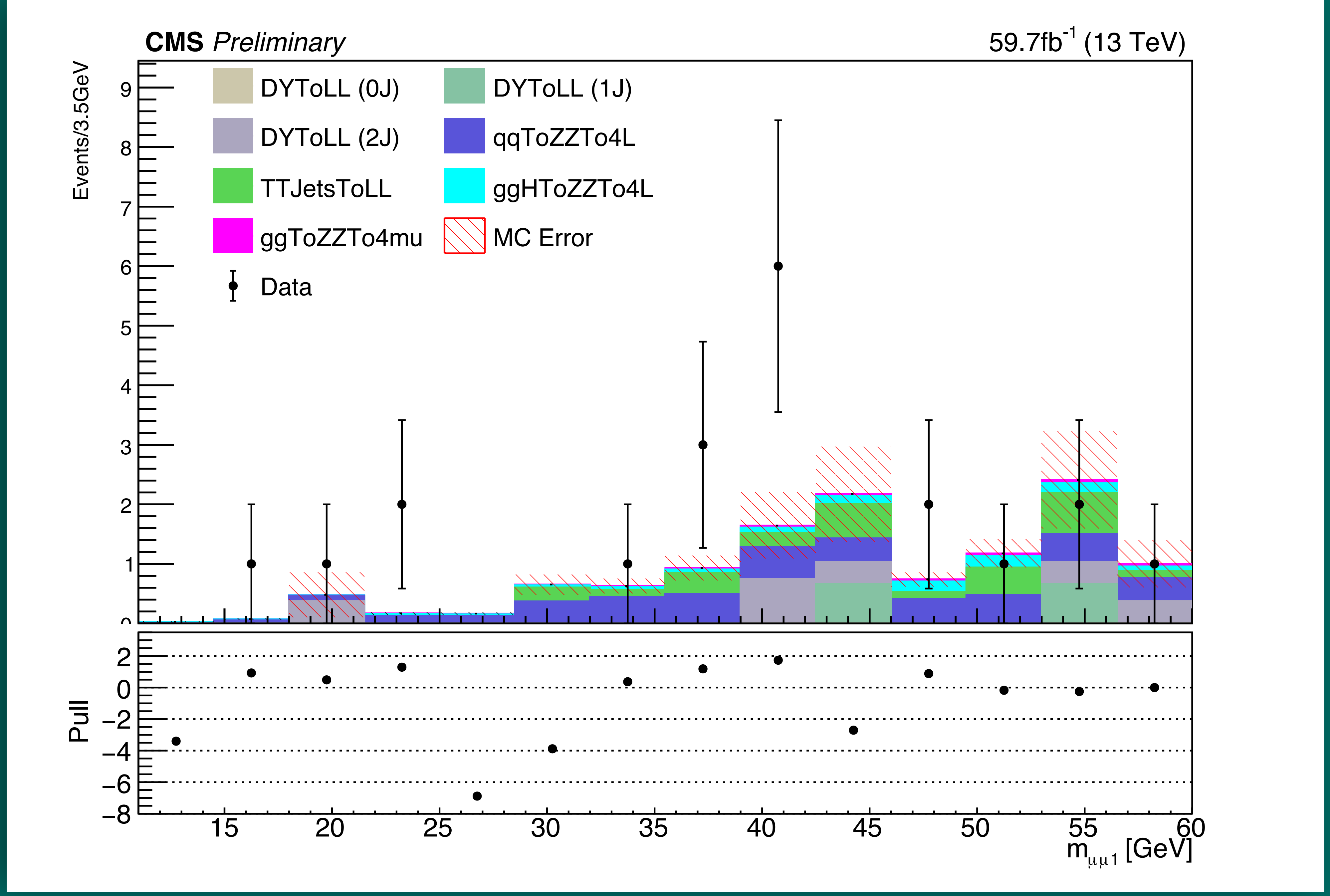

Figure15: MC simulation compared with observed data at SR

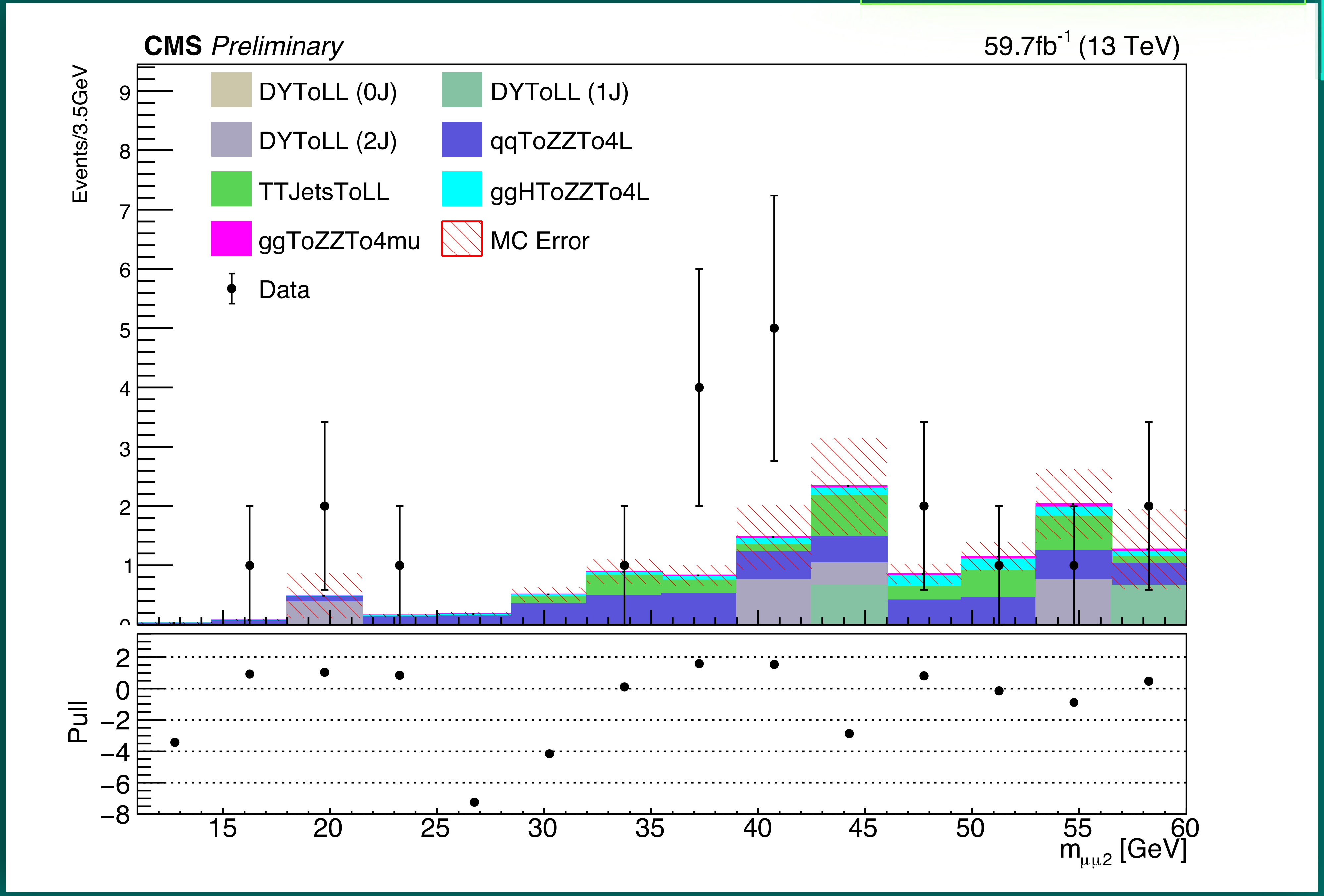

Figure16: MC simulation compared with observed data at SR

Estimated number of background events in the SR

$SR : 12.28 \pm 2.01$

Observed: 20 events

FLORIDA TECH

Unblinding The Signal Region

Below Below Upsilon (ϒ) Background

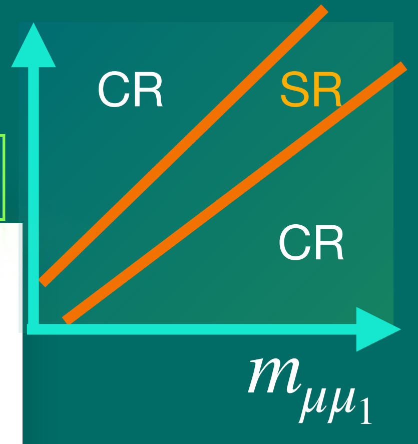

Definition SR and CR: **App. E**

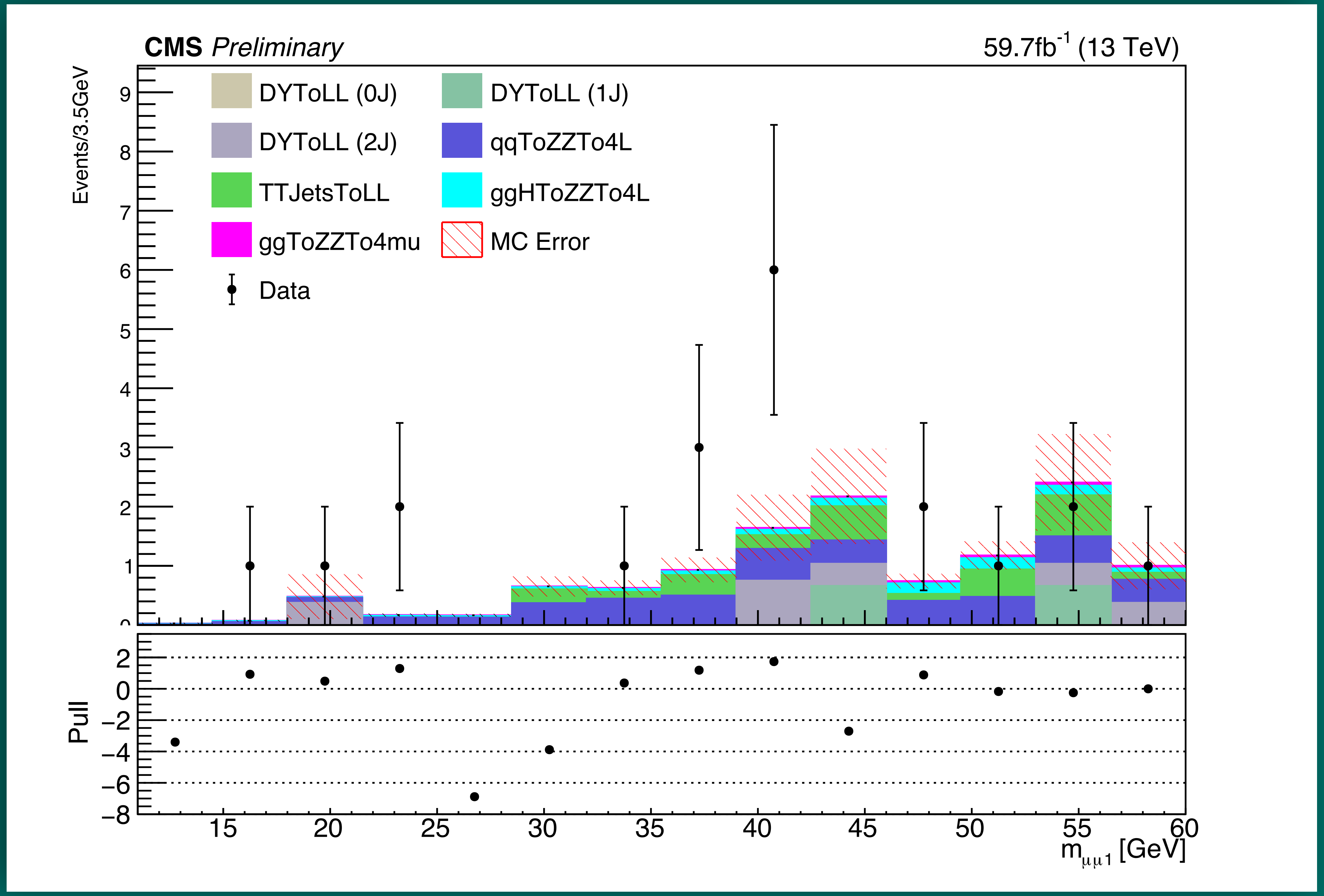

Figure15: MC simulation compared with observed data at SR

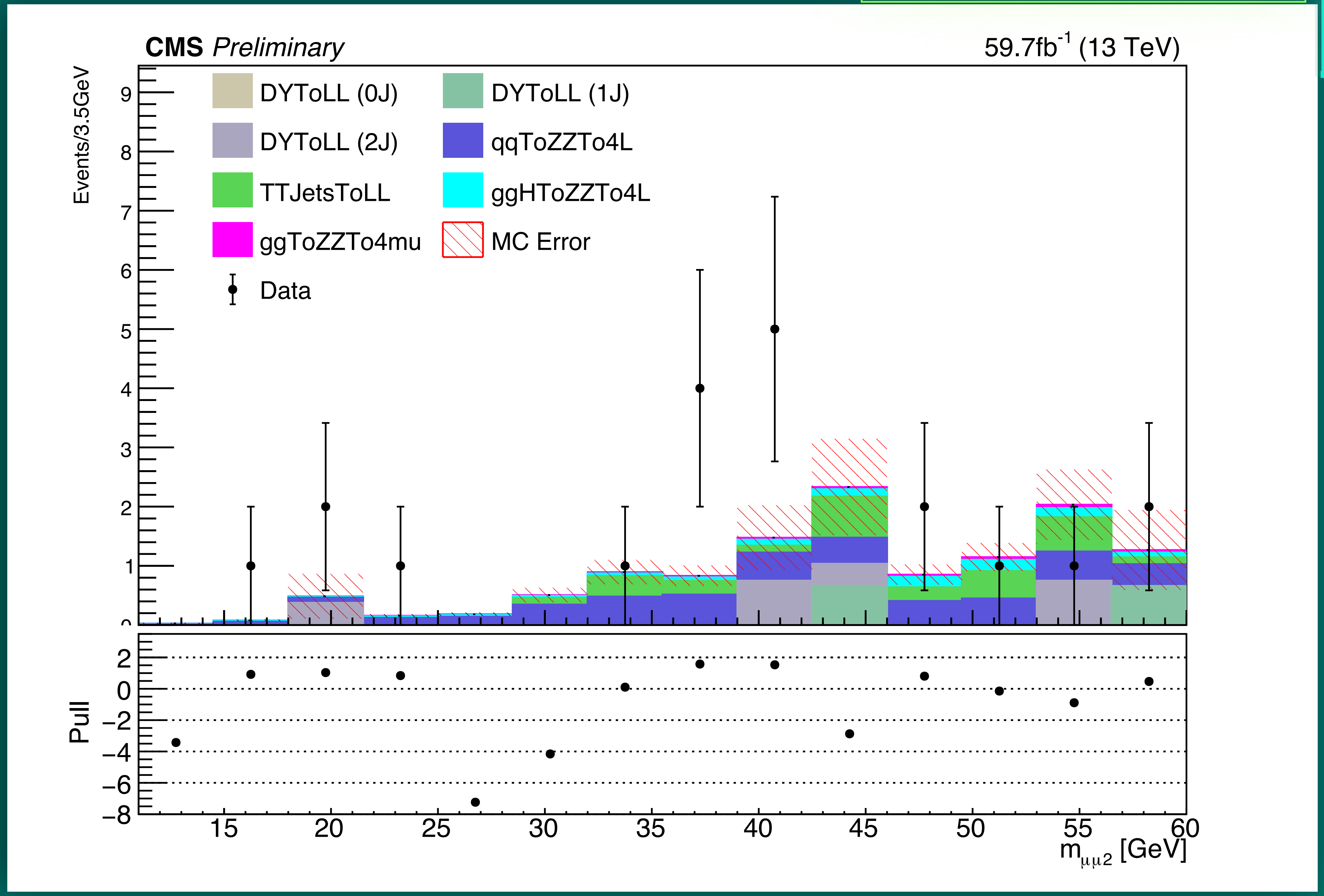

Figure16: MC simulation compared with observed data at SR

Estimated number of background events in the SR

$SR : 12.28 \pm 2.01$

Observed: 20 events

→ consistent with predicted background events, pulls within 2σ (only statistical errors considered)

Unblinding the Signal Region

Observed Limits

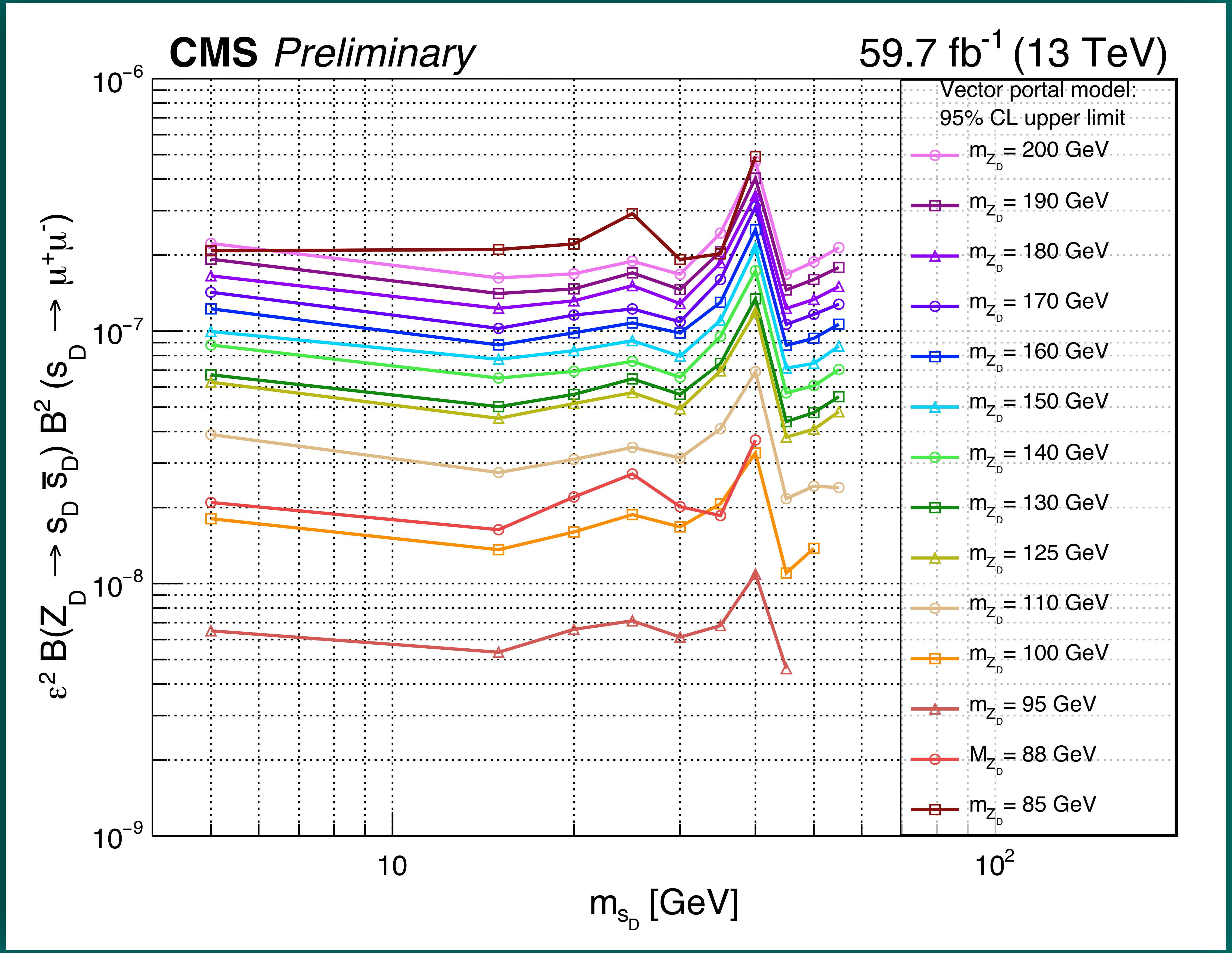

Figure17: Figure13: The observed 95% CL upper limits function of the dark scalar mass m_{s_D} and the dark vector boson mass m_{Z_D}

Unblinding the Signal Region

2018 Conclusion

- In 20-25 GeV region we observe 3 events

- The expected number of events in the said region is ~0.31

- Poisson probability for 0.31 fluctuating to 3 is 0.00364

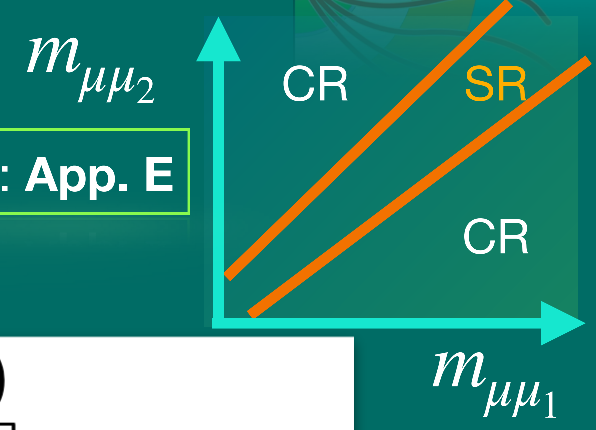

Definition SR and CR: **App. E**

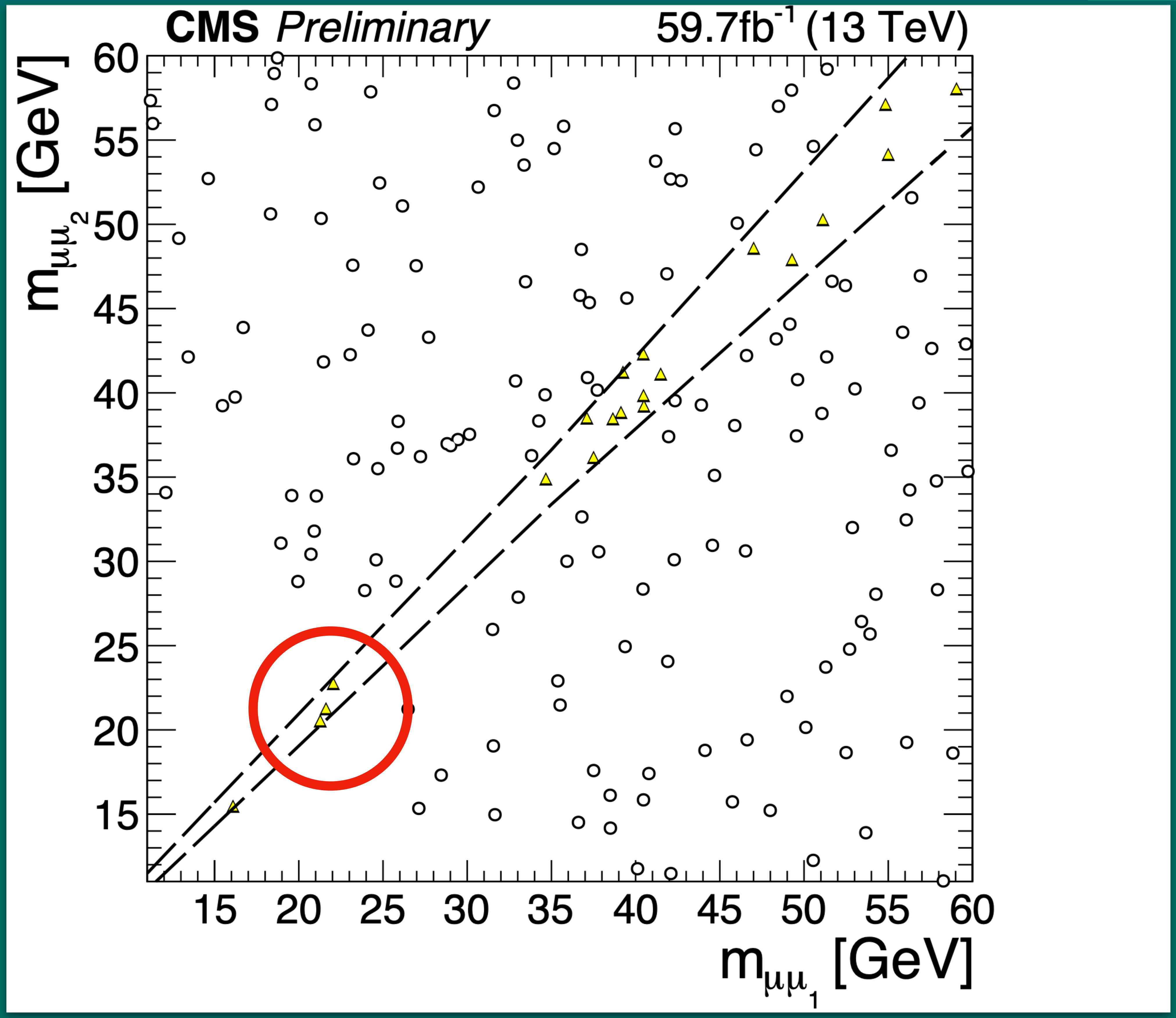

Figure18: Unblinded Signal Region above Υ resonances

Unbinding the Signal Region

2018 Conclusion

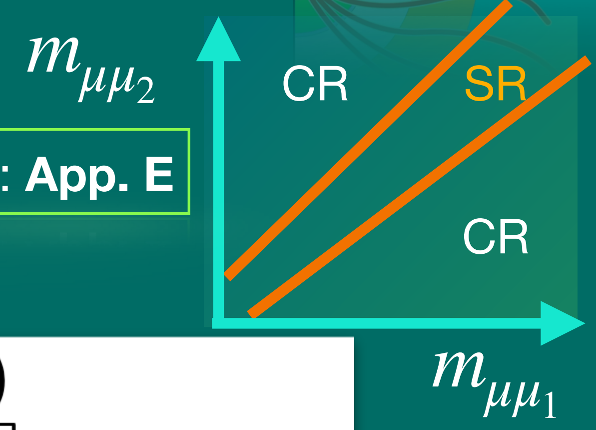

Definition SR and CR: **App. E**

- In 20-25 GeV region we observe 3 events

- The expected number of events in the said region is ~0.31

- Poisson probability for 0.31 fluctuating to 3 is 0.00364

- This could mean the background may not have been well modeled in this region

- This observation lead our research to explore the addition of **2017** CMS data to the our analysis

Brazilian plots: **App.G**

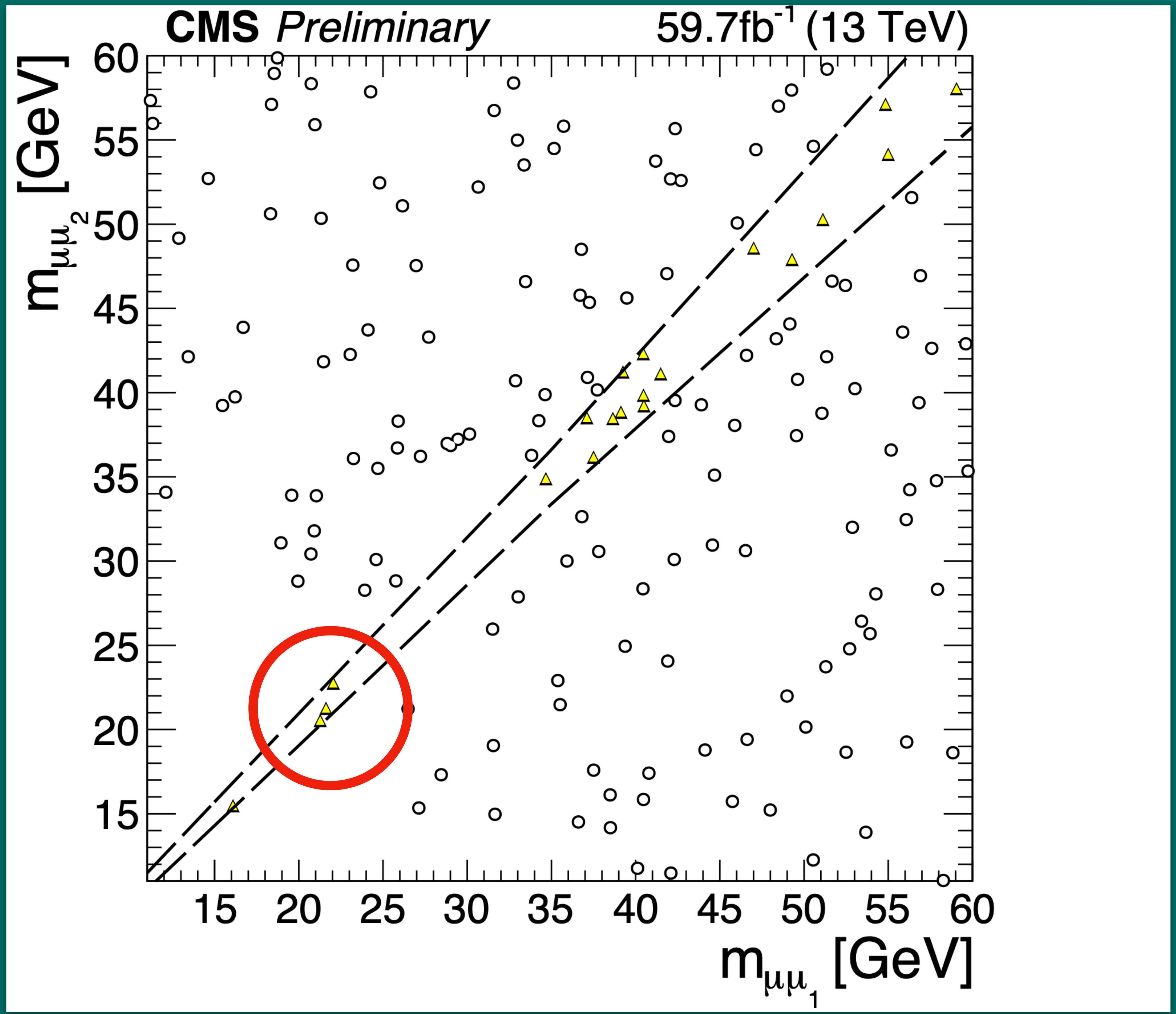

Figure18: Unblinded Signal Region above Υ resonances

2017 Analysis

Tigger Paths and Selections

Prompt Analysis

Trigger Paths
HLT_Mu23_Mu12 (HLT_DoubleL2Mu23NoVtx_2Cha in 2018)*
HLT_Mu18_Mu9_SameSign
HLT_TrkMu12_DoubleTrkMu5NoFiltersNoVtx
HLT_TripleMu_12_10_5

Muon selection
slimmedMuons in MiniAOD
4 PF Loose muon
Two muons: p_T >13 GeV, |eta| < 2
Four muons: p_T >8 GeV, |eta| < 2.4

- *Major contribution (70%-90%) to overall trigger efficiency, important for very boosted signals (low mass large $c\tau$)
- Only available for 2018, main reason we chose not to include 2017 data because no replaceable trigger to use in 2017

2017 Data

Dataset Labels	Number of Events
/DoubleMuon/Run2017B-31Mar2018-v1/MINIAOD	14 501 767
/DoubleMuon/Run2017C-31Mar2018-v1/MINIAOD	49 636 525
/DoubleMuon/Run2017D-31Mar2018-v1/MINIAOD	23 075 733
/DoubleMuon/Run2017E-31Mar2018-v1/MINIAOD	51 589 091
/DoubleMuon/Run2017F-31Mar2018-v1/MINIAOD	79 756 560
Total	218 559 676

2017 Analysis

Model-Independance Performance

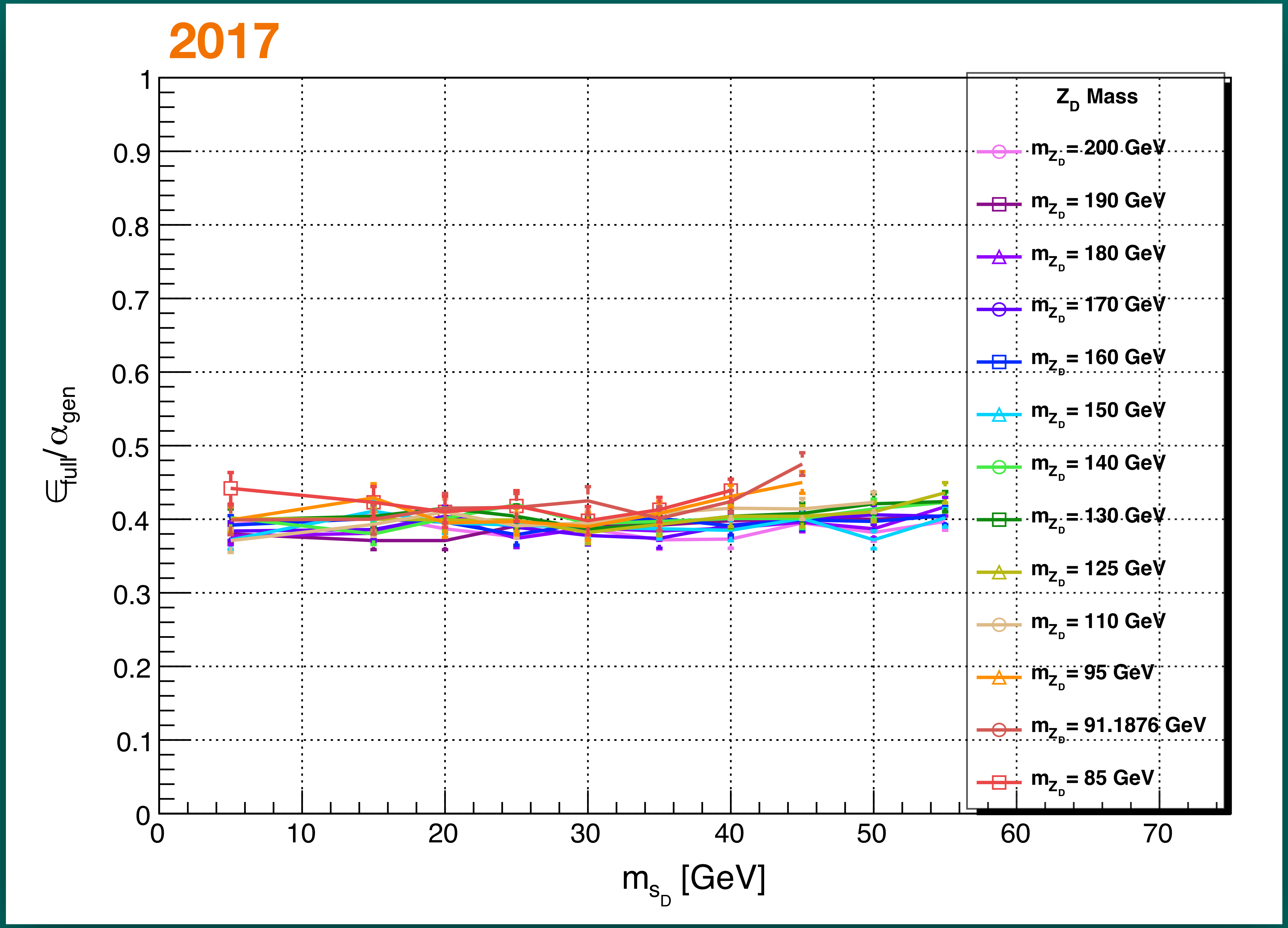

Figure19: Total selection efficiency over generator level selection acceptance, $\epsilon_{Full}/\alpha_{gen}$ as a function of the $s_D$mass for various Z_D masses in the vector portal model. The KM parameter, ϵ, is 10^{-2}

2017 Analysis

Background: Below Υ Resonances

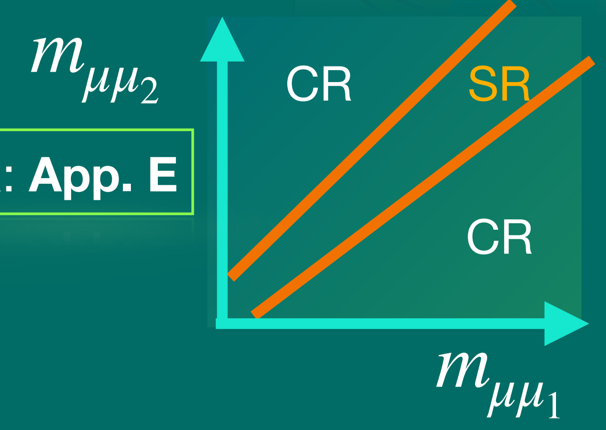

Definition SR and CR: **App. E**

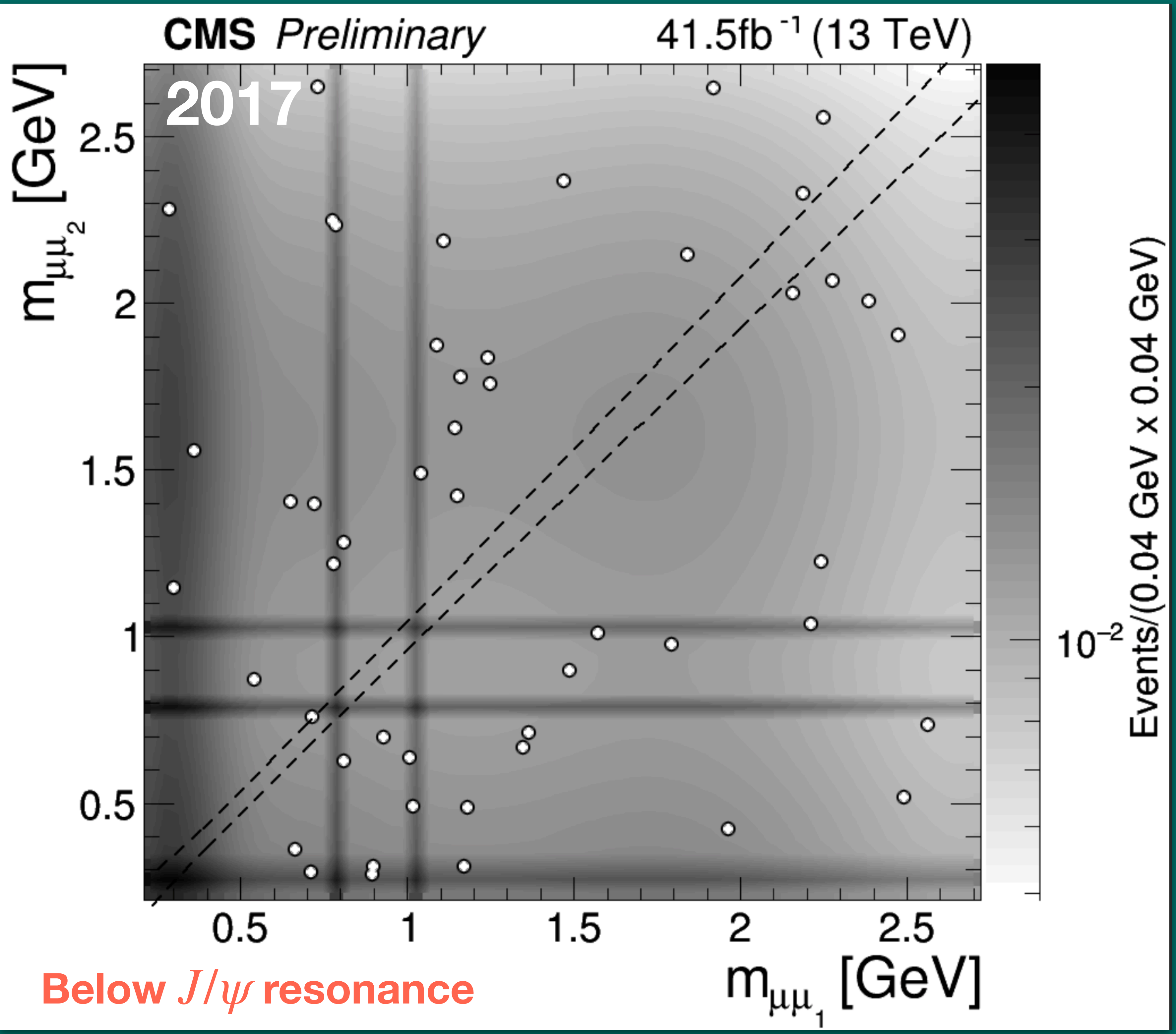

Figure20: 2D QCD background template + data at the CR

- 2D template integral SR/CR = 0.044/0.964
- 2-dimu events at CR: 49 (**SR remain blinded**)
- Estimated BKG events at SR: **2.26 +/- 0.32** (stat.)

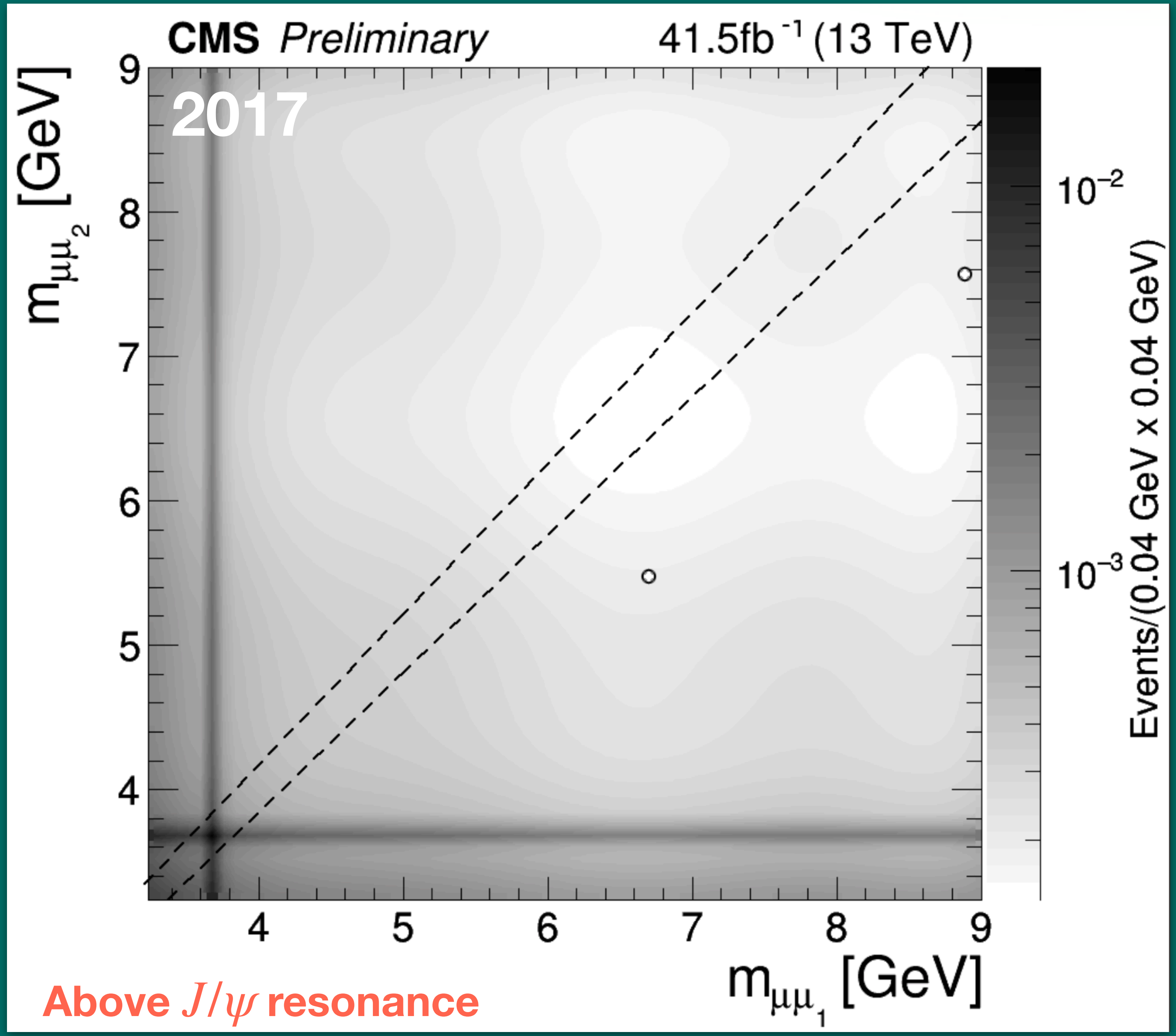

Figure21: 2D QCD background template + data at the CR

- 2D template integral SR/CR = 0.087/0.918
- 2-dimu events at CR: 2 (**SR remain blinded**)
- Estimated BKG events at SR: **0.19 +/- 0.13** (stat.)

2017 Analysis

Background: Above Υ Resonances

Definition SR and CR: **App. E**

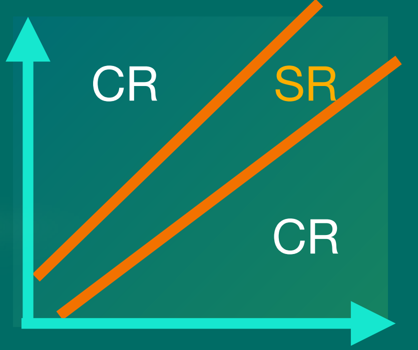

- For 2017 analysis we used QED MC simulated samples in CR for $\mu\mu_1$ and $\mu\mu_2$ similar to the 2018 analysis
- Used Kernel Density Estimation (KDE) to fit the distributions

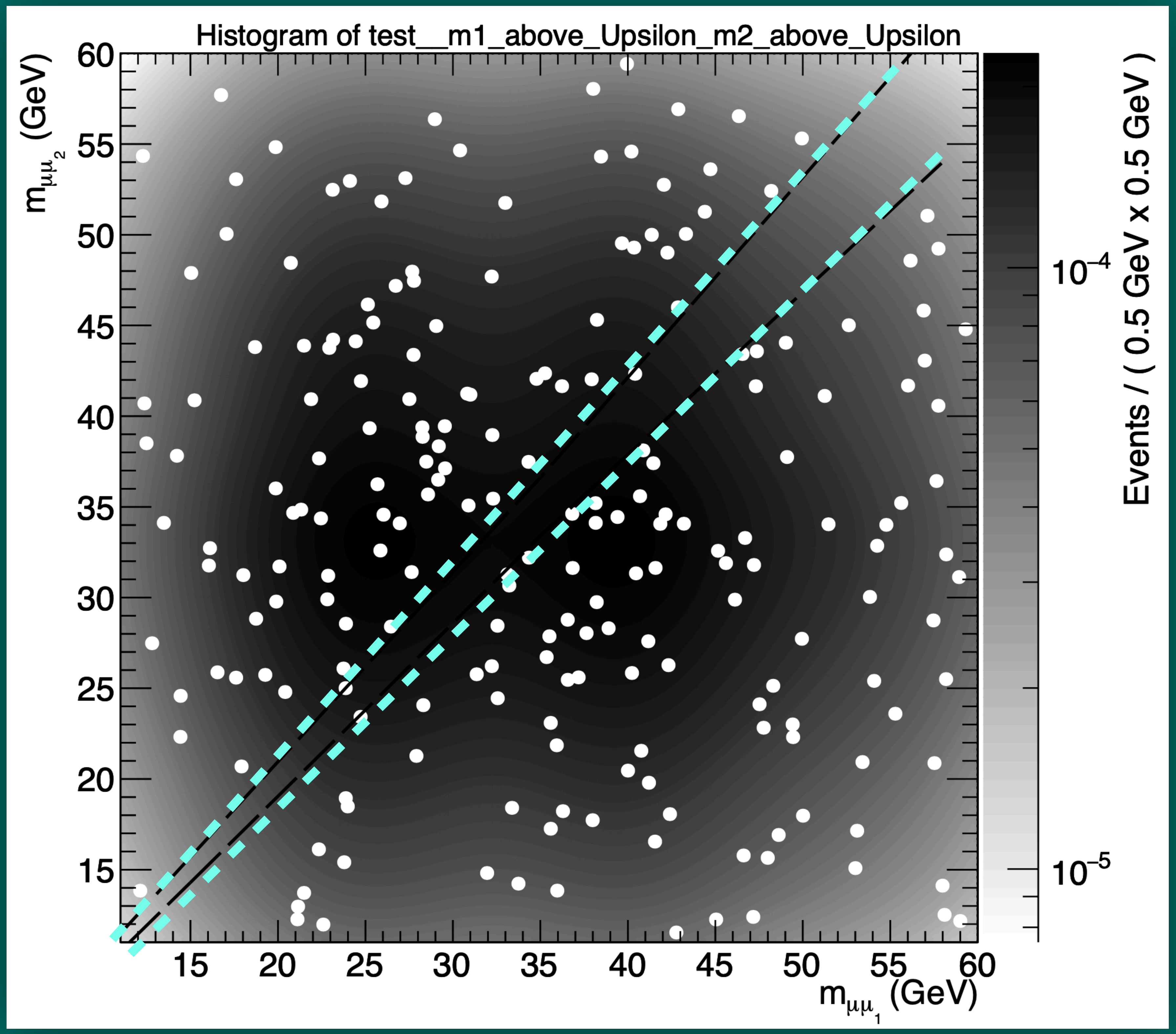

Figure22: 2D KDE background template for above Υ resonance masses

- 2D template integral SR/CR = 0.082/0.918
- 2-dimu events at CR: 212 (**SR remain blinded**)
- Estimated BKG events at SR: **18.97 +/- 1.3** (stat.)

2017 Analysis

Background: Above Υ Resonances

Definition SR and CR: **App. E**

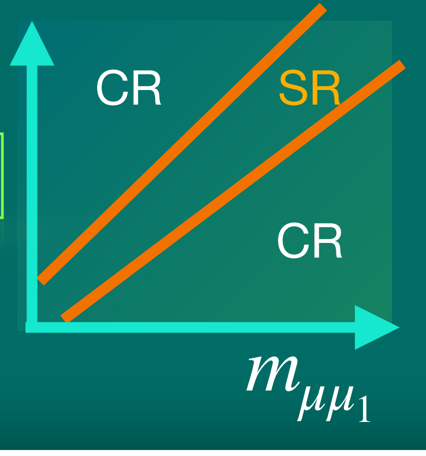

- For 2017 analysis we used QED MC simulated samples in CR for $\mu\mu_1$ and $\mu\mu_2$ similar to the 2018 analysis

- Used Kernel Density Estimation (KDE) to fit the distributions

- Constructed 2D KDE templates

- The signal region in the corridor is still blinded

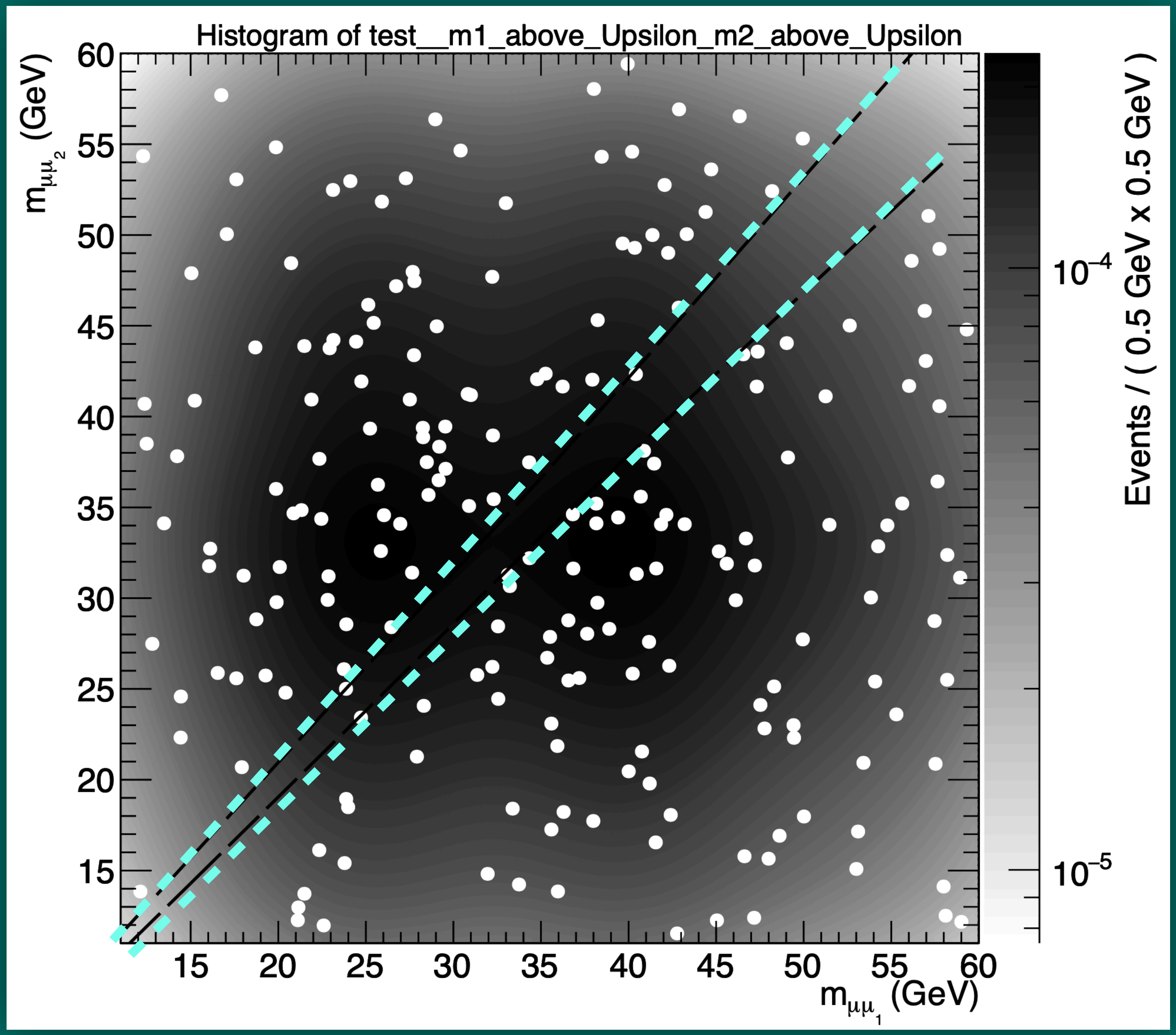

Figure22: 2D KDE background template for above Υ resonance masses

- 2D template integral SR/CR = 0.082/0.918
- 2-dimu events at CR: 212 (**SR remain blinded**)
- Estimated BKG events at SR: **18.97 +/- 1.3** (stat.)

2017 Analysis

2017 Summary

- The expected limit is to be set after scale factor calculations, such as: HLT, NNLO, and reconstruction scale factors

- The results to be combined with 2018 and 2016 results using the Higgs combine tool

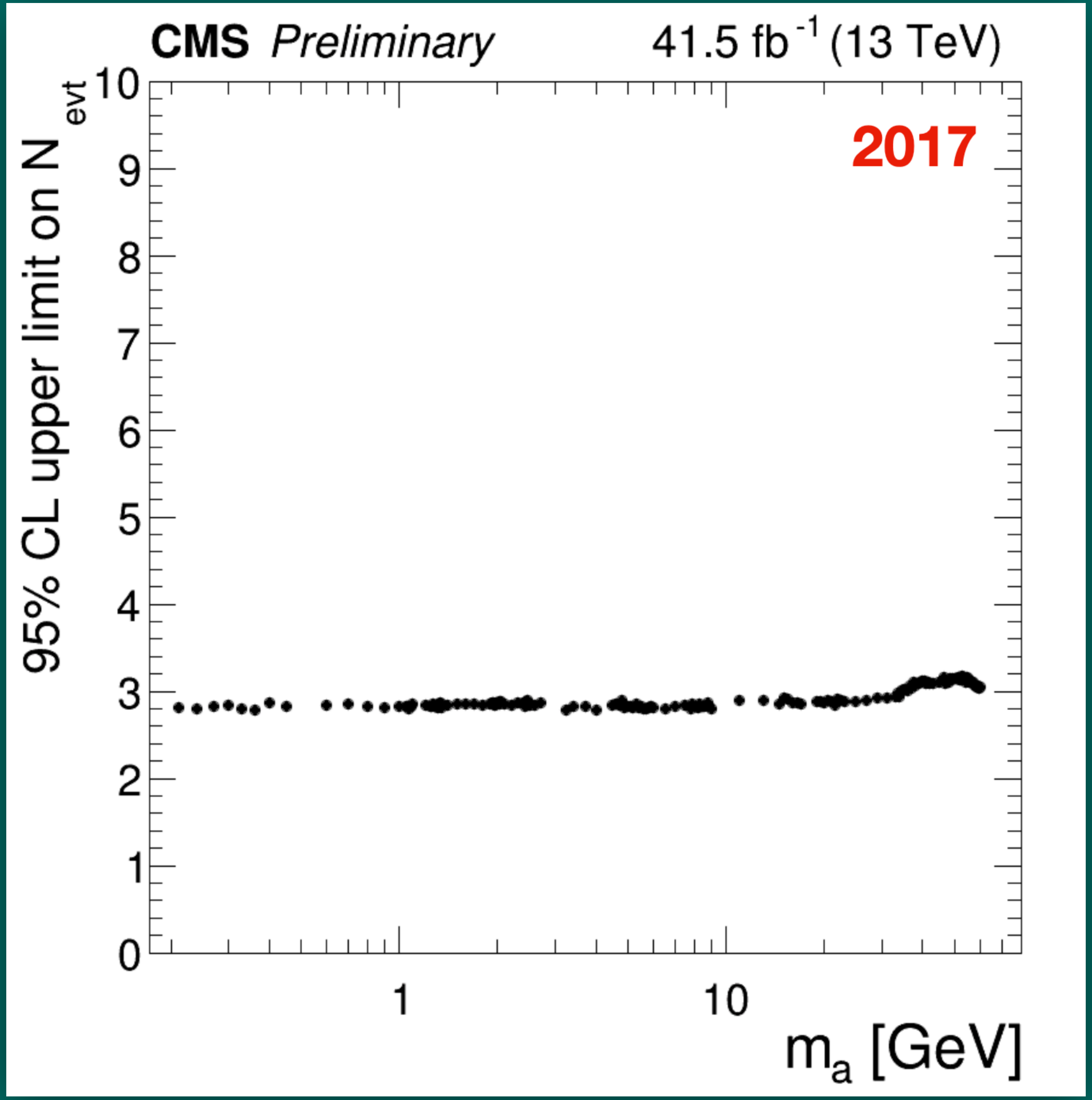

Figure23: Expected model independent 95% CL upper limit on the number of events

2017 Analysis

2017 Summary

- The expected limit is to be set after scale factor calculations, such as: HLT, NNLO, and reconstruction scale factors

- The results to be combined with 2018 and 2016 results using the Higgs combine tool

- Unblind 2017 analysis and produce final limit

- The analysis remains approximately near zero background analysis

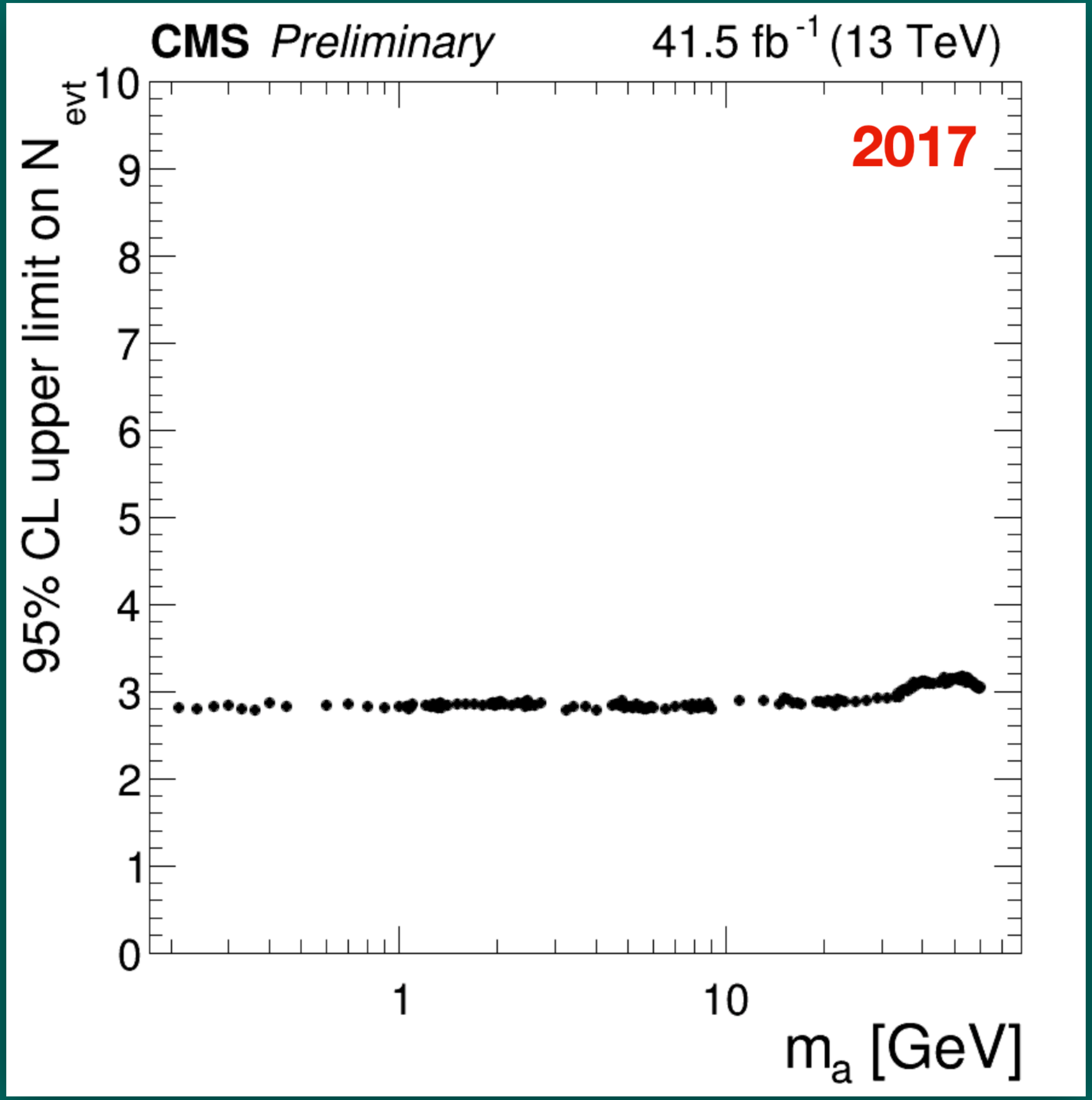

Figure23: Expected model independent 95% CL upper limit on the number of events

Summary

- A model independent analysis for $pp \rightarrow 2a \rightarrow 4\mu$ is represented

- A vector-portal model is introduced as a benchmark dark matter model: $pp \rightarrow Z_D \rightarrow s_D\overline{s_D} \rightarrow 4\mu$

- Model independent upper limits on kinetic mixing parameter, cross-section branching ratio, and acceptance is set

- The 2018 data from CMS is analyzed

- We are adding 2017 data to the analysis to improve the background modeling

References

[1] E. Dudas, Y. Mambrini, S. Pokorski, and A. Romagnoni, “Invisible z’ and dark matter,” Journal of High Energy Physics, vol. 2009, no. 08, p. 014, 2009

[2] J. Goodman and W. Shepherd, “Lhc bounds on uv-complete models of dark matter,” arXiv preprint arXiv:1111.2359, 2011

[3] H. An, X. Ji, and L.-T. Wang, “Light dark matter and zprime dark force at colliders,” Journal of High Energy Physics, vol. 2012, no. 7, pp. 1–25, 2012

[4] J. L. Feng, M. Kaplinghat, H. Tu, and H.-B. Yu, “Hidden charged dark matter,” Journal of Cosmology and Astroparticle Physics, vol. 2009, no. 07, p. 004, 2009.

[5] J. D. Wells, “How to find a hidden world at the large hadron collider,” arXiv preprint arXiv:0803.1243, 2008.

[6] D. Curtin, R. Essig, S. Gori, and J. Shelton, “Illuminating dark photons with high-energy colliders,” Journal of High Energy Physics, vol. 2015, no. 2, pp. 1–45, 2015.

[7] A. M. Sirunyan et al., “A search for pair production of new light bosons decaying into muons in proton-proton collisions at 13 TeV,” Physics Letters B, vol. 796, pp. 131–154, 2019.

[8] D. Abercrombie et al., “Dark Matter Benchmark Models for Early LHC Run-2 Searches: Report of the ATLAS/CMS Dark Matter Forum,” Phys. Dark Univ., vol. 27, p. 100371, 2020.

[9] F. Bishara, R. Contino, and J. Rojo, “Higgs pair production in vector-boson fusion at the LHC and beyond,” Eur. Phys. J. C, vol. 77, no. 7, p. 481, 2017.

Appendix A
Benchmark Models

Dark SUSY

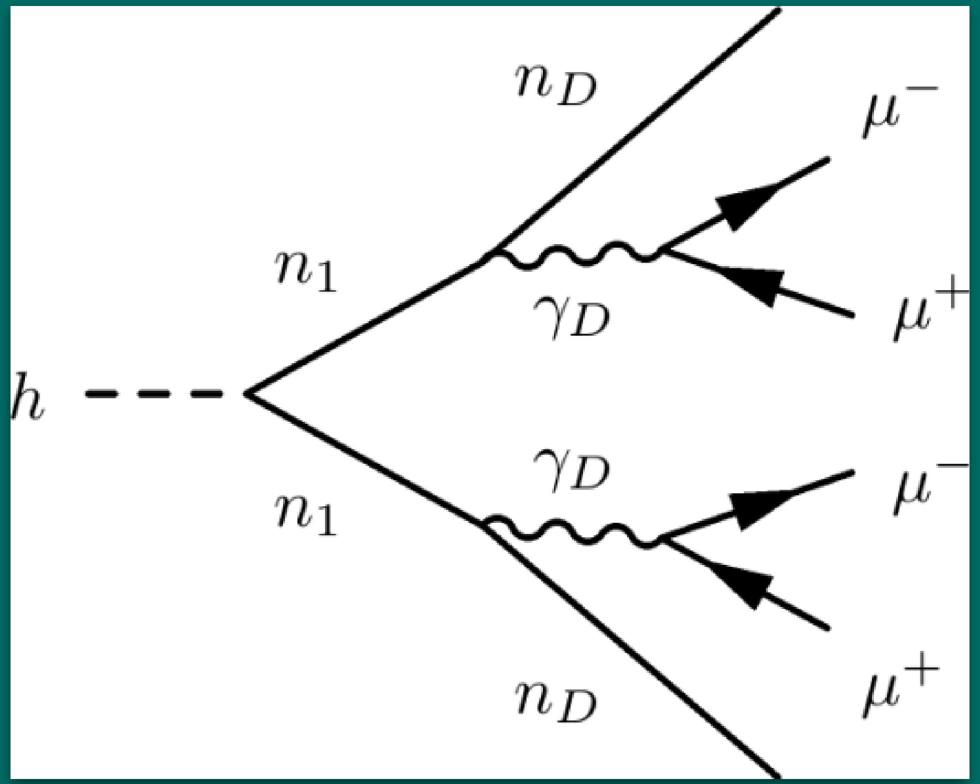

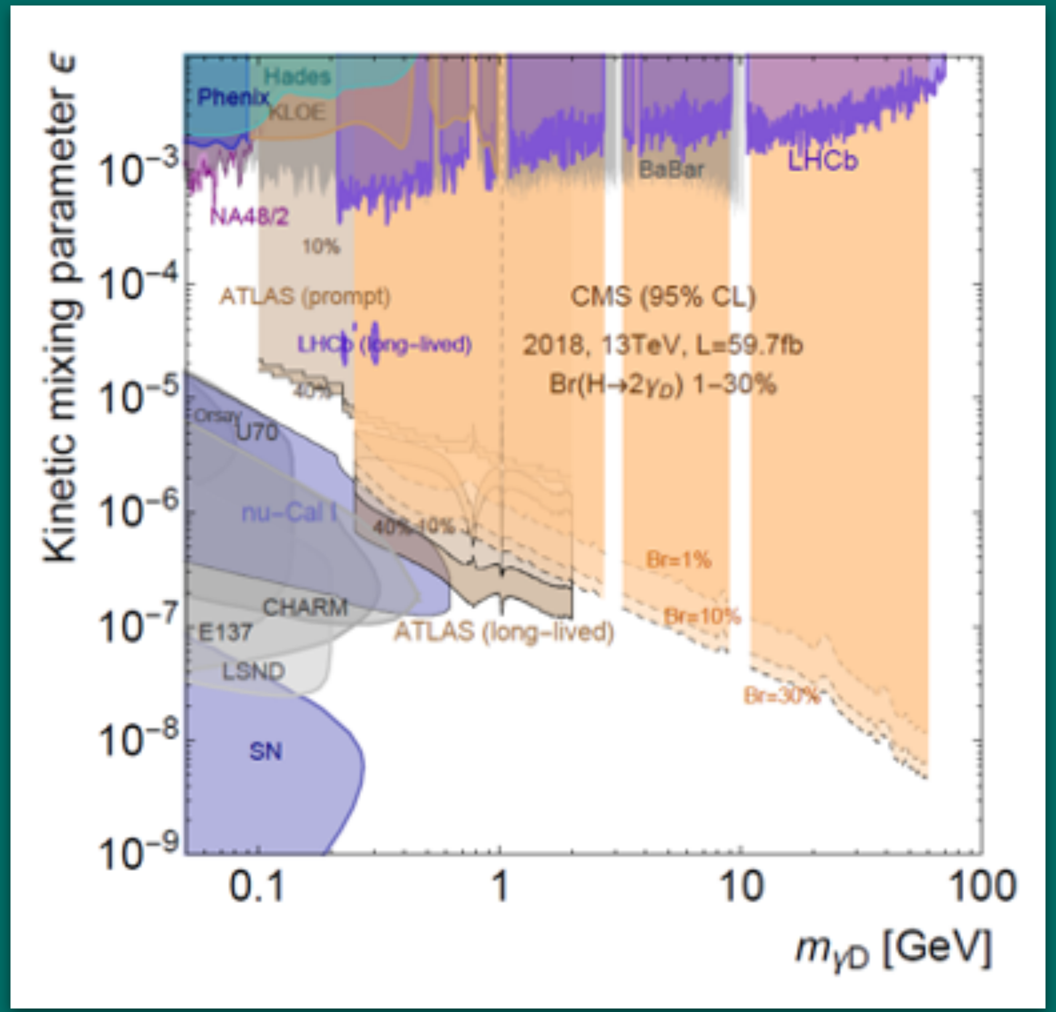

NMSSM

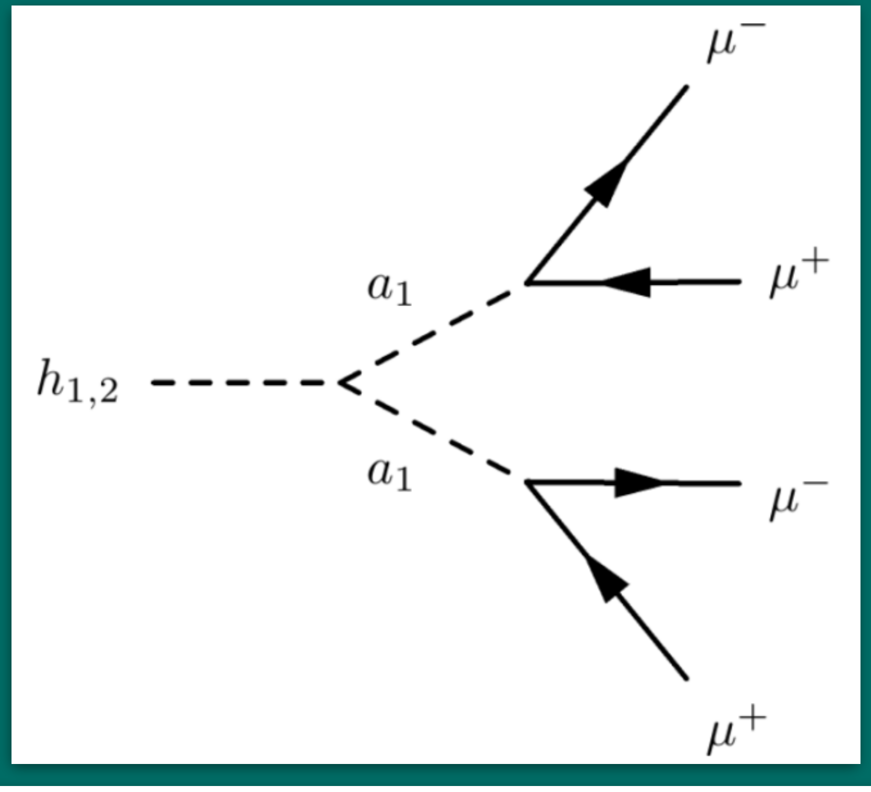

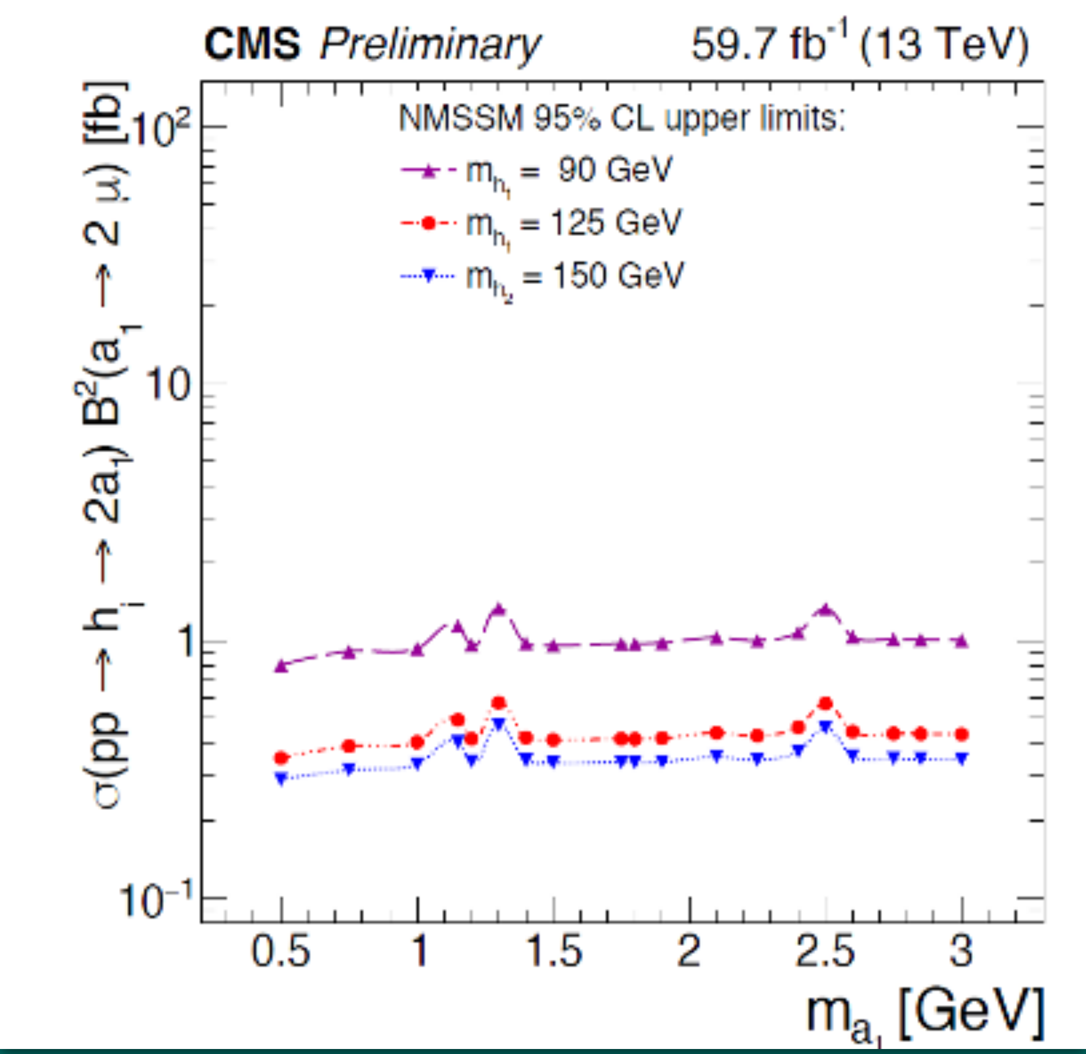

ALP

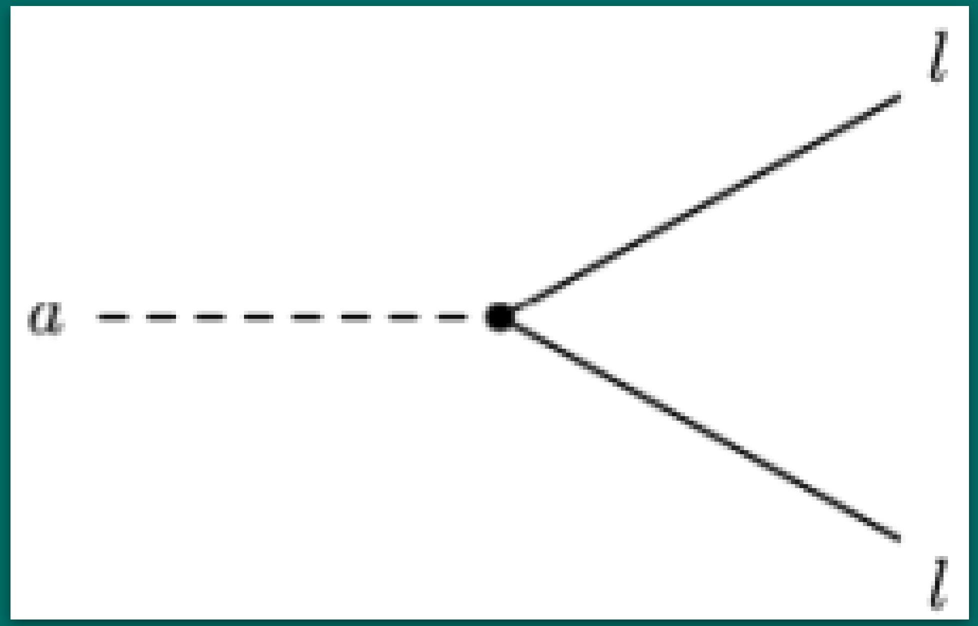

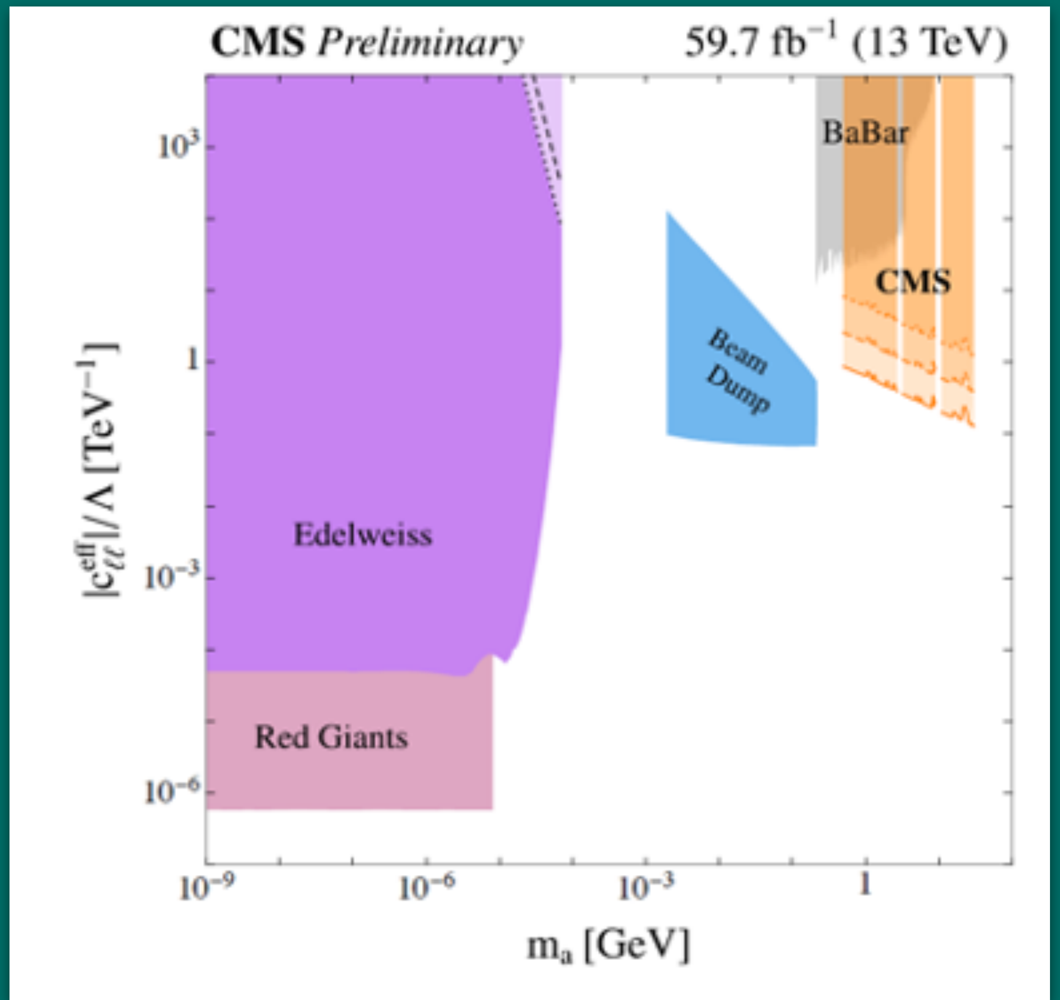

Appendix B

Below ϒ Resonance 1D Mass Templates

From pre-approval talk given by Wei Shi

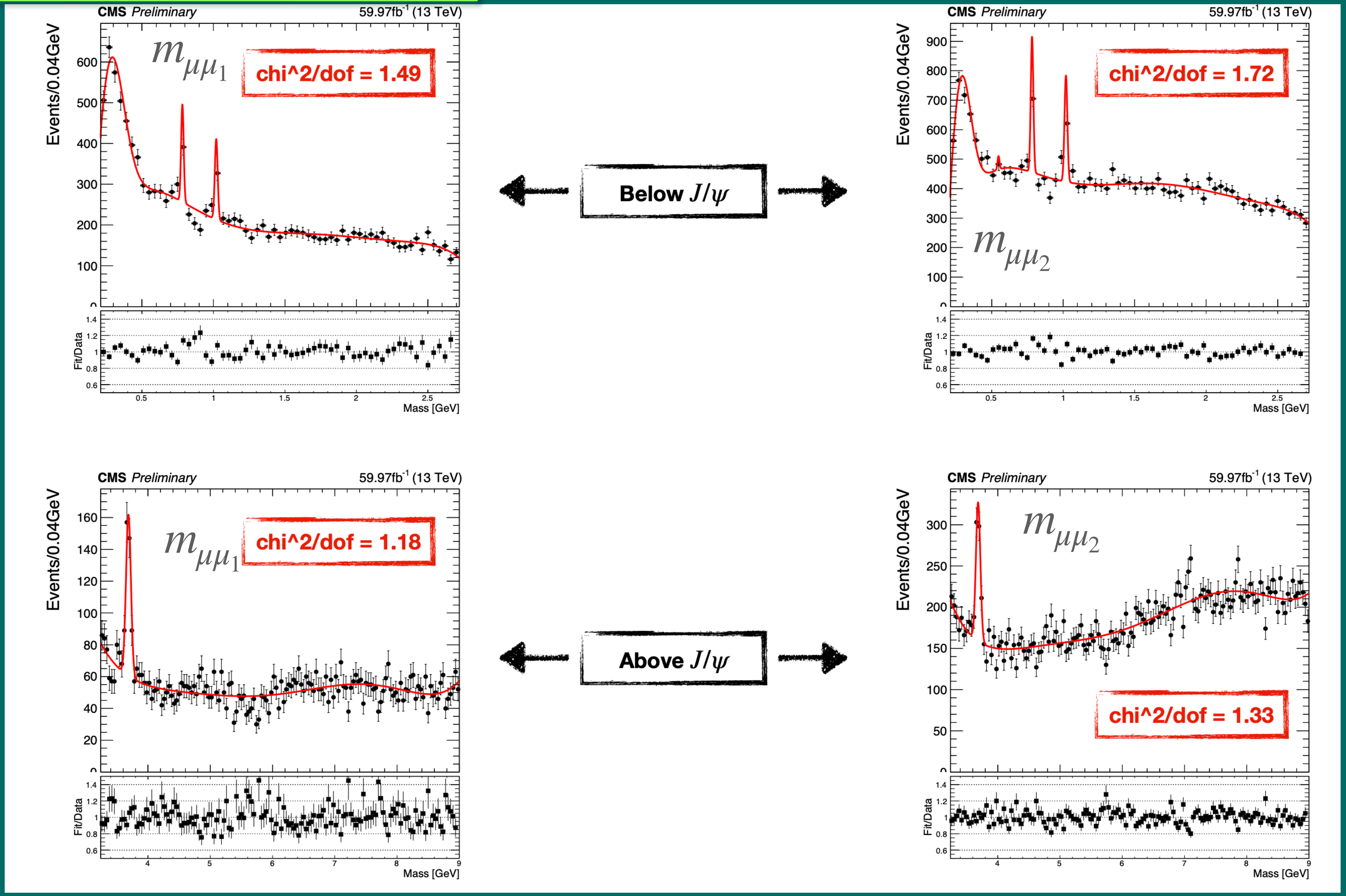

Appendix C

Kernel Density Estimation Above Υ Resonance

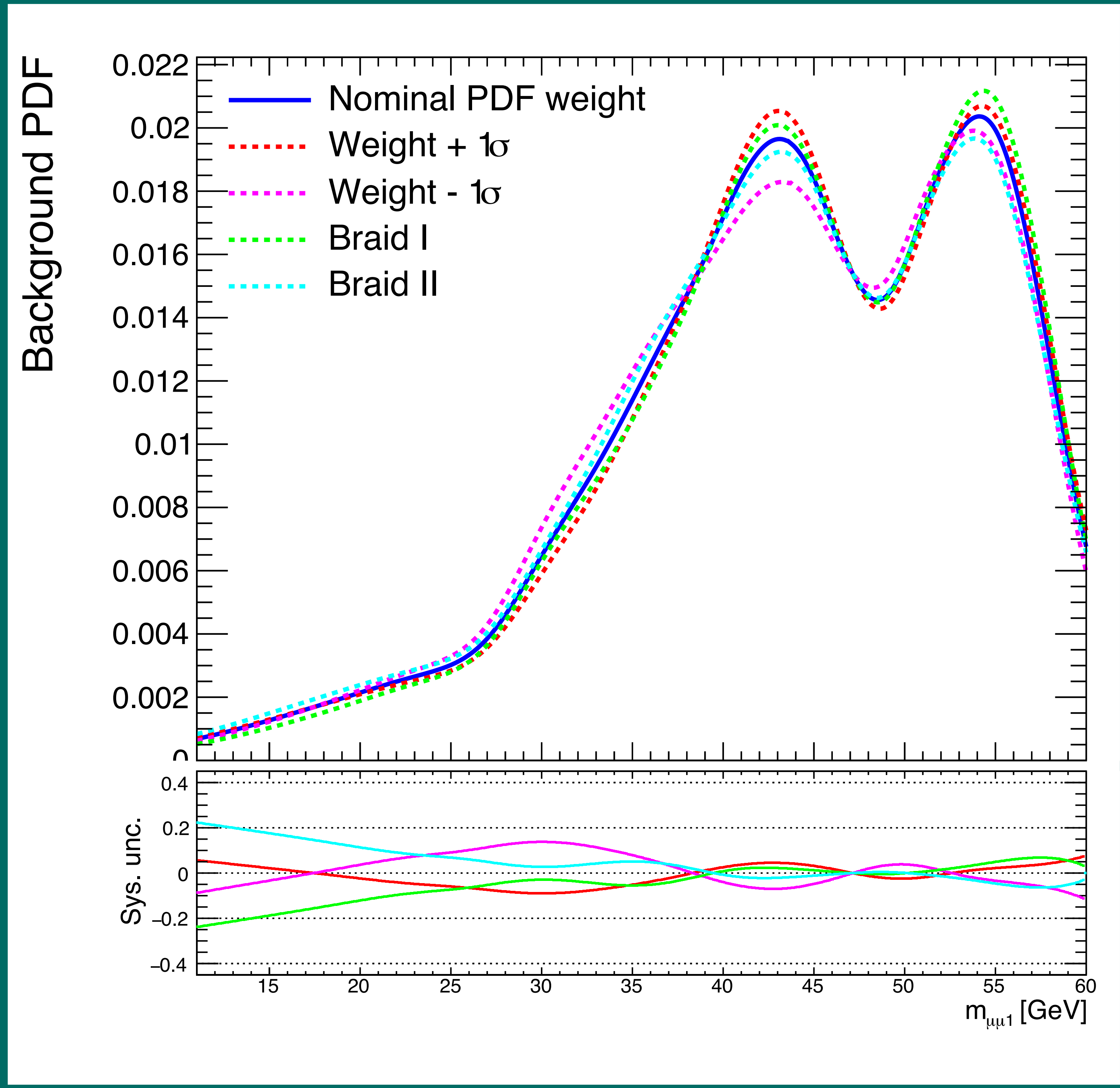

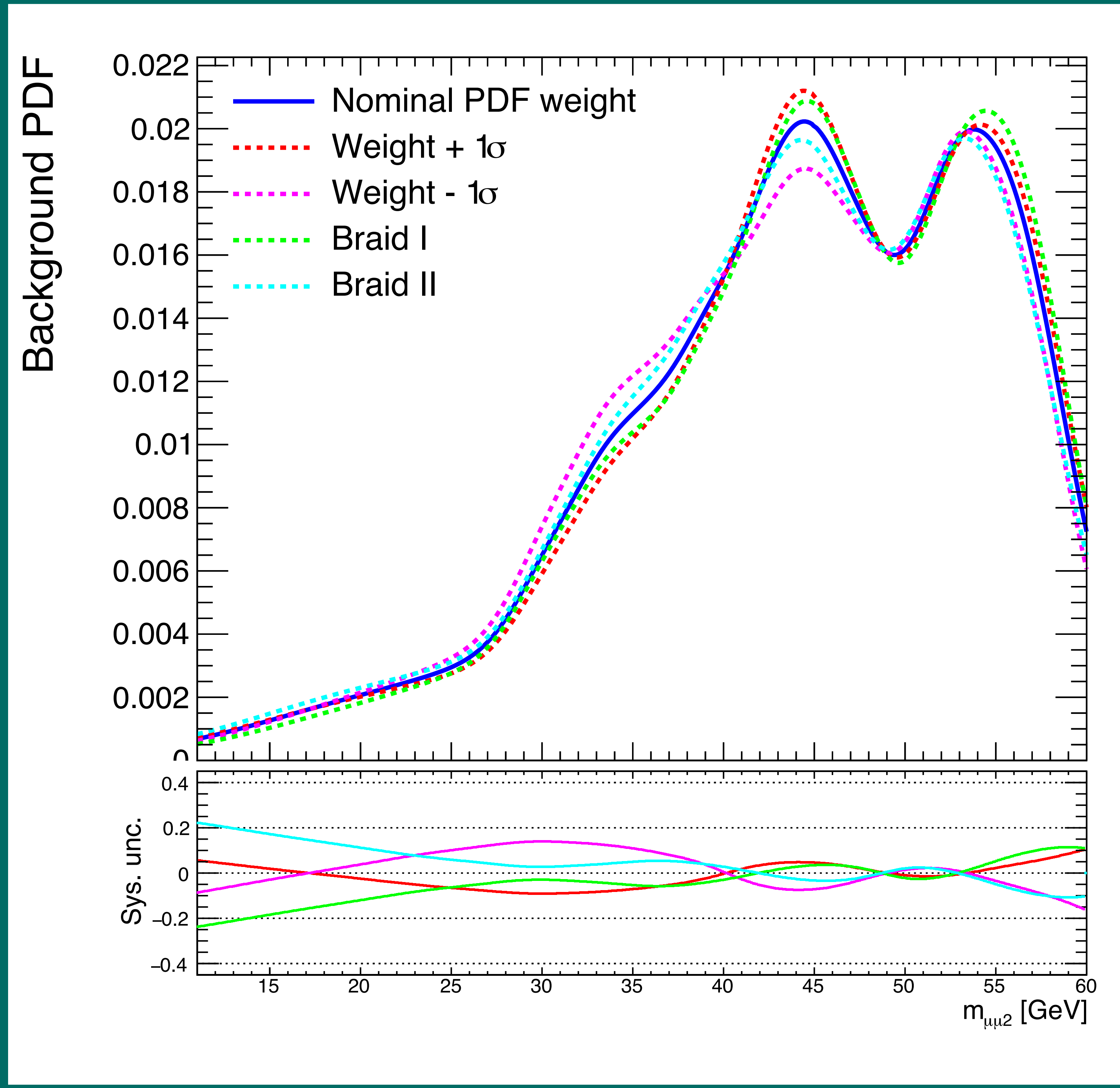

Appendix D
Triggers

- **HLT_DoubleL2Mu23NoVtx_2Cha**
  - Major contribution (70%-90%) to overall trigger efficiency,
    important for very boosted signals (low mass large cTau)
  - Only available for 2018
- **HLT_Mu18_Mu9_SS, HLT_TrkMu12, HLT_TripleMu_12_10_5**
  - Lower p_T improves trigger efficiency
- 2017 Analysis:
  - **HLT_Mu23_Mu12** replaced **HLT_DoubleL2Mu23NoVtx_2Cha**

2018

Trigger Paths
HLT_DoubleL2Mu23NoVtx_2Cha
HLT_Mu18_Mu9_SameSign
HLT_TrkMu12_DoubleTrkMu5NoFiltersNoVtx,
HLT_TripleMu_12_10_5

2017

Trigger Paths
HLT_Mu23_Mu12 (HLT_DoubleL2Mu23NoVtx_2Cha in 2018)
HLT_Mu18_Mu9_SameSign
HLT_TrkMu12_DoubleTrkMu5NoFiltersNoVtx
HLT_TripleMu_12_10_5

Appendix D
Triggers

- **HLT_DoubleL2Mu23NoVtx_2Cha**
  - Major contribution (70%-90%) to overall trigger efficiency,
    important for very boosted signals (low mass large cTau)
  - Only available for 2018

- **HLT_Mu18_Mu9_SS, HLT_TrkMu12, HLT_TripleMu_12_10_5**
  - Lower p_T improves trigger efficiency

- 2017 Analysis:
  - **HLT_Mu23_Mu12** replaced **HLT_DoubleL2Mu23NoVtx_2Cha**

From pre-approval talk given by Wei Shi

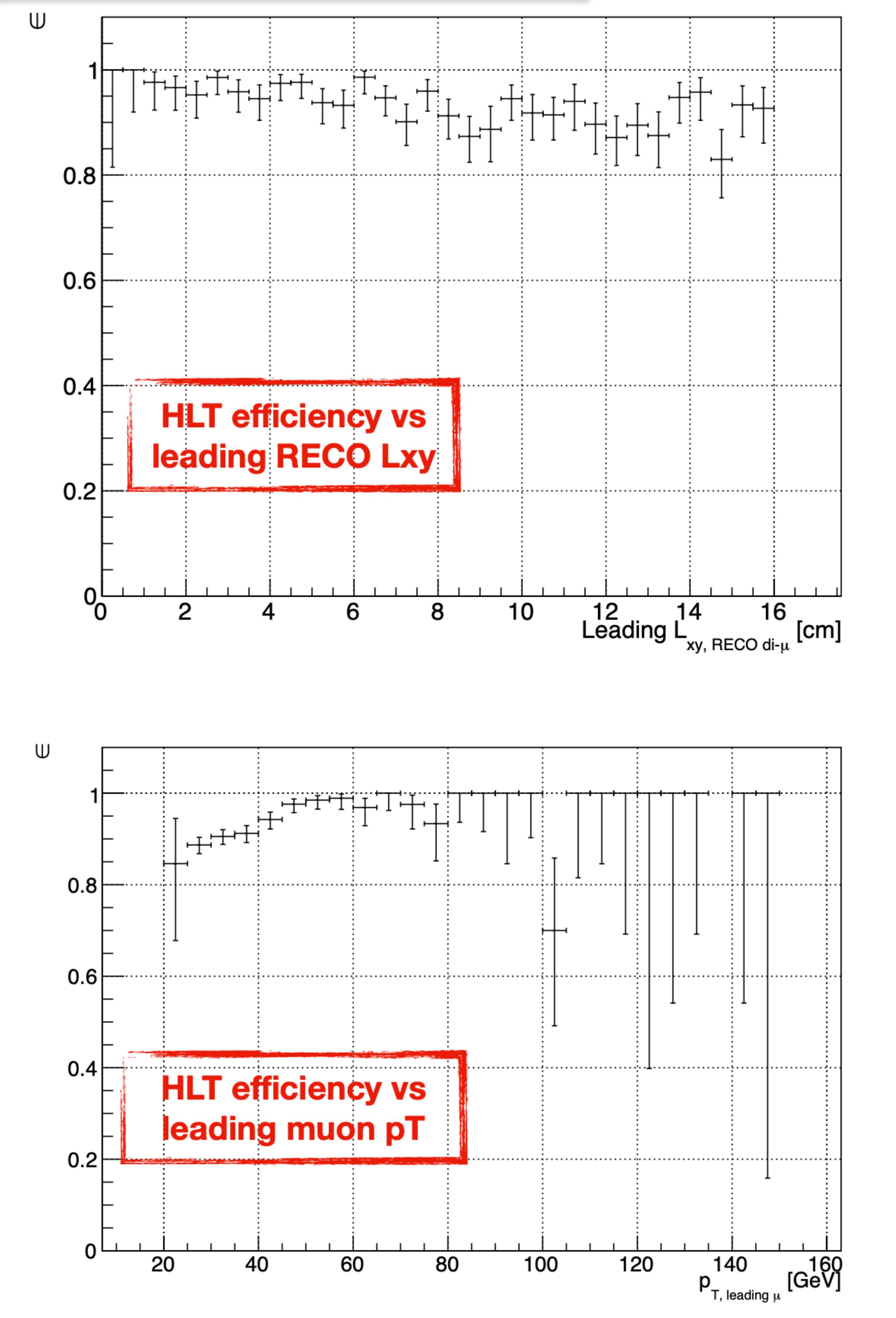

Appendix E

Pixel Hit

- Pixel detector went through and upgrade in 2016
- We require a valid pixel hit in phase-1 detector for at least one muon of each pair
- 4 barrel layers L_{xy} up 16 cm, and 3 forward layers $|L_z|$ up to 51.6 cm

Left: comparative layout of the pixel detector between the layers and disks, before and after the upgrade of pixel detectors.
Right: Transverse-oblique view comparing the pixel barrel layers in the upgraded detector versus pre-upgrade

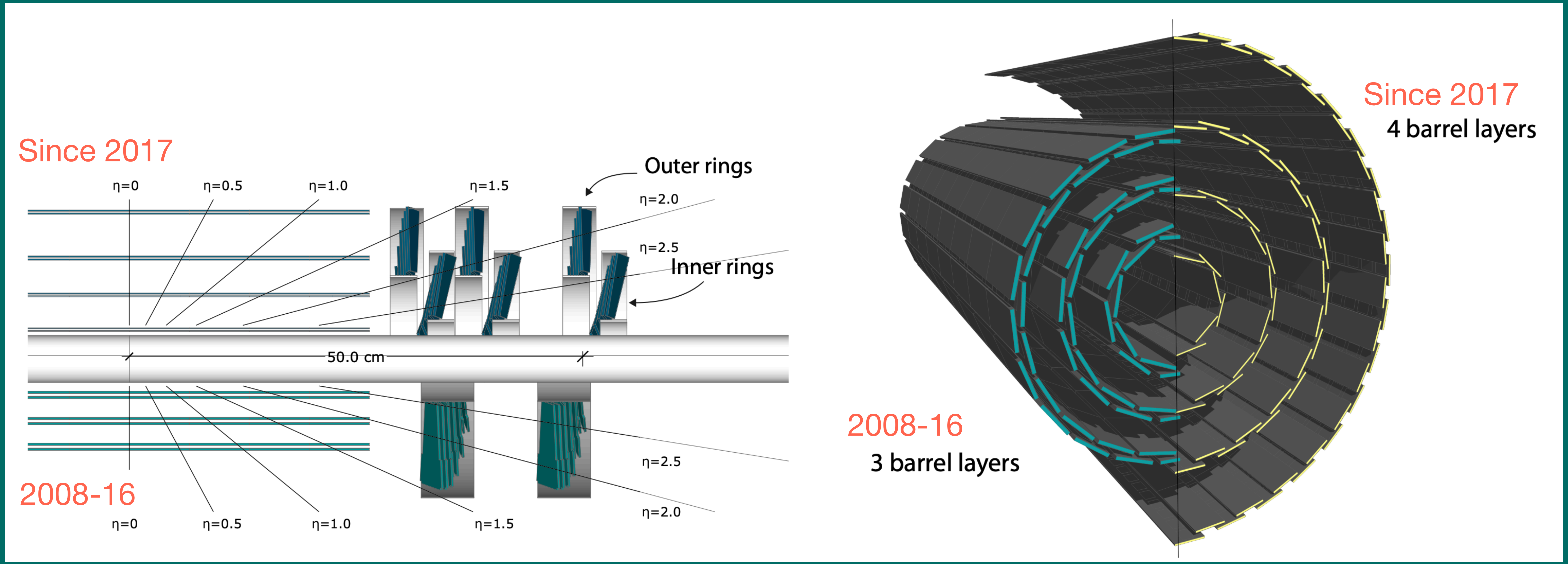

Appendix E

Dimuon Vertex

- dimuon vertex fit probability from KalmanVertexFitter

$$P_{\mu\mu} > P(L_{xy}, f\sqrt{\Delta R}, N_{SA-\mu})$$

$$P(L_{xy}, f\sqrt{\Delta R}, N_{SA-\mu}) = P_0 \times (1 - N_{SA\mu}) \times \exp[-(\frac{L_{xy}}{R_0})^2 \times f(\sqrt{\Delta R})]$$

$$f(\Delta R) = p_0 + p_1 \times \sqrt{\Delta R} + p_2 \times (\Delta R)^2 + p_3 \times (\Delta R)^3 + p_4 \times (\Delta R)^4$$

$p_0 = 0.2,\ R_0 = 10cm,\ p_0 = 8.54,\ p_1 = -50.46,\ p_2 = 109.83,\ p_3 = -92.74,\ p_4 = 36.84$

Appendix E

Defining Control and Signal Regions

- Since the moun pairs are produced from supposedly the same bosons with consistent masses, the invariant mass of muon pairs should be consistent as well

- Conventional way of defining a mass consistency window:
  - The width of the SR window is adjusted by the di-muon mass reconstruction resolution eg., a Gaussian fit to the di-muon mass and the standard deviation 3σ would result in ~99% signal efficiency
  - This method does not work for higher masses ($\gtrsim 10$ GeV)
  - Higher mass: radiative non-gaussian tails
- Instead we define the window width by the efficiencies that we desire

$$m_1 - m_2 = f(\frac{m_1 + m_2}{2})$$

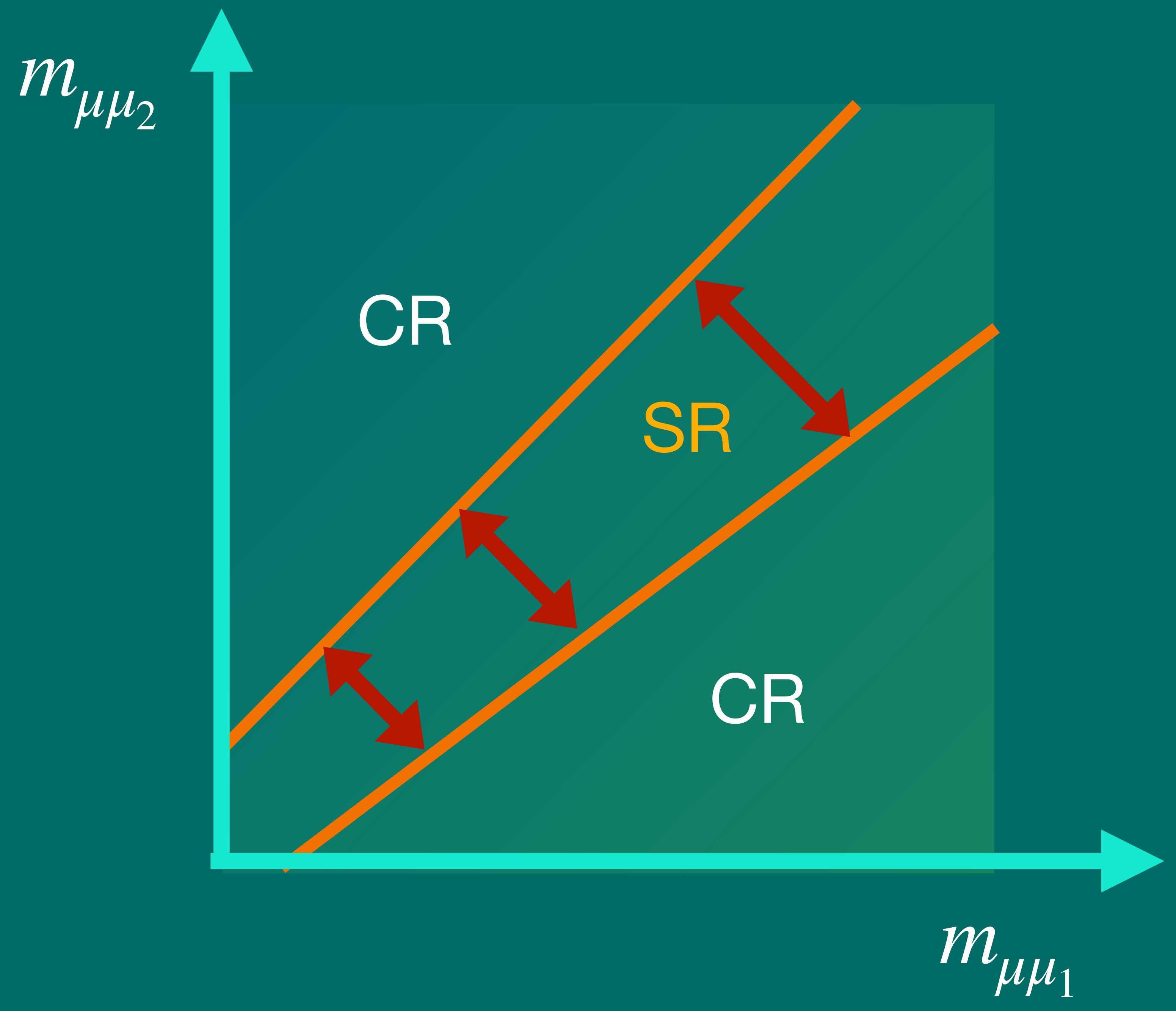

For more on mass window cut see App. E

Appendix E

Mass window

- Choose desired efficiency: calculate the signal significance $(s/\sqrt{S+B})$

- Significance drops at higher masses

- We chose 90% signal efficiency

- Window size is determined based on desired 90% efficiency

$$f(\frac{m_1 + m_2}{2})$$

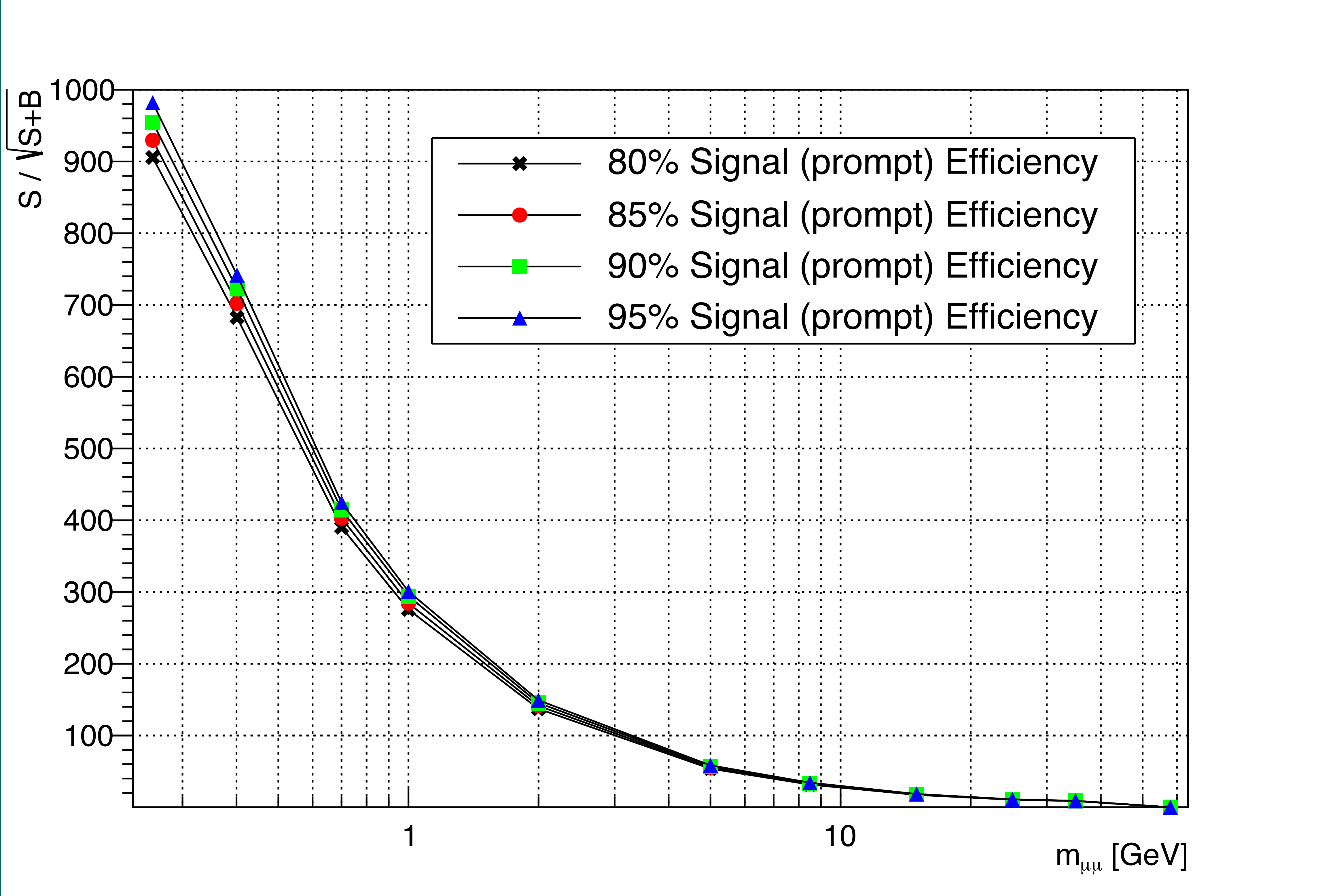

Appendix F

HLT Scale Factor 2018

•Using orthogonal triggers on SingleMuon control dataset and MC simulated events.

•The efficiency of the signal triggers is determined on events passing a set of selection criteria optimized to select WZTo3LNu and ZZTo4l events.

•This is done both on the data and on the MC simulated events. Then the signal HLT efficiency is calculated on the surviving events.

•The cut-flow table of this process is shown on the right.

•The efficiency of the signal HLT on both MC samples is ~0.99, while the efficiency of data is 0.986.

•This results in a trigger scale factor of SF = 0.986/0.99 = 99.6% ± 0.6% (stat.)

Selection	WZTo3LNu	ZZTo4Mu	Data
Pre-selection (if applicable)	301245.23	70517.53	18051620
Passes at least one orthogonal trigger	118895.45	22794.27	18014171
Exactly three muons	22819.88	4019.38	3405670
$\|\eta_i\| < 2.4$	22819.88	4019.38	3405670
$p_{T,1} > 20$ GeV, $p_{T,2} > 20$ GeV, $p_{T,3} > 10$ GeV	1007.26	116.17	373507
Two muons with opposite charge	999.81	115.70	337040
$\|m_{\mu\mu} - m_Z\| < 10$ GeV	835.89	73.05	222817
Medium muon ID	748.68	56.47	12627
$\|d_{xy,i}\| < 0.005$ cm	706.08	48.94	5269
$\|d_{z,i}\| < 0.01$ cm	603.32	39.64	3059
$\text{RelIso}_i < 0.1$	406.95	25.71	437
Passes at least one signal trigger	402.72	25.42	431

Appendix F

HLT Scale Factor 2017

- For 2017 we separate the run eras and emulate the triggers
- The cross-section weighted total MC is calculated
- For each run:
  - $Total\ MC_{eff} = \frac{\sigma_{WZ} \times WZ_{\#events} + \sigma_{ZZ} \times ZZ_{\#events}}{\sigma_{WZ} + \sigma_{ZZ}}$
  - $SF = \frac{data_{eff}}{total\ MC_{eff}}$
- The lumi weighted total SF:
- $Total\ SF = \frac{(4.79 \times 0.908) + (23.19 \times 0.996) + (13.53 \times 0.956)}{41.5}$
- That results in an overall **SF = 0.972**

	Lumi fb^{-1}	WZ eff	ZZ eff	Total MC eff	Data eff	SF
Run B	4.79	0.902	0.912	0.904	0.821	0.908
Run C-E	23.19	0.95	0.96	0.955	0.95	0.994
Run F	13.53	0.996	0.995	0.996	0.953	0.956

Appendix G

Brazilian Plot - Post Fit Observed Limits -2018

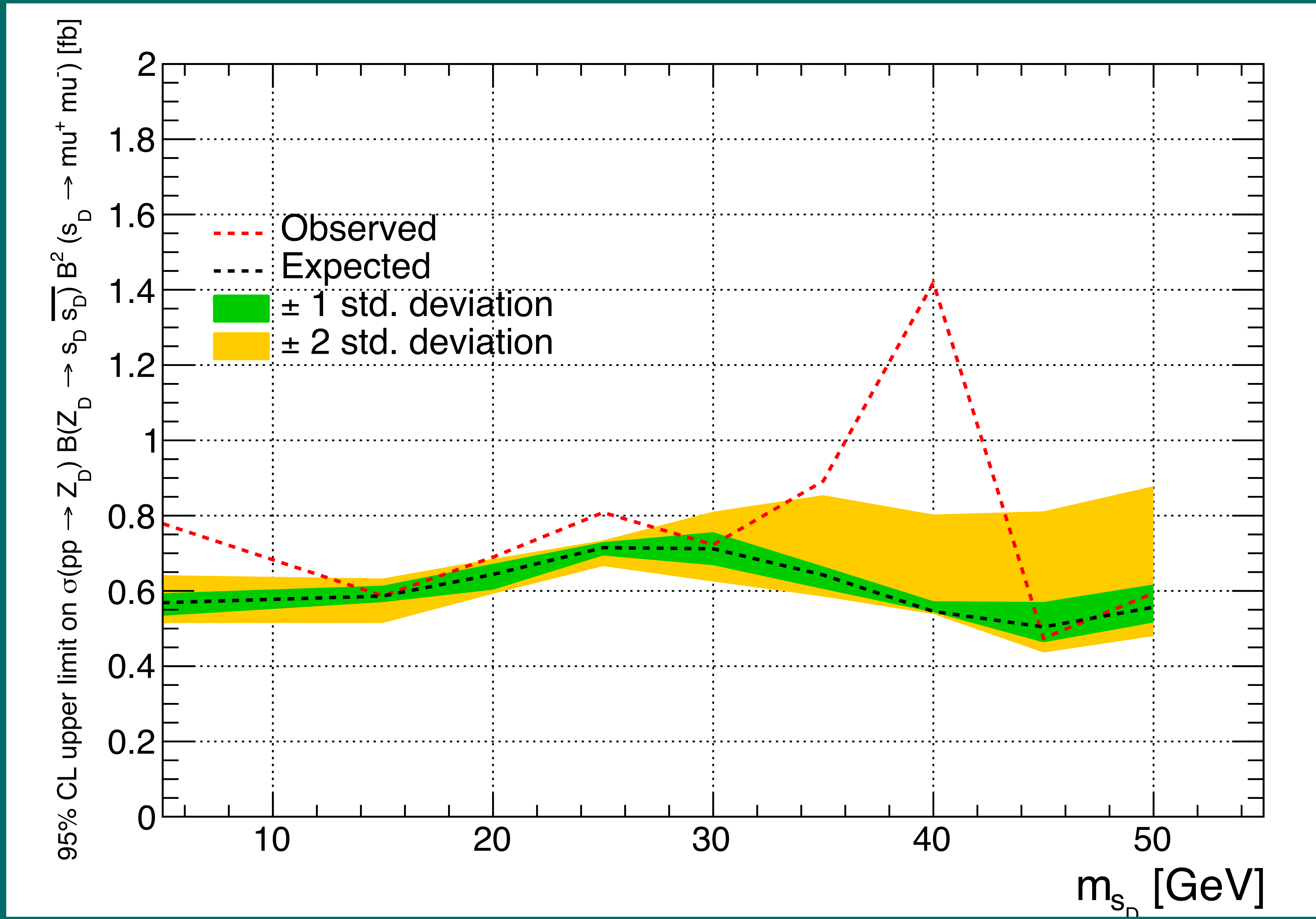

Brazilian bands for m_{ZD} =100 GeV. Expected limits after unblinding

Appendix G

Brazilian Plot - Post Fit Observed Limits -2018

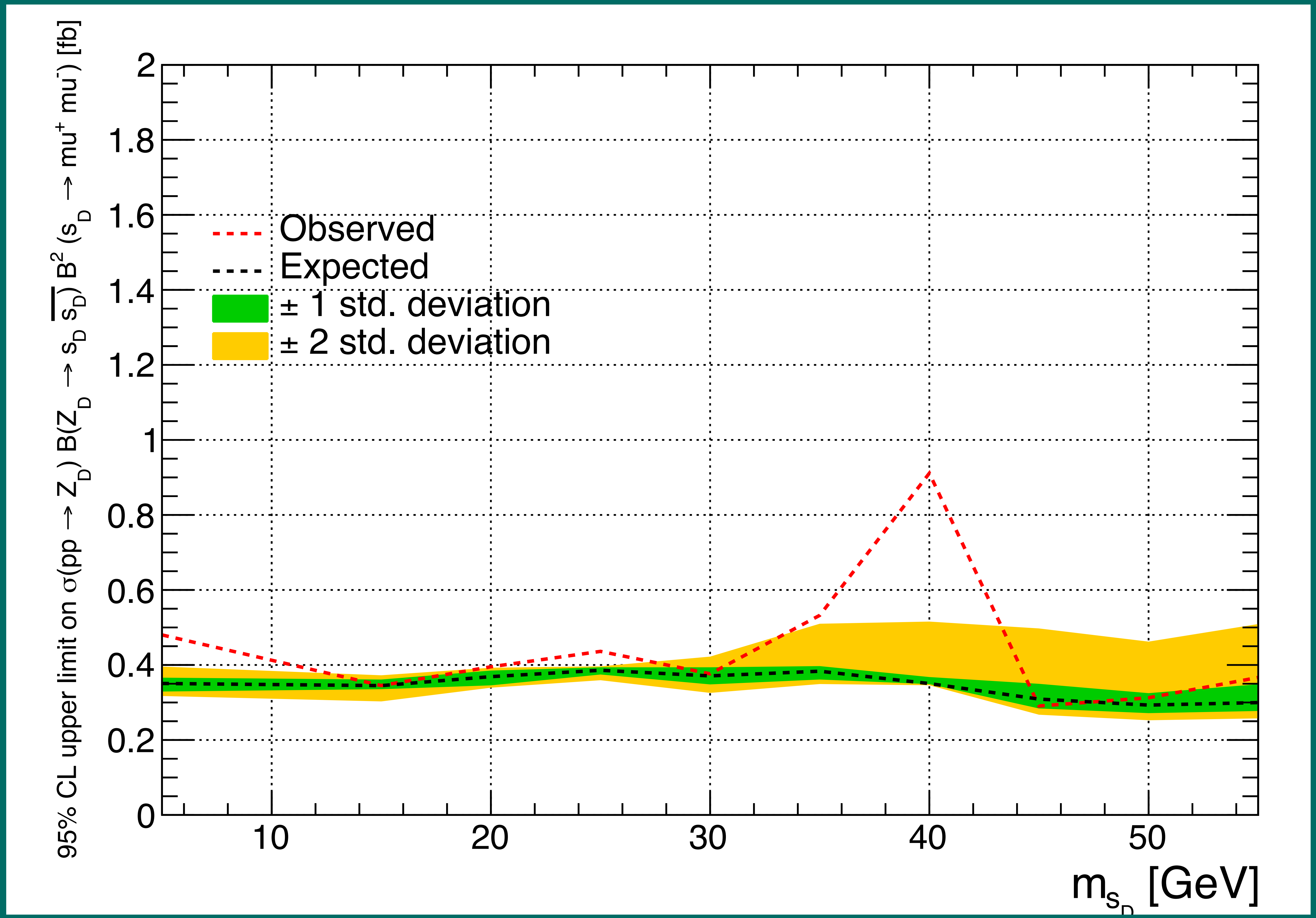

Brazilian bands for m_{ZD} =125 GeV. Expected limits after unblinding

Appendix G

Brazilian Plot - Post Fit Observed Limits -2018

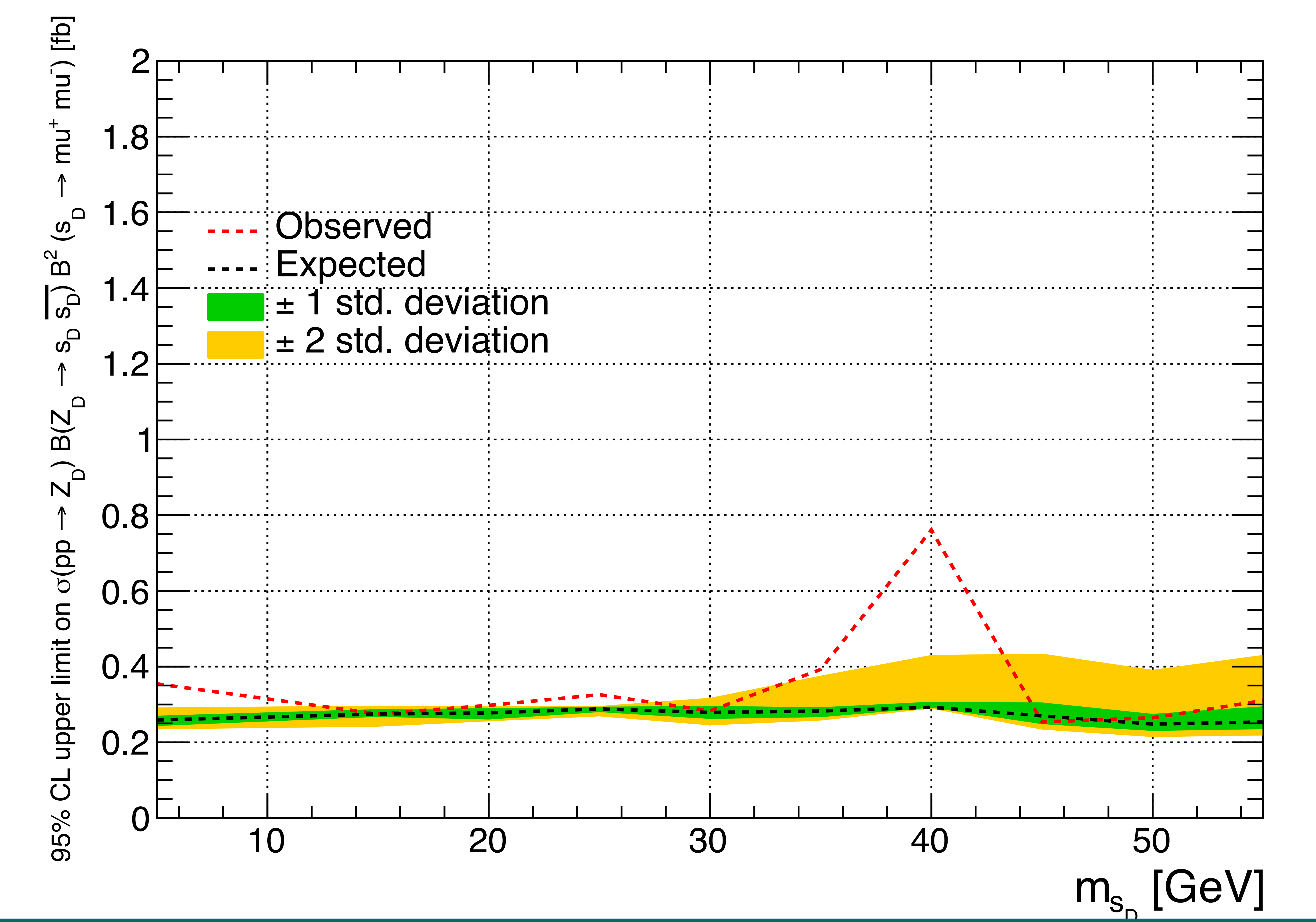

Brazilian bands for m_{ZD} =150 GeV. Expected limits after unblinding

Appendix G

Brazilian Plot - Post Fit Observed Limits -2018

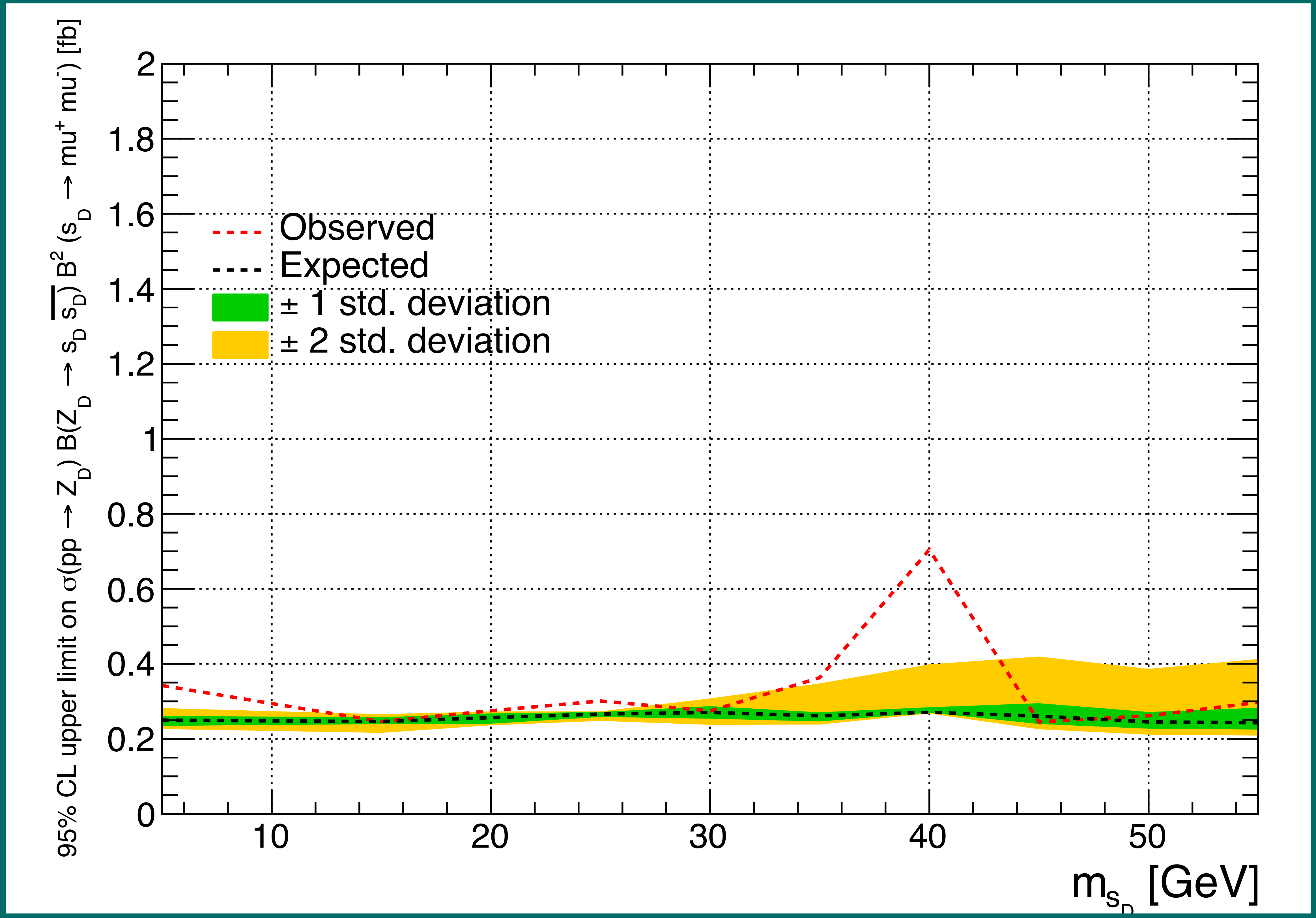

Brazilian bands for m_{ZD} =160 GeV. Expected limits after unblinding

Appendix G

Brazilian Plot - Post Fit Observed Limits -2018

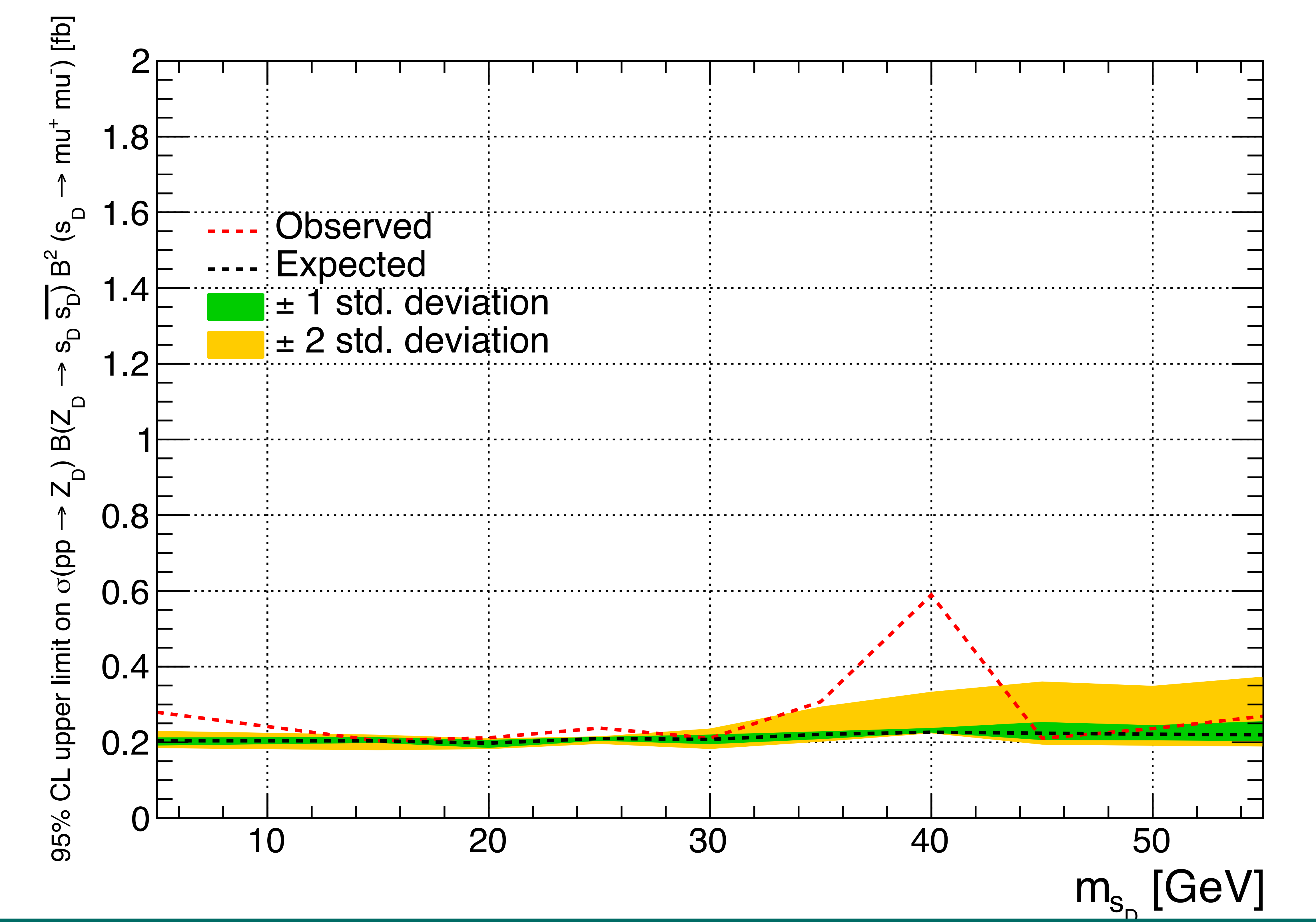

Brazilian bands for m_{ZD} =200 GeV. Expected limits after unblinding

Appendix H

Kinematics of the Model - Hard Process Simulation

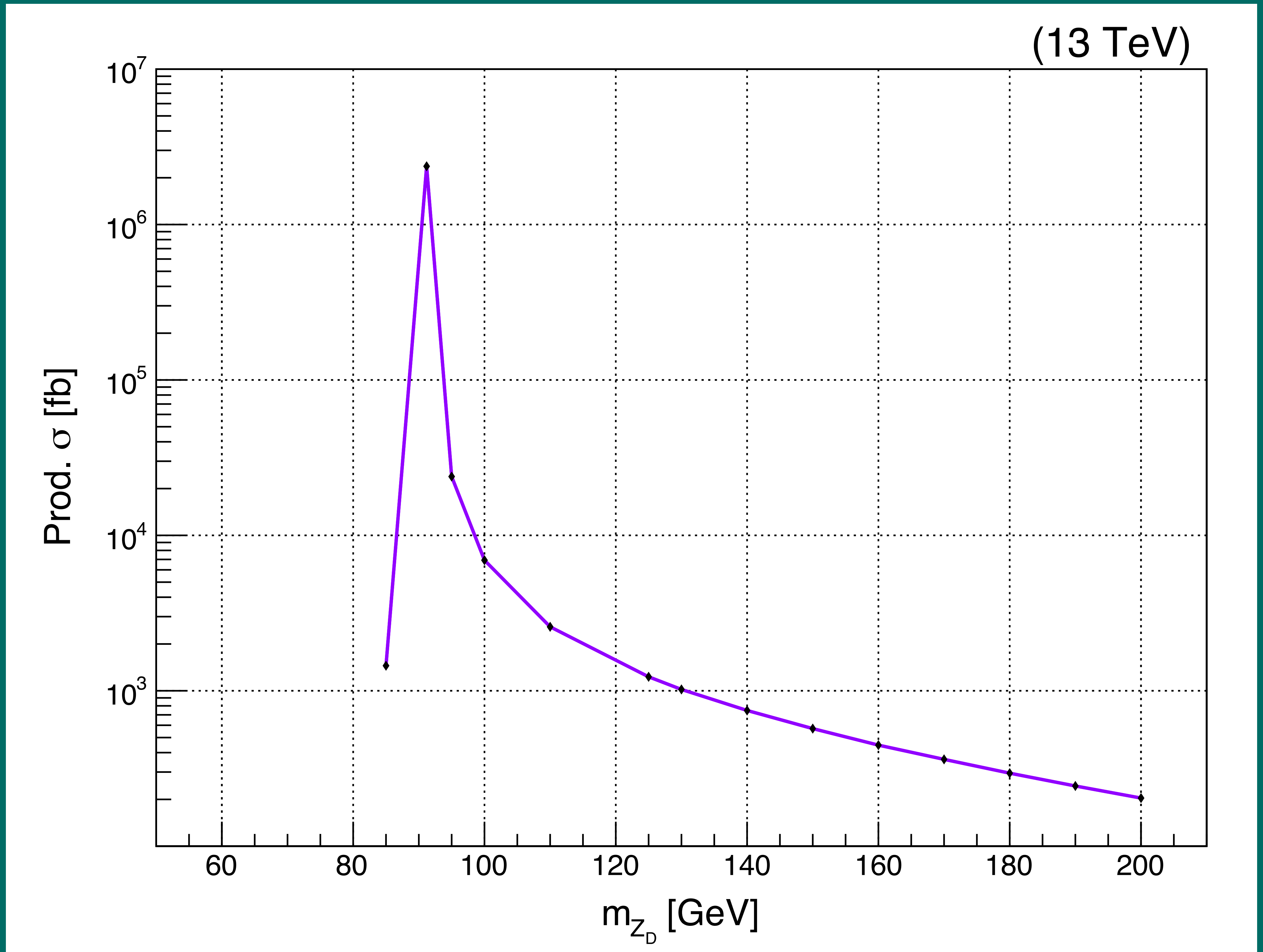

A scan of production cross-section for varying mass of Z_D

Appendix H

Kinematics of the Model - Hard Process Simulation

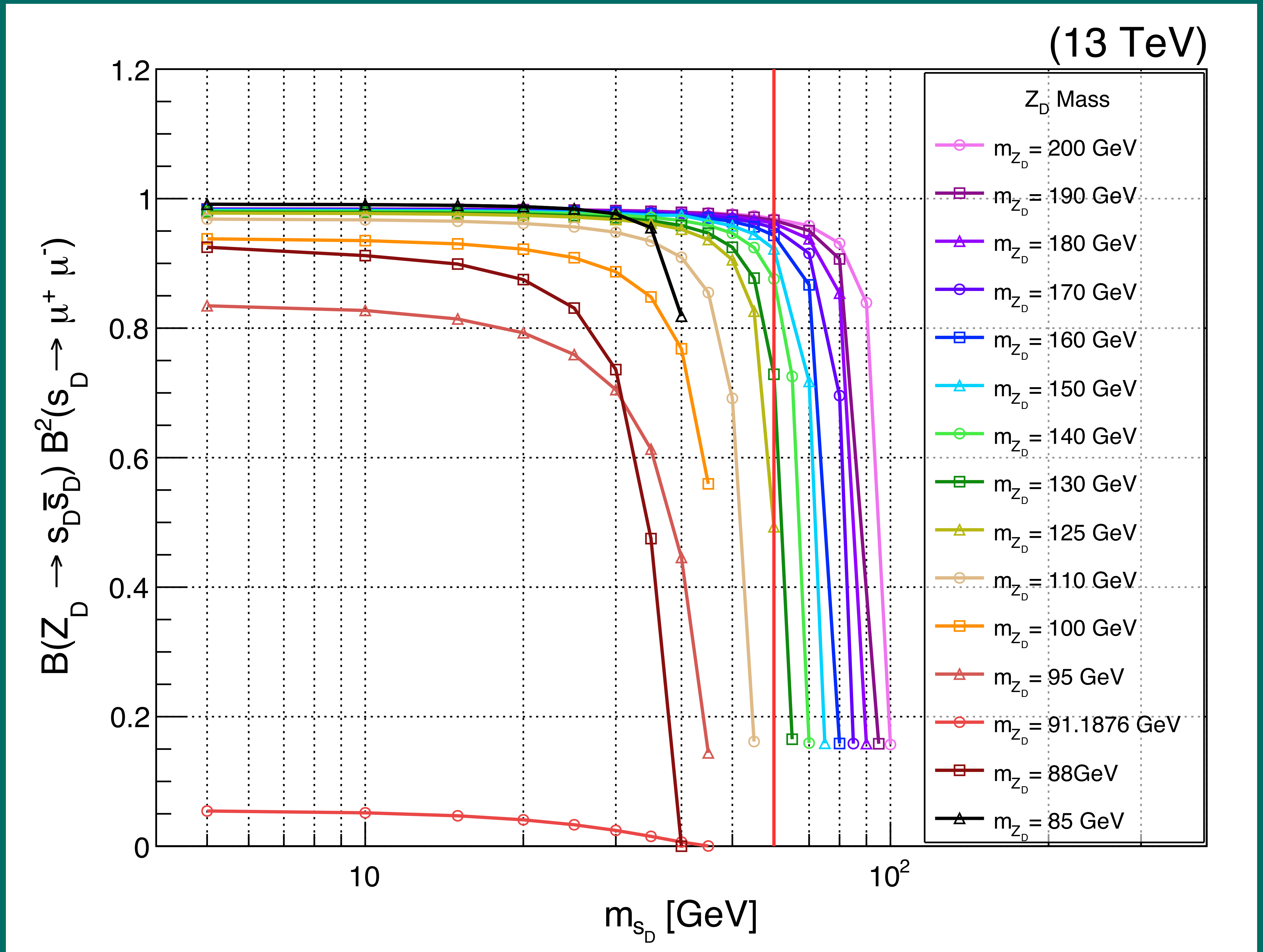

A scan of branching fraction for varying mass of Z_D and s_D

Appendix H

Kinematics of the Model - Hard Process Simulation

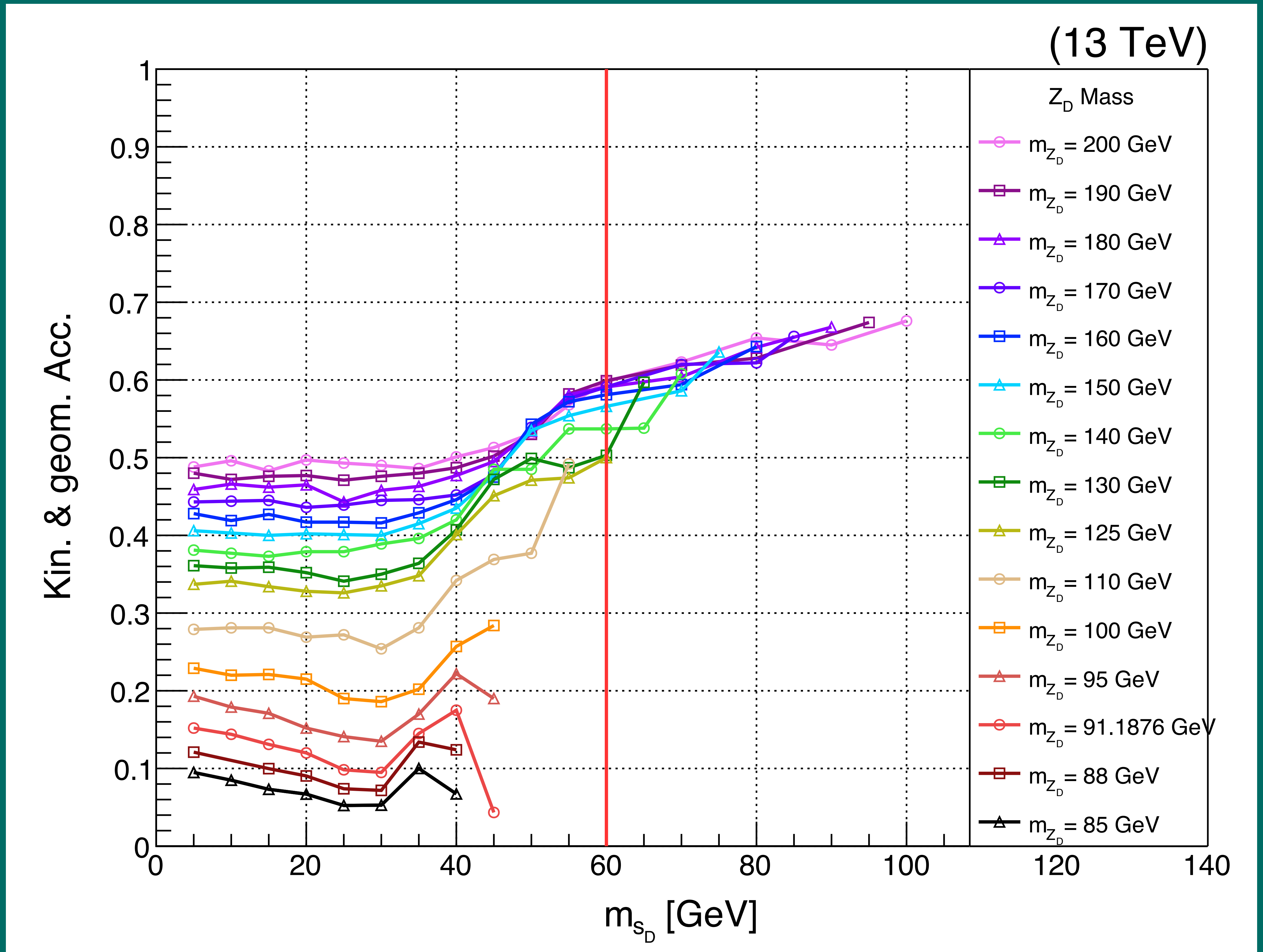

A scan of geometrical and kinematic acceptance of the muon selection for varying mass of Z_D and s_D

Appendix H

Kinematics of the Model - Hard Process Simulation

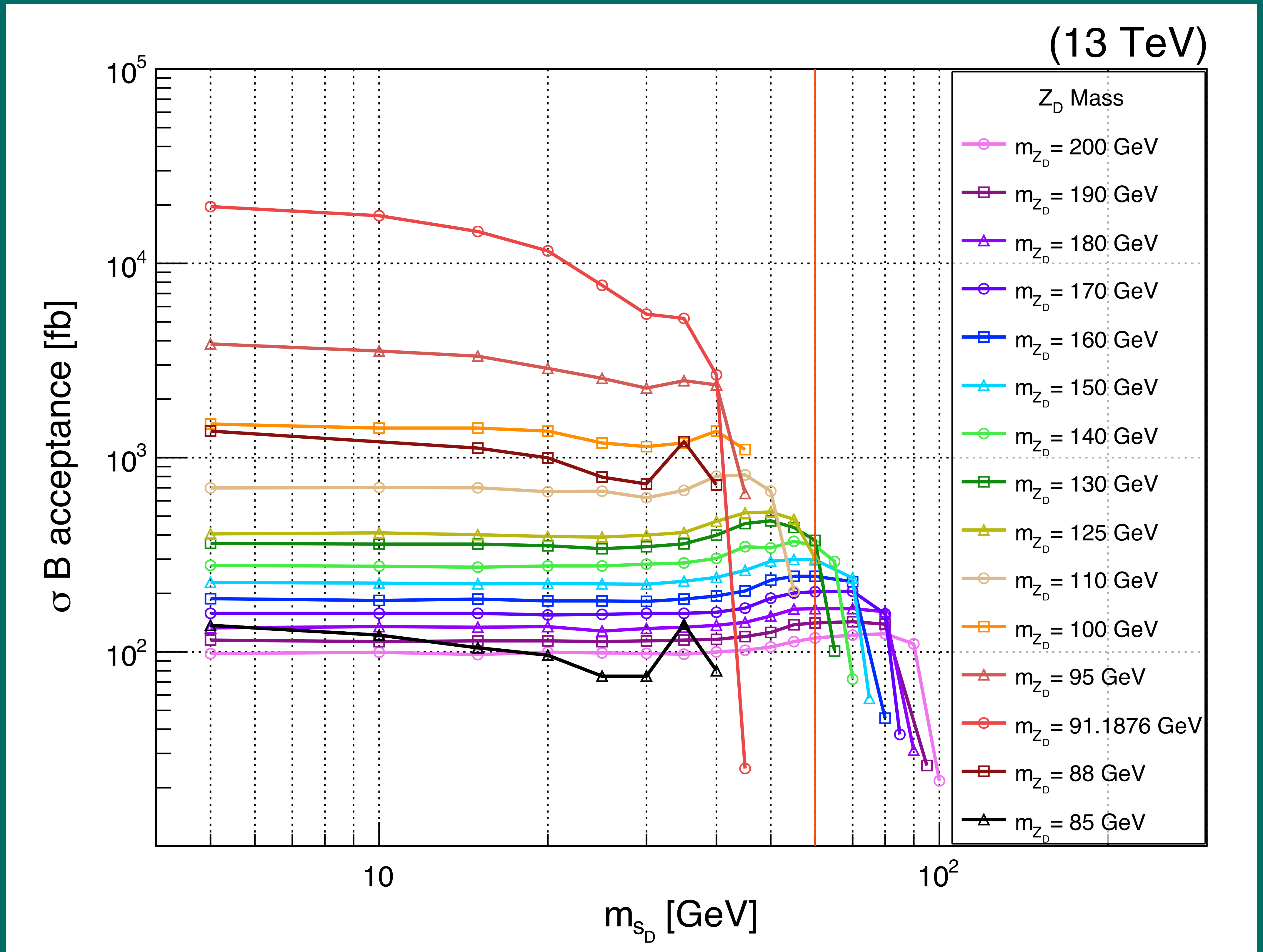

Multiplication production cross-section, branching fraction, and acceptance as an indication of sensitivity for varying mass of ZD and sD

Appendix I

Muon Pairing Algorithm